

10
I29A
#433
copy 3

CIVIL ENGINEERING STUDIES
Structural Research Series No. 433

UIU-ENG-76-2018



EVALUATION OF SAFETY OF REINFORCED CONCRETE BUILDINGS TO EARTHQUAKES

Metz Reference Room
Civil Engineering Department
B106 C. E. Building
University of Illinois
Urbana, Illinois 61801

by
M. PORTILLO GALLO
and
A. H-S. ANG

Technical Report of Research
Supported
by the
National Science Foundation
under Grant GK-36378

UNIVERSITY OF ILLINOIS
AT URBANA-CHAMPAIGN
OCTOBER 1976

EVALUATION OF SAFETY OF REINFORCED CONCRETE
BUILDINGS TO EARTHQUAKES

by

M. Portillo Gallo

and

A.H-S. Ang

Technical Report of Research Supported

by the

NATIONAL SCIENCE FOUNDATION

under

Grant GK-36378

University of Illinois at Urbana-Champaign

October 1976

ACKNOWLEDGMENT

This report is based on the doctoral thesis of M. Portillo Gallo submitted to the Graduate College of the University of Illinois at Urbana-Champaign in partial fulfillment for the Ph.D. degree. The study was directed by A.H-S. Ang, Professor of Civil Engineering, as part of a research program in the Department of Civil Engineering supported partially by the National Science Foundation under grant GK-36378.

The various discussions held with, and constructive comments offered by, Professors W. J. Hall, M. Sozen, and W. Tang during the course of the study are gratefully acknowledged.

TABLE OF CONTENTS

CHAPTER	Page
1. INTRODUCTION	1
1.1 General Remarks	1
1.2 Related Previous Studies	2
1.3 Objectives and Scope of Present Study	4
1.4 Basic Reliability Model	5
1.5 Organization	7
1.6 Notation	8
2. ANALYSIS OF RESISTANCE MODELS	10
2.1 Introductory Remarks	10
2.2 Flexure and Axial Load	10
2.2.1 Equations of Flexural Capacity	10
2.2.2 Uncertainties in Flexural Capacity	12
2.3 Shear	14
2.3.1 Equations for Shear Resistance	14
2.3.2 Uncertainty in Shear Capacity	16
3. MODELING OF STRUCTURAL SYSTEMS FOR DYNAMIC ANALYSIS	22
3.1 Introduction	22
3.2 The Eigenvalue Problem	22
3.2.1 General Formulation	22
3.2.2 The Mass Matrix	23
3.2.3 The Stiffness Matrix	25
3.2.4 Uncertainties in Natural Frequencies and Modal Shapes	34
3.3 Analysis of Uncertainty in Structural Damping	35
3.3.1 Introduction	35
3.3.2 Data from Full-Scale Structures	36
3.3.3 Damping of Model Structures	39
3.3.4 Summary and Conclusions on Damping	40
4. ANALYSIS OF LOAD MODELS AND LOAD EFFECTS	42
4.1 Introductory Remarks	42
4.2 Dead Load	42
4.3 Live Load	43
4.3.1 Introduction	43
4.3.2 Live Load Models	44
4.3.3 Arbitrary-Point-in-Time Load	47
4.3.4 Live Load Effects	47

	Page
4.4 Earthquake Load	50
4.4.1 Introduction	50
4.4.2 Methods of Earthquake Response Analysis	51
4.4.3 Statistics of Maximum Response	53
4.4.4 Maximum Earthquake Load Effects	57
4.5 Total Load Effect	64
5. RELIABILITY OF CURRENT DESIGNS	65
5.1 Introductory Remarks	65
5.2 Risk Implicit in Current Designs	65
6. SUMMARY AND CONCLUSIONS	70
6.1 Summary of Study	70
6.2 Main Conclusions	71
LIST OF REFERENCES	72
APPENDIX	
A. COVARIANCE BETWEEN MATHEMATICAL MODELS	101
B. ANALYSIS OF M_t	104
C. CORRELATION BETWEEN THE TOTAL LOAD ACTING ON TWO FLOORS	106
D. ANALYSIS OF EI	109
E. ANALYSIS OF W_i AND $\{\phi_i\}$	113
VITA	115

LIST OF TABLES

Table		Page
2.1	UNCERTAINTIES IN DESIGN PARAMETERS	14
2.2	BIAS AND UNCERTAINTY OF EQ. 2.12	18
2.3	SUMMARY OF TEST VERSUS CALCULATED VALUES OF v_c FROM TABLE 2, REF. [81] ($0.005 < \rho < 0.01$)	19
2.4	BIAS AND UNCERTAINTY OF EQ. 2.11 FOR v_t	20
3.1	IMPERFECTIONS IN THE ESTIMATION OF EI	29
3.2	SUMMARY OF TEST DATA FROM MATTOCK [59]	31
3.3	SUMMARY OF DAMPING OF FULL-SCALE STRUCTURES	39
4.1	5 DOF SYSTEM: RELATIVE DISPLACEMENT OF THE FLOORS	52
4.2	STATISTICS OF THE AMPLIFICATION FACTORS	55
4.3	SUMMARY OF v/a AND ad/v^2 (HORIZONTAL DIRECTION)	56
4.4	SUMMARY OF COEFFICIENTS IN EQ. 4.50	63
4.5	COEFFICIENTS OF VARIATION OF AMPLIFICATION FACTORS	63
4.6	COEFFICIENT OF VARIATION OF D_i	64
5.1	DESIGN LATERAL FORCES	66
5.2	FAILURE PROBABILITIES OF THE MEMBERS OF STRUCTURE 1 FOR $a = 0.1 g$	68
6.1	CALCULATED FAILURE PROBABILITY	70

LIST OF FIGURES

Figure		Page
2.1	COEFFICIENT OF VARIATION IN FLEXURAL CAPACITY $\bar{f}_c = 4.7 \text{ ksi}$, $\bar{f}_y = 47.7 \text{ ksi}$	80
2.2	COEFFICIENT OF VARIATION OF v_c (EQ. 2.14)	81
2.3	COEFFICIENT OF VARIATION OF v_c (EQ. 2.18)	81
2.4	COEFFICIENT OF VARIATION IN SHEAR CAPACITY	81
3.1	COEFFICIENT OF VARIATION OF TOTAL DEAD AND LIVE LOAD ON A FLOOR	82
3.2	CORRELATION COEFFICIENT BETWEEN TOTAL LOADS ON TWO FLOORS	82
3.3	ASSUMED STRAIN AND STRESS DISTRIBUTION FOR CALCULATION OF EI	83
3.4	MOMENT-CURVATURE RELATIONSHIP OF REINFORCED CONCRETE MEMBERS	84
3.5	COEFFICIENT OF VARIATION OF EI $\bar{f}_c = 4.7 \text{ ksi}$, $\bar{f}_y = 47.7 \text{ ksi}$	85
3.6	END MOMENT-END ROTATION RELATIONSHIP OF ANTI-SYMMETRIC MEMBERS	86
3.7	TYPES OF ELEMENTS TESTED	86
3.8	DAMPING VALUES OBTAINED FROM FORCED VIBRATION TESTS OF FULL-SCALE STRUCTURES (ALL DATA)	87
3.9	DAMPING VALUES OBTAINED FROM FORCED VIBRATION TESTS OF FULL-SCALE STRUCTURES (DATA OF 1965-1973)	87
4.1	LIVE LOAD MODEL	88
4.2	COEFFICIENT OF VARIATION OF UNIT LIVE LOAD INTENSITY	89
4.3	COEFFICIENT OF VARIATION OF LIVE LOAD EFFECT	89
4.4	COEFFICIENT OF VARIATION OF AXIAL LOAD IN A COLUMN SUPPORTING n FLOORS	90
4.5	REDUCTION IN COEFFICIENT OF VARIATION OF AXIAL LOAD IN A COLUMN AS A FUNCTION OF NUMBER OF FLOORS SUPPORTED	90
4.6	BASIC SHAPE OF THE RESPONSE SPECTRUM [69]	91
4.7	CONDITIONAL MEANS OF AMPLIFICATION FACTORS	92
4.8	CONDITIONAL STANDARD DEVIATIONS OF AMPLIFICATION FACTORS	92
5.1	PLAN AND ELEVATION OF STRUCTURES CONSIDERED	93
5.2	MEMBER DIMENSIONS OF STRUCTURE 1 AND STRUCTURE 2	94
5.3	PROBABILITY OF FAILURE OF SEAOC DESIGN, STRUCTURE 1; $a = 0.1 \text{ g}$, $\bar{\beta} = 4\%$	95
5.4	PROBABILITY OF FAILURE OF SEAOC DESIGN, STRUCTURE 2; $a = 0.1 \text{ g}$, $\bar{\beta} = 4\%$	96

Figure		Page
5.5	PROBABILITY OF FAILURE OF INTERIOR BEAM AND COLUMNS AT LEVEL 5 OF STRUCTURE 1, $\bar{\beta} = 4\%$. . .	97
5.6	FAILURE PROBABILITY OF INTERIOR BEAMS FOR DIFFERENT NATURAL PERIODS, $\bar{\beta} = 4\%$. . .	98
5.7	FAILURE PROBABILITY OF INTERIOR COLUMNS FOR DIFFERENT NATURAL PERIODS, $\bar{\beta} = 4\%$. . .	98
5.8	FAILURE PROBABILITY OF INTERIOR BEAMS FOR DIFFERENT DAMPING, $\bar{T} = 1.75$ sec . . .	99
5.9	FAILURE PROBABILITY OF INTERIOR COLUMNS FOR DIFFERENT DAMPING, $\bar{T} = 1.75$ sec . . .	99
5.10	INFLUENCE OF THE NUMBER OF MODES ON PROBABILITY OF FAILURE (INTERIOR BEAMS OF STRUCTURE 1), $\bar{\beta} = 4\%$. . .	100
5.11	INFLUENCE OF THE NUMBER OF MODES ON PROBABILITY OF FAILURE (INTERIOR COLUMNS OF STRUCTURE 1), $\bar{\beta} = 4\%$. . .	100

CHAPTER 1

INTRODUCTION

1.1 General Remarks

Earthquake-resistant design, perhaps more than any other branch of engineering, is characterized by very high levels of uncertainty, because (1) of the unpredictability of the characteristics and intensities of the ground motion of future earthquakes; (2) the lack of precise information on the structural properties, especially those pertaining to the dynamic behavior of systems; and finally, (3) the numerous assumptions and simplifications that the designer is forced to make in order to reduce the complexity of the dynamic problem for practical applications. Under these circumstances, the correct determination of the levels of risk implicit in the design of structures located in seismic areas becomes an important objective of the process of design. In fact, this is the basis for the development of a proper earthquake-resistant design.

Current earthquake-resistant design techniques, as represented by construction codes, recognize the existence of uncertainty, but rely on intuitively determined overall factors of safety to obtain proper designs. As a consequence, the true levels of risk underlying a given design are unknown. Moreover, the results of new investigations and new developments that could reduce the existing uncertainties cannot be incorporated systematically into the design process.

For these purposes, a method of reliability evaluation is required. In this regard, it should establish the basis for the assessment of the reliability of each of the potential modes of failure in a structure under the various earthquake intensities. In doing this, it may be emphasized that meaningful expressions of safety can only be formulated if the uncertainties in the loads and the structural properties, as well as the inaccuracies of the load and resistance prediction models, are duly considered.

Appropriately, several authors have suggested the use of probability concepts in the analysis of structural safety [11, 22, 37, 72].

It is recognized, in particular, that the proper treatment of uncertainty requires concepts of the theory of probability; accordingly, the loads and strengths are treated as random variables, and the reliability of a structure, or conversely of the risk involved in a given design, is expressed in terms of the probability of failure. This study is concerned with such reliability analysis with special reference to reinforced concrete structures subjected to earthquake forces.

1.2 Related Previous Studies

The problem of structural safety involves two main areas of study; the analysis and assessment of uncertainties, and the quantitative evaluation of risk [3]. The analysis of uncertainties associated with earthquake loadings and structural response, may be divided into three groups:

1. Those concerned with the estimation of future earthquake intensities commonly referred to as "seismic risk analysis". In these studies, the maximum ground intensity at a site (usually expressed in terms of the maximum value of the ground displacement, velocity, or acceleration) is expressed in terms of the return period. The first seismic risk models were introduced by Cornell [30], Milne and Davenport [67], and Esteva [35]. Implicit in these models is the assumption that the energy released during an earthquake is concentrated at a point (point-source models). Although this assumption may be acceptable for small earthquakes, it would not be valid for the case of major earthquakes in which the energy is released along fault slips that may be hundreds of kilometers long. To overcome this difficulty, Ang [9] and Der-Kiureghian and Ang [31] developed a model which takes into account the relation between magnitude and the length of the fault slip (line-source model).
2. Those dealing with the modeling of the random earthquake motion itself; appropriately, stochastic models were used for this purpose. Examples of these models include stationary processes,

such as white-noise, continuous Gaussian random process (see for example References [56, 72, 77]), and non-stationary processes, obtained by multiplying a stationary process by a deterministic envelope function of time [7, 53, 83]. These are then used to generate artificial earthquakes, for use in time history analysis, or for the direct estimation of the maximum response statistics through random vibration theory. More recently, response spectra corresponding to specified probability levels have been used to represent the statistical properties of the ground motion at a site. These are obtained through the analysis of normalized earthquake records [21, 69, 71, 89] or by linear regression analysis techniques [36, 64].

3. Those whose objective is the statistical evaluation of the response. In the case of linear structures, the theory of random vibrations is commonly used for this purpose [9, 41, 56, 77, 94, 95]. The results of recent studies [17, 58] seem to indicate that the response spectrum approach may also be used to estimate the statistics of the response of multidegree of freedom systems. In the case of nonlinear systems the response statistics are usually obtained by time-history analysis of artificially generated earthquake motions [78], although some approximations for elasto-plastic systems, or systems with mild nonlinearities are possible through random vibration theory [41, 56, 57]. All of these studies, however, consider the structural properties to be deterministic. The problem of systems with random structural properties subjected to random earthquake motions remains an area for further study.

The problem of structural safety under extreme hazards in general was discussed by Ang [10]. Rosenblueth and Esteva [86] indicated conceptually how the statistics of the load effects may be obtained for the case of earthquakes of prescribed intensity. Similarly, Esteva and Villaverde [36] presented a formulation for the analysis of the probability distribution of the maximum seismic response of systems with imperfectly known properties.

Although these studies are important steps in the analysis of structural safety under earthquake loading, the actual levels of risk

involved in modern earthquake-resistant design of reinforced concrete structures remain unknown because: (1) realistic values of the uncertainties in the properties of structures under dynamic loading are not available; and (2) a general procedure that includes the uncertainties in the load effects and the structural response evaluation has not yet been developed.

1.3 Objectives and Scope of Present Study

This study is intended to provide a basis for determining the level of risk involved in current earthquake-resistant designs, with special reference to reinforced concrete structures. For this purpose, the loads and structural properties are assumed to be statistically independent random variables. It is also assumed that the first and second moment statistics of these variables are sufficient to estimate the required risks.

As a first step, the basic variabilities of the loads and structural properties, as well as the inaccuracies in the loads and resistance prediction methods are carefully examined and assessed; the required risks are then obtained by evaluating the probabilities of failure, in flexure and shear, of individual components of reinforced concrete buildings designed in accordance with current design codes when subjected to earthquakes of prescribed intensities. In this regard, available reliability model [8, 11] is used as the basis of the reliability analysis (see Sect. 1.4).

Only linear structures are considered, and "failure" pertains to the first sign of distress in one or more members of a structure. Thus, failure means that a structure (or structural element) has been stressed beyond the elastic range; in particular, this does not necessarily mean that collapse or even serious structural damage has occurred, unless the structural elements are not provided with adequate ductility. However, from the observation of the performance of modern structures during earthquakes [101], there is evidence to indicate that when a structure becomes inelastic, architectural damage usually occurs which may represent an important portion of the total cost of the building

(especially in framed structures). On this basis, the probability of failure calculated herein represents the risk of some (may be only local) structural damage.

1.4 Basic Reliability Model

Existing reliability model [8, 11] will form the basis for this study. The essence of this model may be described as follows.

Let Y be a random variable representing, for example, the resistance, R , or the applied load effect, S , in a given member of a structure. Invariably, Y is a function of other variables; e.g.,

$$Y = f(X_1, X_2, \dots, X_n) \quad (1.1)$$

Presumably, the model for Y , as represented by the function of Eq. 1.1, as well as X_1, \dots, X_n , would represent reality exactly. In practice, however, this is not possible; f and X_1, \dots, X_n must be predicted or estimated, and thus are subject to prediction errors. To adjust for an imperfect prediction, corrective factors N_f and N_{X_i} are introduced, such that

$$f = N_f \hat{f} \quad (1.2)$$

and

$$X_i = N_{X_i} \hat{X}_i \quad (1.3)$$

where \hat{f} is the empirical or theoretical function adopted as a model of f , and \hat{X}_i is the model of X_i . Here, N_f , N_{X_i} and \hat{X}_i are random variables with means \bar{N}_f , \bar{N}_{X_i} and \bar{x}_i , and coefficients of variation (c.o.v.) Ω_{N_f} , Δ_{X_i} and δ_{X_i} , respectively. The uncertainties associated with the basic variability in X_i are, therefore, measured by δ_{X_i} ; whereas Δ_{X_i} represents the prediction uncertainty in X_i . Consistent with the first-order approximation, Δ_{X_i} will be ascribed entirely to the uncertainty in the predicted \bar{x}_i . Furthermore, the mean values \bar{N}_f and \bar{N}_{X_i} represent,

respectively, the bias in the model \hat{f} (usually a deterministic function) and the estimated mean \bar{x}_i .

By first-order approximation, the total c.o.v. of X_i then (by virtue of Eq. 1.3) is

$$\Omega_{X_i} = \sqrt{\delta_{X_i}^2 + \Delta_{X_i}^2} \quad (1.4)$$

Similarly, the total c.o.v. of f is

$$\Omega_f = \sqrt{\delta_f^2 + \Delta_f^2} \quad (1.5)$$

where δ_f represents the basic variability about the model function \hat{f} ; $\delta_f = 0$ if \hat{f} is deterministic.

Substituting Eqs. 1.2 and 1.3 into Eq. 1.1, and using a first-order approximation, the mean and c.o.v. of Y are easily found to be [99]

$$\mu_Y = \bar{N}_f \hat{f} (\bar{N}_{X_1} \bar{X}_1, \bar{N}_{X_2} \bar{X}_2, \dots, \bar{N}_{X_n} \bar{X}_n) \quad (1.6)$$

and

$$\begin{aligned} \Omega_Y^2 = \Omega_f^2 &+ \frac{\bar{N}_f^2}{\mu_Y^2} \left[\sum_{i=1}^n \left(\frac{\partial f}{\partial X_i} \right)_\mu^2 \bar{N}_{X_i}^2 \bar{X}_i^2 \Omega_{X_i}^2 + \right. \\ &\left. \sum_{\substack{i=1 \\ i \neq j}}^n \sum_{j=1}^n \left(\frac{\partial f}{\partial X_i} \right)_\mu \left(\frac{\partial f}{\partial X_j} \right)_\mu \rho_{X_i, X_j} \bar{N}_{X_i} \bar{N}_{X_j} \bar{X}_i \bar{X}_j \Omega_{X_i} \Omega_{X_j} \right] \quad (1.7) \end{aligned}$$

in which ρ_{X_i, X_j} is the correlation coefficient between X_i and X_j . Procedures for estimating the basic variabilities and prediction uncertainties, as well as ρ_{X_i, X_j} , from typical sources of information are given in Refs. [99, 105].

In some cases, the component variables X_1, \dots, X_n may be functions of other variables; e.g.,

$$X_i = g_i(Z_1, Z_2, \dots, Z_m) \quad \text{for } i = 1, \dots, n \quad (1.8)$$

In such cases, the mean and c.o.v. of X_i may be found using a procedure similar to the one just described for Y . The estimation of the correlation coefficient (or covariance) between X_i and X_j , necessary for the estimation of Ω_Y (see Eq. 1.7) may be difficult to obtain in general. However, if the correlation between X_i and X_j exists because of functional relationships (e.g., X_i and X_j are functions of certain common variables), an approximate expression for $\text{COV}[X_i, X_j]$, consistent with the first-order approximation, is given by (see Appendix A),

$$\text{COV}[X_i, X_j] = \bar{N}_{g_i} \bar{N}_{g_j} \sum_{\ell=1}^p \left(\frac{\partial g_i}{\partial Z_\ell} \right)_\mu \left(\frac{\partial g_j}{\partial Z_\ell} \right)_\mu \bar{N}_{Z_\ell}^2 \bar{Z}_\ell^2 \Omega_{Z_\ell}^2 \quad (1.9)$$

where Z_ℓ , for $\ell = 1, \dots, p$ are the variables common to both X_i and X_j .

Finally, for statistically independent R and S , the failure probability is easily obtained for prescribed distributions [8]. In particular, for the case of lognormally distributed R and S

$$P_f = 1 - \Phi \left[\frac{\ln \left(\frac{\mu_R / \mu_S \sqrt{1 + \Omega_S^2}}{1 + \Omega_R^2} \right)}{\sqrt{\ln [(1 + \Omega_R^2)(1 + \Omega_S^2)]}} \right] \quad (1.10)$$

where $\Phi(-)$ is the standard normal probability distribution function.

1.5 Organization

Chapter 2 contains the formulation of resistance models, in flexure and shear, of typical beams and columns found in reinforced concrete earthquake-resistant designs.

Chapter 3 contains an analysis of structural system models for dynamic response determination. Its purpose is to assess the variabilities in the properties of reinforced concrete structural systems and those underlying their mathematical idealization. The dynamic properties of the systems, mainly, natural frequencies, model shapes, and damping, are examined.

The analysis and modeling of loads are discussed in Chapter 4. Various dead and live load models are reviewed relative to the determination of loads for seismic consideration. Different methods for specifying the ground motion inputs are studied; these include the time-history approach, response spectrum techniques, and random vibration analysis. Mean-values and coefficients of variation of the maximum response of multi-degree-of-freedom systems calculated using these models are compared, and the adequacy of the response spectrum approach to represent earthquake motions is discussed. On these bases, the statistics of the total load effects, as obtained from the simultaneous action of dead, live, and earthquake loads are assessed.

Risk levels involved or implicit in present design codes are evaluated in Chapter 5. For this purpose, typical designs of reinforced concrete structures are obtained by applying the provisions of the SEAOC code [90], and the probabilities of failure are evaluated accordingly.

Chapter 6 contains the summary and principal conclusions of this study.

1.6 Notation

When applicable, conventional ACI notation is used herein. The other basic symbols used in this study are as follows:

- D random variable describing the unit dead load (psf units)
- E random variable describing the earthquake load
- L random variable describing the unit live load (psf units)
- P_f probability of failure
- R random variable describing member resistance
- S_i random load effect from load i
- \bar{X} predicted mean of random variable X

Δ_X	prediction uncertainty in X
δ_X	coefficient of variation (c.o.v.) of X
μ_X	mean value of X
ρ_{X_i, X_j}	correlation coefficient between X_i and X_j
σ_X	standard deviation of X
Ω_X	total uncertainty in X , equal to $\sqrt{\delta_X^2 + \Delta_X^2}$

CHAPTER 2

ANALYSIS OF RESISTANCE MODELS

2.1 Introductory Remarks

The purpose of this chapter is to formulate resistance models needed in the reliability analysis of reinforced concrete structures under dynamic loading. Resistances in flexure, shear, and axial load are considered.

Because of the way that members are fabricated or constructed, the resistances between any two points along a member are invariably highly correlated. In particular, the yield strengths and areas of reinforcing bars may be assumed to be perfectly correlated along a member; however, the flexural and shear reinforcements may be assumed to be statistically independent.

2.2 Flexure and Axial Load

2.2.1 Equations of Flexural Capacity -- For the purpose of this study, flexural failures are assumed to occur when the tension reinforcement yields (tension failure), or when the strain at the extreme edge of the concrete compression zone reaches a maximum value of $\bar{\epsilon}_{cu} = 0.004$ (compression failures). Properly then, the flexural resistance should be expressed in terms of the yield moment capacity, M_y , in the case of tension failure; whereas the ultimate moment capacity, M_t , should be used for this purpose in the case of compression failure. However, the difference between M_t and M_y in the first case is very small, and, for practical purposes, M_t may be used instead of M_y . On this basis, the ultimate moment, M_t , will be used in formulating the flexural strength of reinforced concrete members in general.

The ultimate moment capacity of reinforced concrete members is not affected by load reversals if adequate shear capacity is provided [16, 27, 40, 87]. Thus, expressions for M_t may be obtained through the application of the "ultimate strength" theory of reinforced concrete [49, 61]. For rectangular sections, having the steel placed parallel to the two end faces (neglecting slenderness effects)

$$M_t = [P + A_s f_s - A'_s (f'_s - k_3 f'_c)] \left[1 - \eta \frac{P + A_s f_s - A'_s (f'_s - k_3 f'_c)}{f'_c b d} \right] d + A'_s (f'_s - k_3 f'_c) (d - d') - P \left(\frac{d - d'}{2} \right) \quad (2.1)$$

in which conventional ACI notation [4] is used; M_t is measured from the mid-height of the section, which corresponds to the plastic centroid in the case of symmetrically reinforced sections; $\eta = k_2/k_1 k_3$ is a parameter describing the characteristics of the concrete stress block distribution [49, 61]; and P is the applied axial load.

If the compression reinforcement yields (i.e., $f'_s = f_y$), f_s may be found by solving a strain compatibility equation simultaneously with the stress-strain curve of the reinforcement. This gives

$$f_s = c_1 + \sqrt{c_1^2 + c_2} \leq f_y \quad (2.2)$$

in which

$$c_1 = \frac{1}{2} \left[\frac{A'_s}{A_s} (f_y - k_3 f'_c) - E_s \epsilon_{cu} - \frac{P}{A_s} \right] \quad (2.3)$$

$$c_2 = \left[\frac{k_1 k_3 f'_c b d}{A_s} + \frac{A'_s}{A_s} (f_y - k_3 f'_c) - \frac{P}{A_s} \right] E_s \epsilon_{cu} \quad (2.4)$$

Similarly, if the tension reinforcement yields (i.e., $f_s = f_y$), then

$$f'_s = c_3 - \sqrt{c_3^2 + c_4} \leq f_y \quad (2.5)$$

where

$$c_3 = \frac{1}{2} \left[E_s \epsilon_{cu} + k_3 f'_c + \frac{A_s}{A'_s} f_y + \frac{P}{A'_s} \right] \quad (2.6)$$

and

$$c_4 = \left[\frac{k_1 k_3 f'_c b d'}{A'_s} - k_3 f'_c - \frac{A_s}{A'_s} f_y - \frac{P}{A'_s} \right] E_s \epsilon_{cu} \quad (2.7)$$

2.2.2 Uncertainties in Flexural Capacity -- If the axial load is zero, as in the case of pure bending of beams, the flexural strength is fully defined by the section and material properties, and the statistics of M_t may then be evaluated from Eq. 2.1. The limitations on the maximum amount of tension reinforcement in structures subjected to seismic loading [4, 90], makes tension failures nearly certain [33]; that is, the stress in the tensile reinforcement can be assumed to be equal to the yield stress. This is not necessarily true, however, for the compression reinforcement. If $f'_s < f_y$, then Eq. 2.5 must first be substituted into Eq. 2.1 before the statistics of M_t can be evaluated. A possible approximation for this later case, that greatly simplifies the amount of numerical computation, is obtained by substituting f'_s in Eq. 2.1 by $c_5 f_y$, where $c_5 = \bar{f}'_s / \bar{f}_y$ (i.e., c_5 is assumed to be constant). The error introduced in Ω_{M_t} is negligible, as has been verified numerically. This is also true for the case in which $P \neq 0$.

In the case of beam-columns, that is when $P \neq 0$, there is no closed form function describing jointly the behavior of M and P , needed to evaluate the respective uncertainties. The uncertainty analysis is therefore complicated by the resistance being a function of the relative load effects. Resistance and load are no longer statistically independent, and simplifications must be sought.

Ellingwood and Ang [33] assumed the applied moment and applied axial thrust to be perfectly correlated, and computed the statistics of the axial capacity in terms of material strengths, section parameters and load eccentricity. This assumption, however, does not seem appropriate for the case of structures subjected to seismic loading, because in many cases, moments and axial loads, may be induced by different types of loads. For example, in the case of an interior column of a symmetrical building, the axial load depends almost entirely on the dead and live loads, whereas the moment is due almost entirely to the earthquake load. Since the correlation between the load effects of different loads is small (in this

study they are assumed to be statistically independent), it is more appropriate to assume that moments and axial loads are statistically independent.

In computing the statistics of M_t from Eq. 2.1, two types of column failures may be identified: when the axial load is small (i.e., $P < P_B$), the section fails by yielding of the tensile reinforcement (tension failures), and $f_s = f_y$; whereas for high axial loads (i.e., $P > P_B$) failure is governed by the concrete reaching its ultimate strain, while the tensile reinforcement is still elastic (compression failure), and Eq. 2.2 must be substituted into Eq. 2.1 before the statistics of M_t can be estimated. Since P and P_B are random variables, it is generally not possible to know whether a tension or a compression failure will govern the design [33, 86]. However, in the case of reinforced concrete structures designed against earthquake loads, most columns are subjected to low axial loads, i.e., $P < P_B$ [20], except in the case of extremely tall buildings; thus, failure can be assumed to occur through tensile yielding. For simplicity this will be assumed in the following (the adequacy of this assumption will be verified in the analysis of specific design examples). However, if needed, various procedures to include the possibility of compression failures may be included [33].

On the basis of the above assumptions, the relevant statistics of the flexural capacity of reinforced concrete beams and columns found in structures designed to resist earthquake forces are determined with Eq. 2.1 where $f_s = f_y$ and $f'_s = (f'_s/\bar{f}_y)f_y = c_5 f_y$. For this purpose, the statistics of the material and section properties given in Ref. [33] (as summarized in Table 2.1) are used. The statistics of P may be determined as described in Chapter 4. Expressions for the partial derivatives of M_t with respect to its component variables needed in the evaluation of Ω_{M_t} , are given in Appendix B.

The total coefficients of variation are summarized in Fig. 2.1 for the following: (a) symmetrically doubly reinforced beams, as a function of the reinforcement ratio $\bar{\rho}$; (b) unsymmetrically doubly reinforced beams, as a function of the ratio of compressive to tensile reinforcement $\bar{\rho}'/\bar{\rho}$; and (c) symmetrically reinforced columns, as a function of the applied load

to the balanced load, \bar{P}/\bar{P}_B . It may be observed from this figure that, in the case of beams, Ω_{M_t} is almost constant for all values of the reinforcement ratio; whereas for columns, Ω_{M_t} depends on the axial load \bar{P}/\bar{P}_B and, of course, also on the uncertainty in P .

TABLE 2.1 UNCERTAINTIES IN DESIGN PARAMETERS

Parameter	Predicted Mean	Basic Variability	Prediction Uncertainty	Total Uncertainty
f_y (Nominal 40 ksi)	47.7 ksi	0.09	0.12	0.150
f_y (Nominal 60 ksi)	64.0 ksi	0.07	0.12	0.139
f_c (Nominal 3 ksi)	3.5 ksi	0.12	0.18	0.216
f_c (Nominal 4 ksi)	4.7 ksi	0.12	0.18	0.216
A_s		0.02	0.03	0.036
b		0.04	0.02	0.045
d		0.07	0.05	0.086
h		0.04	0.02	0.045
$k_1 k_3$	0.72	0.12	0.05	0.130
η	0.59	0.05	0.00	0.050
ϵ_{cu}	0.004	0.12	0.10	0.156

2.3 Shear

2.3.1 Equations for Shear Resistance -- The other mode of potential failure is through shear. The members are subjected to load reversals, as expected of structures under earthquake loading. In this regard, shear failure of a member is assumed to occur before the corresponding yield moment capacity is exceeded.

The so-called "shear-failure" is in fact a failure under combined shear and bending plus, occasionally, axial load and torsion [1, 14]. Shear stresses are transferred from one plane to another in various ways: shear stress in the uncracked concrete; interface shear transfer; dowel action; arch action; and through the shear reinforcement. Expressions for the shear capacity of reinforced concrete members that take into account all of these shear transfer mechanisms are not available. Usually, the so-called "truss-analogy" is used for this purpose [14]. In this context, the shear capacity of a section is expressed as

$$V_t = V_c + V_s \quad (2.8)$$

where V_c is the "shear carried by the concrete" at ultimate, and V_s is the shear carried by the transverse reinforcement. For the purpose of this study, Eq. 2.8 will suffice.

The shear carried by the concrete, assumed to be equal to that causing the first diagonal crack in a member without shear reinforcement, may be expressed as

$$V_c = v_c bd \quad (2.9)$$

where v_c is an average stress (the nominal shear stress) assumed to be uniform over the area bd . The shear force carried by the web reinforcement is calculated on the assumptions that the inclined cracking has a horizontal projected length, d , and the reinforcement is yielding. If the stirrups are vertical and of the same size, then [14].

$$V_s = \frac{d}{s} A_v f_y \quad (2.10)$$

where s is the stirrup spacing and A_v the stirrup area. The shear capacity is then

$$V_t = v_c bd + \frac{d}{s} A_v f_y \quad (2.11)$$

Tests in which load reversals were applied indicated that the behavior of beams is not significantly affected by the application of a

few number of relatively high loads, provided that the longitudinal reinforcement is kept within the elastic range [5, 14]. On this basis, information obtained from members loaded in one direction (no reversal) may be applied to the case of members subjected to load reversals. However, if the flexural reinforcement yields, test results indicated the necessity of ignoring the concrete shear-resisting mechanism -- at least its contribution [74] must be reduced.

A number of semi-rational expressions have been developed to predict the shear cracking load of reinforced concrete members [1, 60, 81, 82, 106]. According to ACI [1, 4], the shear stress at cracking may be calculated by

$$v_c = 1.9 \sqrt{f'_c} + 2500 \rho \frac{Vd}{M} \leq 3.5 \sqrt{f'_c} \quad (2.12)$$

If axial load is present, Eq. 2.12 can still be used, except that M is substituted by

$$M_m = M - P \left(\frac{4h - d}{8} \right) \quad (2.13)$$

However, v_c should satisfy

$$v_c \leq 3.5 \sqrt{f'_c} \sqrt{1 + 0.002 \frac{P}{bh}} \quad (2.14)$$

2.3.2 Uncertainty in Shear Capacity -- For purposes of this study, the statistics of v_c are evaluated on the basis of Eqs. 2.12 through 2.14. In doing this, it is assumed that the applied axial load and shear are statistically independent. Moreover, based on the analysis of various available expressions for v_c , it was determined that the ratio V/M_m (or V/M when $P = 0$) in Eq. 2.12 may be assumed to be a random variable, statistically independent of the applied shear, with mean \bar{V}/\bar{M}_m and coefficient of variation, Ω_{V/M_m} . Suitable values of Ω_{V/M_m} were obtained by comparing the total c.o.v. of v_c obtained from Eq. 2.12 with those obtained from Eq. 2.14 and the expressions developed by Zsutty [106], Rajagopalan and Ferguson [81], and Ragan [82]. On this basis, $\Omega_{V/M_m} = 0.10$ is estimated when $P = 0$; whereas Ω_{V/M_m} varies from 0.17 (when $\Omega_P = 0.20$)

to 0.25 (when $\Omega_p = 0.60$) for members with axial compression.

If M_m is substituted for M in Eq. 2.12, the mean and the c.o.v. of v_c are

$$\bar{v}_c = 1.9 \sqrt{\bar{f}'_c} + 2500 \bar{\rho} \left(\frac{\bar{V}}{\bar{M}_m} \right) \bar{d} \quad (2.15)$$

and

$$\Omega_{v_c} = \frac{1}{\bar{v}_c} \left[\left(\frac{1.9 \sqrt{\bar{f}'_c}}{2} \right)^2 \Omega_{f'_c}^2 + \left(2500 \bar{\rho} \left(\frac{\bar{V}}{\bar{M}_m} \right) \bar{d} \right)^2 (\Omega_{A_s}^2 + \Omega_b^2 + \Omega_{V/M_m}^2) \right]^{1/2} \quad (2.16)$$

However, if Eq. 2.14 controls, then

$$\bar{v}_c = 3.5 \sqrt{\bar{f}'_c} \sqrt{1 + 0.002 \frac{\bar{P}}{\bar{b} \bar{h}}} \quad (2.17)$$

and

$$\Omega_{v_c} = \frac{1}{2} \left[\Omega_{f'_c}^2 + \left(\frac{0.002 \bar{P}/\bar{b} \bar{h}}{1 + 0.002 \bar{P}/\bar{b} \bar{h}} \right)^2 (\Omega_p^2 + \Omega_b^2 + \Omega_h^2) \right]^{1/2} \quad (2.18)$$

Figure 2.2 shows the coefficient of variation obtained from Eq. 2.14 for the cases of $\Omega_{V/M_m} = 0.10$ ($P = 0$) and $\Omega_{V/M_m} = 0.17$ ($P \neq 0$, $\Omega_p = 0.20$). Also included for comparison is Ω_{v_c} obtained by assuming $\Omega_{V/M_m} = 0$. Similarly, Ω_{v_c} as obtained from Eq. 2.18 is illustrated in Fig. 2.3 as a function of the axial load.

Test results [1, 81] indicate that the ACI equations underestimate the nominal shear strength for members with reinforcement ratios greater than about 1 to 1.5% and low Vd/M values, but may yield unconservative results for members with lower amounts of reinforcement. For the purpose of a reliability analysis, this bias must be corrected. This may be accomplished through the analysis of test data in the form of test versus calculated values of v_c (or V_c/bd). For the case in which v_c is calculated through Eq. 2.12, the bias and uncertainty of this equation are obtained on the basis of the data reported in References [1, 81]; the results are summarized in Table 2.2.

TABLE 2.2 BIAS AND UNCERTAINTY OF EQ. 2.12

Data Source	Case	Bias	Prediction Uncertainty
Rajagopalan et al. [81]; Table 2	$P = 0; 0.005 < \rho < 0.01$	0.96	0.16
ACI-ASCE Com. 326 [1]; Table 5.20	$P = 0, \rho > 0.01$	1.18	0.16
ACI-ASCE Com. 326 [1]; Table 7.4	$P \neq 0$	1.29	0.12

The bias and prediction uncertainties shown above were evaluated as the mean-value and c.o.v. of the ratio of test to calculated values of v_c . These may be illustrated using the test data of Ref. [81] as shown in Table 2.3, which gives

$$E [v_{c \text{ test}}/v_{c \text{ calc}}] = 0.96$$

$$\text{c.o.v. of } v_{c \text{ test}}/v_{c \text{ calc}} = 0.16$$

No data is available to evaluate the error in Eq. 2.14; thus, it will be assumed herein that the results obtained for Eq. 2.12 may be applied also for Eq. 2.14.

The mean and c.o.v. of V_t may be evaluated using Eqs. 2.11 through 2.18; obtaining

$$\bar{V}_t = [\bar{v}_c \bar{b} \bar{d} + \frac{\bar{d}}{\bar{s}} \bar{A}_v \bar{f}_y] \quad (2.19)$$

and

$$\begin{aligned} \Omega_{V_t}^2 = & \left[\frac{r_s}{r_s + 1} \right]^2 \left[\Omega_{v_c}^2 + (1 - c) \Omega_b^2 \right] + \\ & \left[\frac{1}{r_s + 1} \right]^2 \left[\Omega_s^2 + \Omega_{A_v}^2 + \Omega_{f_y}^2 \right] + \Omega_d^2 \end{aligned} \quad (2.20)$$

TABLE 2.3 SUMMARY OF TEST VERSUS CALCULATED VALUES OF v_c
FROM TABLE 2, REF. [81] ($0.005 < \rho < 0.01$)

Beam	v_c test (psi)	v_c^* calc. (psi)	v_c test/ v_c calc.
S-2	132	138	0.96
S-3	111	128	0.87
S-4	99	135	0.73
S-5	122	124	0.98
S-9	90	118	0.76
A2	157	137	1.15
A3	128	107	1.19
A4	132	124	1.07
V-a-19	112	117	0.96
V-a-20	117	122	0.96
VI-b-21	126	124	1.01
VI-b-23	133	134	0.99
IV-13A2	145	109	1.33
267	86	108	0.80
246	88	124	0.71
180	87	138	0.63
143	104	101	1.03
152	117	108	1.08
153	114	108	1.06
103	132	130	1.01
104	118	120	0.98
107	90	122	0.74
116	138	124	1.11
164	123	138	0.89
166	142	143	1.00
166	132	142	0.93
B56E2	103	92	1.13

* v_c calc. is based on Eq. 2.12 where Vd/M is assumed to be equal to d/a , in which a is the shear span.

where:

$$r_s = \frac{\bar{v}_c \bar{b} \bar{d}}{\frac{\bar{d}}{s} \bar{A}_v \bar{f}_y} \quad (2.21)$$

and

$$c = 2 - \frac{3.8 \sqrt{\bar{f}'_c}}{\bar{v}_c} \quad (2.22)$$

or

$$c = \frac{0.002 \bar{P}/\bar{b} \bar{h}}{1 + 0.002 \bar{P}/\bar{b} \bar{h}} \quad (2.23)$$

depending on whether Eq. 2.12 or 2.14 is used to estimate the shear capacity.

All but the c.o.v. of s and A_v have thus far been defined. Since stirrups are normally formed with smaller reinforcing bars, $\Omega_{A_v} = \Omega_{A_s}$ may be used. No data is available to evaluate the uncertainties in s , but as these pertain to errors in spacing the stirrups, it seems reasonable to assume that the uncertainties in s are about the same as those of d [33].

An inspection of the data shown in Refs. [1, 42] indicates that Eq. 2.11 underestimates the shear capacity of members with shear reinforcement, even after the bias in v_c has been removed. The bias and prediction uncertainty in V_t may be estimated from the ratio of observed to calculated values of V_t (or V_t/bd), after the bias of v_c has been removed.

The results are summarized in Table 2.4

TABLE 2.4 BIAS AND UNCERTAINTY OF EQ. 2.11 FOR V_t

Data Source	Case	Bias	Prediction Uncertainty
ACI-ASCE Com. 326 [1]; Table 6.1	$P = 0$	1.14	0.16
Haddadin, et al. [42]; Table 2	$P \neq 0$	1.23	0.11

It may be mentioned that the bias shown in Table 2.4 for the case of $P = 0$ has a tendency to decrease as the amount of web reinforcement increases. This is consistent with the observation that stirrups designed according

to ACI [4] tend to be more conservative for low percentages of web reinforcement [14].

The total c.o.v. of V_t is illustrated in Fig. 2.4 as a function of r_s . As the amount of web reinforcement increases (small r_s), the influence of v_c (and of Ω_{v_c}) on the total shear capacity becomes less important resulting in a smaller coefficient of variation [33]. The presence of axial load also decreases Ω_{V_t} (whereas it increases Ω_{v_c} ; see Fig. 2.2). This is mainly due to the difference in the bias and prediction uncertainty for this case, and the case of no axial load. It may also be observed from Fig. 2.4 that the c.o.v.'s for the total shear capacity obtained on the basis of Eqs. 2.12 and 2.14 agree very closely when the mean values of v_c from the two equations are equal.

CHAPTER 3

MODELING OF STRUCTURAL SYSTEMS FOR DYNAMIC ANALYSIS

3.1 Introduction

The necessary modeling of structural systems for dynamic response analysis, and the key parameters associated therewith are summarized herein. The variabilities in the dynamic properties of reinforced concrete structural systems, such as the natural frequencies, modal shapes, and damping, and the uncertainties associated with the mathematical idealization for purpose of dynamic analysis, are assessed.

Only framed structures without shear-walls are considered. It is assumed that the systems are stressed within the elastic limit and that no stiffness degradation occurs; thus, their behavior may be assumed to be approximately linearly elastic, even under load reversals.

3.2 The Eigenvalue Problem

3.2.1 General Formulation -- The eigenvalue problem of linear structural systems is formulated in terms of the characteristic equation

$$([K] - \lambda_i [M])\{\phi_i\} = 0 \quad (3.1)$$

where $[K]$ and $[M]$ are, respectively, the effective stiffness and mass matrices, λ_i is the i^{th} eigenvalue, and $\{\phi_i\}$ is the i^{th} eigenvector. The i^{th} natural frequency of the system is given by

$$\omega_i = \sqrt{\lambda_i} = \left[\frac{\{\phi_i\}^t [K] \{\phi_i\}}{\{\phi_i\}^t [M] \{\phi_i\}} \right]^{1/2} \quad (3.2)$$

and the participation factor corresponding to the i^{th} mode is

$$\gamma_i = \frac{\{\phi_i\}^t [M] \{I\}}{\{\phi_i\}^t [M] \{\phi_i\}} \quad (3.3)$$

where $\{I\}$ is a unit vector.

Since both the stiffness and mass matrices are random, the natural frequencies, modal shapes, and participation factors are, in general, also random scalars or random vectors. Several approximate methods for solving the eigenvalue problem of systems with random structural properties are available [43, 46, 88]. Further approximations for reinforced concrete buildings are possible; these are described in the sequel.

3.2.2 The Mass Matrix -- For practical applications, the total mass of a framed structure may be idealized as lumped masses concentrated at the floor levels. The mass concentrated at the i^{th} story level of a building may be expressed as $M_i = W_i/g$, in which W_i is the total load (dead + live load) acting at that level, and g is the acceleration of gravity. Since g may be assumed to be constant, it follows that

$$\overline{M}_i = \frac{\overline{W}_i}{g} \quad (3.4)$$

and

$$\Omega_{M_i} = \Omega_{W_i} \quad (3.5)$$

Similarly, the correlation coefficient between the masses of two floors, M_i and M_j is

$$\rho_{M_i, M_j} = \rho_{W_i, W_j} \quad (3.6)$$

The total load acting on the i^{th} floor may be expressed as

$$W_i = [D_i + L(A_i)] A_i \quad (3.7)$$

where D_i and $L(A_i)$ are the average dead and live load intensities, and A_i is the area of the floor under consideration. For statistically independent D and L it follows that

$$\overline{W}_i = [\overline{D}_i + \overline{L(A_i)}] A_i \quad (3.8)$$

and

$$\Omega_{W_i} = \left[\frac{\bar{D}_i^2 \Omega_{D_i}^2 + \overline{L(A_i)}^2 \Omega_{L(A_i)}^2}{(\overline{L(A_i)} + \bar{D}_i)^2} \right]^{1/2} \quad (3.9)$$

A plot of Ω_{W_i} as a function of the floor area, obtained on the basis of the dead load and live load models described in Chapter 4, is shown in Fig. 3.1. It may be observed from this figure that the results obtained with the two live load models (the white-noise and Peir's) are very close. Also it may be observed that Ω_{W_i} is not sensitive to the mean value of the dead load; at least, not for typical dead to live load ratios found in office buildings. This is especially true for large areas, as in the case of the total floor area of a building. Thus, a reasonable approximation is to take $\Omega_{W_i} = 0.12$ for all floors (see Fig. 3.1); this is assumed in the sequel.

The correlation coefficient between the total loads on two floors, W_i and W_j , is

$$\rho_{W_i, W_j} = \frac{\text{COV} [W_i, W_j]}{\sigma_{W_i} \sigma_{W_j}} \quad (3.10)$$

If the areas of the two floors are approximately the same, and considering the dead load for the two floors to be equal and perfectly correlated (but statistically independent of the live load) it follows that

$$\rho_{W_i, W_j} = \frac{\bar{D}^2 \Omega_D^2 + \text{COV} [L(A_i), L(A_j)]}{\bar{D}^2 \Omega_D^2 + \overline{L(A)}^2 \Omega_{L(A)}^2} \quad (3.11)$$

in which $A_i = A_j = A$ and $D_i = D_j = D$.

Expressions for the $\text{COV} [L(A_i), L(A_j)]$ (and for ρ_{W_i, W_j}), obtained with the load models described in Chapter 4, are given in Appendix C. Fig. 3.2 shows ρ_{W_i, W_j} obtained with Eq. 3.11 as a function of the floor area. It is observed that ρ_{W_i, W_j} becomes fairly constant for large areas and that it increases with \bar{D} . In particular, it becomes of the order of 0.9 for $\bar{D} \approx 100$ psf and $A \geq 2000$ ft². Since dead load intensities in office buildings are typically of the order of 100 psf or more, and the total floor areas are commonly larger than 2000 ft², it is reasonable to assume

that the total load in two different floors of a building are highly correlated. Accordingly, for the purpose of this study, the total loads on two different floors will be considered to be perfectly correlated.

On the basis of the above discussions, the mass matrix may be expressed as

$$M = M^* [\bar{M}] \quad (3.12)$$

where M^* is a random variable with mean equal 1.0 and c.o.v. $\Omega_{M^*} = \Omega_M = 0.12$, and $[\bar{M}]$ is a deterministic matrix consisting of the mean values of the floor masses obtained from Eq. 3.4.

3.2.3 The Stiffness Matrix -- The stiffness matrix of a structural system is obtained from the stiffness matrices of its elements. For the case of framed structures (without shear walls) of moderate height, the effects of axial and shear deformations are usually unimportant and may be neglected. Thus, the stiffness matrix of the i^{th} element of the system may be expressed as

$$K^i = \frac{EI_i}{L_i} \begin{bmatrix} 12 & 6L & -12 & 6L \\ 6L & 4L^2 & -6L & 2L^2 \\ -12 & -6L & 12 & -6L \\ 6L & 2L^2 & -6L & 4L^2 \end{bmatrix}$$

where EI_i is the equivalent flexural rigidity, and L_i the length of the element. In general, any uncertainty in L is negligible. Hence, the only uncertainty in the element stiffness matrix is associated with the flexural rigidity EI .

The ij^{th} stiffness coefficient of the system, k_{ij} , may be expressed as

$$k_{ij} = \sum_{\ell=1}^n (C_{\ell} EI_{\ell}) \quad (3.13)$$

where C_{ℓ} is a constant (i.e., $12/L_{\ell}^3$, $4/L_{\ell}^2$, ..., etc.) and EI_{ℓ} is the flexural rigidity of the ℓ^{th} element connecting into the i^{th} joint.

In order to estimate the statistics of k_{ij} through Eq. 3.13, expressions for EI_{ℓ} are required. In formulating these, it is assumed that the members of a structure subjected to earthquake loading may be stressed up to, but not exceeding, their yield capacity. It is further assumed that representative equivalent rigidities, of reinforced concrete members, even for the case of load reversals, may be obtained from the ratio of the yield moment capacity to yield curvature at the critical section [12], i.e.,

$$EI = \frac{M_y}{\phi_y} \quad (3.14)$$

In computing the yield moment and curvature, a linear strain and stress distribution, as shown in Fig. 3.3, is assumed. On this basis, it follows that

$$M_y = C_c(d' - \frac{c}{3}) + T_s(d - d') + P(\frac{d - d'}{2}) \quad (3.15)$$

and

$$\phi_y = \frac{\epsilon_y}{d - c} = \frac{f_y}{E_s(d - c)} \quad (3.16)$$

where:

$$c = \{ -[\rho'(n-1) + \rho''n] + \sqrt{[\rho'(n-1) + \rho''n]^2 + 2[\rho'(n-1) d'/d + \rho''n]} \} d$$

$$C_c = \frac{1}{2} b \frac{c^2}{d - c} \frac{f_y}{n}$$

$$T_s = A_s f_y$$

$$n = E_s/E_c = \text{modular ratio}$$

$$\rho'' = \frac{A_s + P/f_y}{bd}$$

Equations 3.15 and 3.16 are valid as long as the stress-strain curve for concrete is linear (i.e., for $f_{c \max} \leq 0.7 f'_c$), and the stress in the compression reinforcement is below its yield stress. However, reasonable values of EI can be obtained from the above formulation, even for cases in

which these conditions are violated. This may be observed from Fig. 3.4 where values of EI calculated by Eqs. 3.14 through 3.16 are plotted together with moment-curvature relationships obtained by a more exact method [80]. The only exception occurs for columns with high axial loads and low reinforcement ratios. This is not of major concern in earthquake-resistant structures, because most columns found in reinforced concrete buildings that are designed to resist earthquake motions are subjected to low axial loads (i.e., less than the "balance" load), except in the case of very tall buildings.

The statistics of EI may be found from Eqs. 3.14 through 3.16. For these purposes, expressions for the partial derivatives of EI with respect to the basic variables are needed; these are shown in Appendix D. The modulus of elasticity of steel is assumed to be constant -- equal to 29,000 ksi. The statistics of the modulus of elasticity of concrete are obtained, based on the equation of ACI 318-71 [4] for normal weight concrete; i.e.,

$$E_c = 57000\sqrt{f'_c}$$

from which,

$$\bar{E}_c = 57000\sqrt{\bar{f}'_c}$$

and

$$\Omega_{E_c} = \Omega_{f'_c}/2$$

The variabilities of the other variables involved in Eqs. 3.14 through 3.16 are summarized in Table 2.1 [33].

The coefficient of variation of EI is shown in Fig. 3.5a for the case of symmetrically doubly reinforced beams as a function of the reinforcement ratio $\bar{\rho}$. Similar information is summarized in Fig. 3.5b for unsymmetrically doubly reinforced beams as a function of the ratio of compressive to tensile reinforcement, $\bar{\rho}'/\bar{\rho}$; and in Fig. 3.5c for symmetrically reinforced concrete columns as a function of the ratio of the applied axial load to the balanced load, \bar{P}/\bar{P}_B . It may be observed from these figures that the c.o.v. of EI is not very sensitive to $\bar{\rho}$ or $\bar{\rho}'/\bar{\rho}$, or to \bar{P}/\bar{P}_B when $\Omega_p < 0.30$. In computing the equivalent flexural rigidity of reinforced concrete columns, only the axial load due to the dead and live loads is considered. From the load

models to be described in Chapter 4, it may be shown that Ω_p is less than 0.30 for typical dead to live load ratios found in office buildings. Under these circumstances, a reasonable approximation is to take a single value of the c.o.v. of EI for all members. Based on Figs. 3.5a through 3.5c, a value around 0.20 appears reasonable.

Before proceeding further, it is important to examine and assess any imperfection underlying the estimation of EI by Eqs. 3.14 through 3.16. For this purpose, consider a typical flexural member of a reinforced concrete frame subjected to anti-symmetric bending (as in the case of a structure subjected to earthquake motions). Also, take a simple beam subjected to a concentrated load at mid-span (these are shown in Fig. 3.6). It may be seen that the end moment-end rotation relationship of the anti-symmetric member is the same as the ratio of the mid-span moment to the mid-span deflection divided by half the span length of the simple beam (see Fig. 3.6). It follows that the moment-rotation relationship of anti-symmetric members can be evaluated empirically by studying the test data for simple beams [12].

Similarly, the assessment of uncertainties in the equation for the rigidity of anti-symmetric members may be based on test data obtained from simple beams loaded at mid-span. In this regard, it may be observed that the ratio of measured to calculated values of EI is the same as the ratio of calculated to measured values of the mid-span deflection corresponding to the first yielding of the tension reinforcement. This may be shown as follows: let P_y be the load causing first yielding in the tension reinforcement and d_y the corresponding measured mid-span deflection. Then, an estimate of the true (or measured) equivalent flexural rigidity is given by

$$EI = \left(\frac{P_y}{d_y} \right) \frac{L^3}{48} \quad (3.17)$$

Similarly, if \hat{EI} is the theoretical flexural rigidity (obtained, for example, from Eqs. 3.14 to 3.16), the calculated mid-span deflection is

$$\hat{d}_y = \frac{P_y}{\hat{EI}} \frac{L^3}{48} \quad (3.18)$$

Then, it follows that

$$\frac{EI}{\hat{EI}} = \frac{\hat{d}_y}{d_y} \quad (3.19)$$

On the basis of the above discussion, the uncertainty associated with the equation for EI is estimated by examining test data for simple beams, in the form of calculated versus test values of the mid-span deflection at first yielding of the tension reinforcement.

Mattock [59] and Corley [29] tested, respectively, 31 and 40 beams with simple supports and loaded at mid-span. No axial load was applied to the test specimens. The theoretical yield deflections were obtained based on the idealized bending moment diagram developed in Appendix IV of Ref. [59]. The results obtained from these investigations are summarized in Table 3.1.

TABLE 3.1 IMPERFECTIONS IN THE ESTIMATION OF EI

Data Source	No. of Tests	Bias	Prediction Uncertainty
Beams with Concentrated Loads			
Mattock [59]	31	0.79	0.20
Corley [29]	40	0.64	0.20
McCollister, et al. [63]	19	0.79	0.15
Burns, et al. [26]	17	0.81	0.04
Yamashiro & Siess [103]	12	0.93	0.14
All data	119	0.76	0.21
Beams with Uniform Load			
ACI Com. 435 [2]	30	1.08	0.11
Yu & Winter [104]	90	1.05	0.14
Branson [25]	107	1.02 (with top reinforcement)	0.22
Branson [25]		0.95 (without top reinforcement)	0.12

Yamashiro and Siess [103] investigated the moment-rotation characteristics of reinforced concrete members subjected to bending, shear, and axial load. The axial load varied from 0 to about 60% of the balanced load. The results of tests performed by Burns, et al. [26] and by McCollister, et al. [63] were also included. The type of members tested are shown in Fig. 3.7. In computing the yield deflections, a linear curvature distribution along the span was used. The curvature distribution for the stub was estimated empirically. These results are also summarized in Table 3.1. If the deformation in the stub is neglected, the bias shown in Table 3.1 is reduced by about 20% and the prediction uncertainty remains approximately the same.

Data on uniformly loaded members is also included for comparison purposes [2, 25, 104]; these included some tests of continuous and T-beams. Theoretical deflections were estimated using the fully-cracked sections for simple beams, and the average moment-of-inertia of the positive and negative moment regions for continuous beams. The results obtained from these tests are also shown in Table 3.1.

The evaluation of the bias and prediction uncertainty of EI, as shown in Table 3.1, may be illustrated using the data of Mattock [59], which are summarized below in Table 3.2; this set of data gives

$$E [d_{y \text{ calc.}} / d_{y \text{ test}}] = \text{bias} = 0.79$$

$$\text{c.o.v. of } d_{y \text{ calc.}} / d_{y \text{ test}} = \text{prediction uncertainty} = 0.20$$

It may be observed from Table 3.1 that the equation bias obtained on the basis of the uniformly loaded beams is clearly different from those of simple beams subject to concentrated loads applied at mid-span. One explanation of this behavior is given in Reference [103]. It is based on the observation that, in regions with high shear and moments, the cracks in reinforced concrete members are inclined rather than vertical, causing concentrated rotations. Since the behavior of structural members subjected to earthquake loads is closer to that of beams under concentrated loads, the results for uniformly loaded beams will be ignored.

TABLE 3.2 SUMMARY OF TEST DATA FROM MATTOCK [59]

Beam	d_y test	d_y calc.	d_y calc./ d_y test
A1	0.098	0.065	0.67
A2	0.374	0.272	0.73
A3	1.100	1.116	1.01
A4	0.119	0.070	0.59
A5	0.321	0.297	0.93
A6	1.249	1.203	0.96
B1	0.230	0.143	0.62
B2	0.523	0.514	0.98
B3	0.244	0.147	0.60
B4	0.760	0.582	0.77
C1	0.112	0.068	0.60
C2	0.327	0.274	0.84
C3	1.117	1.050	0.94
C4	0.147	0.079	0.54
C5	0.448	0.336	0.75
C6	1.452	1.205	0.83
D1	0.203	0.135	0.66
D2	0.635	0.550	0.87
D3	0.278	0.160	0.58
D4	0.784	0.648	0.83
E1	0.143	0.085	0.59
E2	0.411	0.344	0.84
E3	1.460	1.348	0.92
F1	0.134	0.083	0.62
F2	0.360	0.335	0.93
F3	1.300	1.398	1.08
G1	0.240	0.173	0.72
G2	0.770	0.687	0.89
G3	0.270	0.165	0.61
G4	0.840	0.731	0.87
G5	0.660	0.659	1.00

There are differences between the bias, and the prediction uncertainty, obtained through simple-beam tests from those for beams with stubs (see Table 3.1). However, it is believed that this difference is mainly due to the wider range of variables considered by Mattock and Corley, and by the use of an empirical curvature distribution in the stub used by Yamashiro and Siess. Also, it is recognized that the presence of the stub influences the location of the failure section [103].

The information of these investigations was combined in various ways (such as lumping all data together, computing simple or weighted averages of the means and c.o.v. obtained by the various investigators, etc.). On the basis of the results summarized in Table 3.1, a bias of 0.76 and prediction uncertainty of 0.20 in the estimation of EI appear reasonable.

The analysis of EI, up to this point, is based on the assumption that a member has been subjected to stresses close to its yield capacity. If this is not the case, equivalent flexural rigidities calculated on the basis of the above formulation might not be applicable; in particular, the mean value of the member stiffness may be greatly underestimated.

On the basis of these results and on those shown in Figs. 3.5a through 3.5c, the total c.o.v. of EI of reinforced concrete beams and columns is

$$\Omega_{EI} = \sqrt{(0.20)^2 + (0.20)^2} = 0.28 \quad (3.20)$$

Even if the stiffness of individual members can be estimated correctly, there may be inaccuracies in the stiffness matrix of complete structures. This is due, in part, to the idealizations that are usually made in constructing the stiffness matrix (for example, taking the center-to-center distance between supports as the effective length of the elements, neglecting shear deformations in the joints, etc.), and to the fact that members in a structure do not behave exactly the same as simple beams.

The imperfections in the estimation of k_{ij} may be assessed by systematically comparing stiffness coefficients obtained experimentally and theoretically (i.e., by Eq. 3.13 through 3.16). For this purpose, the results of a series of tests on one-story portal frames [13, 15, 16, 40, 92] were examined. The stiffness matrices of the frames were constructed using equivalent rigidities calculated on the basis of Eqs. 3.14 through 3.16. The center-to-center distances were used as the effective length of the members. The results of the investigations were reported in the form of load-deformation (P- Δ) diagrams, thus comparisons were made by plotting the theoretical stiffness on the P- Δ diagrams.

In general, for the case of first loading, the agreement between the theoretical stiffness and the ones obtained by joining the origin and the points in which first yielding occurs on the experimental P- Δ curves was good. There was no systematic bias between the theoretical and the experimental results, once the bias in EI is corrected. However, in some cases, reduction in the stiffness of the frame was observed for cyclic loading. Most of the reduction took place in the first few cycles and then stabilized as the number of cycles increased [16, 92]. This behavior was also observed by Ruiz and Winter [87] in tests of simply-supported beams to load reversals. This is due, mainly, to the loss of bond between the reinforcement and the concrete, and to the redistribution of cracks along the length of the member.

A two-story frame tested by Hidalgo and Clough [48] was also examined. The structure was about 1/4 scale of a typical 2-story building. The flexibility matrix was determined experimentally and then inverted to obtain the stiffness matrix. The results obtained by comparing the theoretical and experimental results were similar to those of the one-story frame described above.

On the basis of the results above, suitable values for the bias and prediction uncertainty in the formulation of the stiffness matrix of reinforced concrete structural systems are estimated to be 1.0 and 0.20, respectively. In this regard, it may be mentioned that it has been assumed that no stiffness degradation occurs as a result of bond and shear stresses; if this is not the case, additional bias correction may be necessary.

In order to estimate the statistics of the stiffness coefficients from Eq. 3.13, the correlation coefficients (or covariance) between the equivalent rigidities of the members must first be determined. Because of common construction and workmanship, it is likely that the properties of the members in a given structure would be highly correlated. Thus, a plausible approximation is to assume that these are perfectly correlated. It follows then that

$$\bar{k}_{ij} = \sum_{\ell=1}^n (C_{\ell} \bar{EI}_{\ell}) \quad (3.21)$$

and

$$\Omega_{kij}^2 = (0.20)^2 + \frac{1}{k_{ij}^2} \left[\sum_{\ell=1}^n (c_{\ell} \overline{EI}_{\ell}) \Omega_{EI_{\ell}} \right]^2 \quad (3.22)$$

Then, in light of Eq. 3.20

$$\Omega_{kij} = \sqrt{(0.20)^2 + (0.28)^2} = 0.34, \text{ for all } i,j \quad (3.23)$$

On these bases, the stiffness matrix of a structural system may be expressed as

$$[K] = K^* [\overline{K}] \quad (3.24)$$

in which K^* is a random variable with mean $\overline{K^*} = 1.0$ and c.o.v. $\Omega_{K^*} = \Omega_{kij} = 0.34$ (for all i,j), and $[\overline{K}]$ is a deterministic matrix consisting of the mean stiffness coefficients obtained with the mean flexural rigidities of the members. Eq. 3.24 implies that the stiffness coefficients in $[K]$ are constant factors of each other.

3.2.4 Uncertainties in Natural Frequencies and Modal Shapes --

It was shown in Sect. 3.2.3 that the floor masses, as well as the member stiffnesses, may be assumed to be perfectly correlated and with equal coefficients of variation. Since the modal shapes depend only on the relative value of these quantities, it follows (as shown in Appendix E) that the modal shapes are deterministic vectors, depending only on the means of the mass and stiffness matrices. Moreover, replacing $[M]$ with $M^*[\overline{M}]$ in Eq. 3.3, it may be observed that the participation factor is also a deterministic quantity.

The i^{th} natural frequency is found by substituting Eqs. 3.12 and 3.24 into Eq. 3.2; yielding

$$\omega_i = \left[\frac{\{\phi_i\}^t [\overline{K}] \{\phi_i\}}{\{\phi_i\}^t [\overline{M}] \{\phi_i\}} \right]^{1/2} \left[\frac{K^*}{M^*} \right]^{1/2} \quad (3.25)$$

from which it follows that the mean and total coefficient of variation of ω_i are, respectively,

$$\bar{\omega}_i = \left[\frac{\{\phi_i\}^t [\bar{K}] \{\phi_i\}}{\{\phi_i\}^t [\bar{M}] \{\phi_i\}} \right]^{1/2} \quad (3.26)$$

and

$$\Omega_{\omega_i} = \left[(0.10)^2 + \frac{1}{4} (\Omega_{K^*}^2 + \Omega_{M^*}^2) \right]^{1/2} \quad (3.27)$$

where an additional uncertainty of 0.10 is ascribed to the estimation of ω_i reflecting the influence of non-structural elements, soil-structure interactions, etc. With $\Omega_{K^*} = 0.34$ and $\Omega_{M^*} = 0.12$, Eq. 3.27 yields $\Omega_{\omega_i} = 0.21$.

3.3 Analysis of Uncertainty in Structural Damping

3.3.1 Introduction -- Damping is the third important dynamic property of structures. Unlike the natural frequencies and modal shapes, the damping of the structure cannot be evaluated on the basis of the damping in the individual components. Perhaps the only way to represent the energy dissipation characteristics of structural systems is by means of equivalent damping, of the viscous type (denoted hereafter by β), obtained experimentally through dynamic tests** of full-scale structures. Damping depends on the stress level (and on the cracking level, in the case of reinforced concrete members [62, 102]). Thus, non-destructive and low-amplitude vibration tests will produce damping values that underestimate the true energy dissipation capacity of structures subjected to intense excitations. Since ultimately it is the response of structures subjected to strong earthquake motions that is of interest, the results of small vibration tests should be modified when applied to structures subjected to high seismic excitations.

It is the purpose here to analyze the damping of reinforced concrete structures subjected to earthquakes. It is assumed that the structures are stressed up to but not exceeding their yield capacities. Test results on full-scale and model structures of reinforced concrete and steel-

** The term "dynamic test" is used here to indicate that a structure has been excited dynamically either by artificial means, or by natural causes (see Ref. [51]).

reinforced concrete are the basis for these evaluations.

The dynamic tests included in this study are summarized below. The test procedures are well known or are reported elsewhere (see for example [51]).

Full-Scale Structures

Forced Vibration Tests: (Low to very low amplitudes)

Rotating Eccentric Weight Exciter

Man-excited Vibration

Transient Vibration Tests: (Low to high amplitudes)

Micro-tremors

Wind-excited Vibrations

Blast and Explosion

Natural Earthquakes

Model Structures

Forced Vibration Tests

Rotating eccentric weight exciter

Shaking table

Forced-static Tests

3.3.2 Data from Full-Scale Structures -- A number of forced vibration tests of actual structures using rotating eccentric weight exciters have been reported [6, 19, 34, 38, 39, 55, 70, 73, 79, 84, 85, 93, 98]. Damping values were estimated from the resonance curves. Results of such tests are summarized in Fig. 3.8, where the estimated damping coefficients (for the 1st mode) are plotted against the respective natural frequencies of the test structures (the natural frequencies are determined from the tests). The mean value of β from all the tests was 6.0% of critical and the corresponding c.o.v. is 0.62 (from 67 measurements). The dispersion of the data is immediately apparent from Fig. 3.8. Certain trend between frequency and damping may be observed -- damping appears to decrease with increasing period of the structure. The same trend was also observed by Tanaka, et al. [98]. What is striking is the fact that damping values as high as 10% (or more) of critical were measured under very small vibrations. It may be observed, however, that the results of references [6, 19, 70], obtained from tests conducted before 1960, gave

consistently higher values of damping than more recent tests.

If the damping factors from these earlier tests were removed, the resulting plot would be as shown in Fig. 3.9. The values enclosed by dotted lines in Fig. 3.9 involve considerable soil-structure interaction [84, 85], which may explain the high damping values. If these results are also ignored, damping values higher than 5% were obtained in only two cases (see Fig. 3.9). The remaining data give a mean value of 2.73% of critical and a coefficient of variation of 0.57 (if the data from Refs. [84, 85] are included, then $\bar{\beta} = 3.59\%$ and $\delta_{\beta} = 0.71$). It may also be observed from Fig. 3.9 that the correlation between frequency and damping, observed earlier in Fig. 3.8, no longer exists. It is believed that damping values obtained from tests of old structures are not directly applicable to modern structures which are lighter and more flexible than older constructions. In this light, the data shown in Fig. 3.9 is probably the most representative of the structural damping of modern reinforced concrete buildings subjected to low-amplitude excitations.

Man-excited vibration tests are reported in References [100, 102]. The vibration amplitudes were extremely small. Damping was also calculated from the resonance curve. The mean and c.o.v. obtained from 6 measurements were 1.22% of critical and 0.19, respectively. As expected, very low damping factors were reported.

Tanaka [98] reported damping values estimated from the response of reinforced concrete and steel-reinforced concrete structures to micro-tremors. Damping was estimated by means of the power spectral density of the response. The mean damping, estimated from 30 measurements, was 2.7% of critical with a coefficient of variation of 0.43.

A 10-story building subjected to wind excitations was studied by Ward and Crawford [102]. The damping, estimated using the power spectral density, was 1% of critical in both translational directions.

Damping coefficients of 4 buildings, ranging from 20 to 30 stories, were calculated by Blume [18] from the response of structures to nuclear explosions. The modal damping values were calculated by reconciling the empirical and theoretical responses while keeping the elastic properties of the structure constant. From 30 such measurements, a mean value of 5.67% of critical and a c.o.v. of 0.51 were obtained. Damping coefficients

estimated by this procedure are naturally affected by errors in the estimation of the natural frequencies and modal shapes of the systems.

Hart, et al. [44, 45], Tanaka, et al. [98] and Tajimi [97] calculated damping values from the response of structures to natural earthquakes using Fourier-transform techniques, power spectral densities, and auto-correlation analysis, respectively. Seven buildings subjected to the San Fernando Earthquake were studied by Hart, et al. Estimated damping coefficient for the first mode ranged from 2.8 to 16.4% of critical and observed maximum ground accelerations varied from 0.10 to 0.27 g. Five of these buildings were analyzed in a separate study [101]; it was found that four of these buildings responded inelastically during the earthquake, whereas one responded within the elastic limit. An equivalent damping of 10% of critical was calculated for this building by reconciling the theoretical and measured responses against 4.9% estimated by Hart. No further information was found on the remaining two buildings; however, the undamped response spectra calculated by Hart for these two buildings seem to indicate that the response could have been within the elastic range. The mean and coefficient of variation of the equivalent damping obtained from the last three buildings were 4.10% and 0.17. If the data of all buildings is considered, $\bar{\beta}$ becomes 7.39 and $\delta_{\beta} = 0.58$.

The buildings studied by Tanaka, et al. [98] (17 in all) under natural earthquakes were also analyzed under forced vibration and micro-tremors (the damping values calculated from these tests were already discussed). This reference, therefore, is useful in comparing damping values for the same building under different types of excitations. The observed maximum ground acceleration ranged from 0.062 g to 0.22 g. $\bar{\beta}$ (obtained from 30 observations) is 3.33%, compared with 3.13% from forced-vibration tests and 2.70% from micro-tremors; whereas $\delta_{\beta} = 0.50$, against 0.55 and 0.43 from the forced-vibration tests and micro-tremors.

Tajimi [97] measured the response of one building to the Matsushiro earthquakes. The maximum ground acceleration of one of the earthquakes was 0.14 g. Damping estimates from different response records yielded values ranging from 1.6 to 5.7% of critical for the first translational mode. A number of comparisons between the measured and calculated responses based on modal analysis yielded values between 3 and 5% of critical.

The various results described above are summarized in Table 3.3 below.

TABLE 3.3 SUMMARY OF DAMPING OF FULL-SCALE STRUCTURES

Testing Procedure	$\bar{\beta}$	Variability, δ_{β}	No. of Tests
Man-excited Vibrations	1.22	0.19	6
Micro-Tremors	2.65	0.45	32
Rotating Eccentric Weight Exciter	2.73	0.57	30
Natural Earthquakes	3.52	0.45	37
Blast and Explosions	5.67	0.51	30

These results seem to confirm the common belief that damping increases with the level of excitation.

3.3.3 Damping of Model Structures -- Tests on model structures may be used to establish a quantitative relation between damping and excitation level. With this information, damping values obtained from low-amplitude vibration tests of full-scale structures may be used to estimate the damping expected at higher excitations.

McCafferty and Moody [62] investigated the dynamic characteristics of reinforced concrete beam-column specimens at four levels of cracking. Experimental damping values were as follows: 1.7% of critical for uncracked specimens, 2.4% for minor cracks, 2.7% for intermediate cracks, and a wide range of values (from 2.4% to 6%) for severely cracked specimens.

Hidalgo and Clough [48] tested a two-story reinforced concrete model structure (1/4 scale) representing a typical small apartment or office building. The structure was subjected to various amplitude levels by means of a shaking table. Damping coefficients obtained from these tests varied from 1.0% for the uncracked structure to 3.7% just before the structure yielded. Damping was calculated from free vibration tests.

Shiga, et al. [92] tested two types of models: (1) space frames (1/2 - 1/4 scale) which were single-story and two-story reinforced concrete bents, loaded with a small-amplitude exciter; (2) reinforced concrete

portal frames which were subjected to large oscillations on a vibrating table. Damping values of the single-story space frames were calculated through free vibration and forced vibration tests. The free vibration tests yielded damping values between 1 and 1.5% (using the logarithmic decrement of the vibration), whereas damping factors between 1 and 3% were observed in the forced vibration tests. 1% damping was obtained through forced vibration of the two-story space frames when the deflection was smaller than the cracking deflection. Equivalent damping factors for the reinforced portal frames calculated from the area of the hysteresis loop (corresponding approximately to the yield deflection) were estimated to be of the order of 8% of critical.

Using a similar procedure, Shiga and Ogawa [91] found damping coefficients of the order of 2.5% of critical for reinforced concrete portal frames at amplitudes of vibration that are approximately equal to 70% of the yield deflection.

3.3.4 Summary and Conclusions on Damping -- The main observations and conclusions obtained from the above analysis of reported data are as follows:

(a) Equivalent damping values vary, on the average, proportionally to the amplitude of vibration.

(b) In some cases, damping appears to decrease with the natural period [98]; however, when data from different sources are lumped together this effect practically vanishes. Thus, damping and natural periods may be assumed to be statistically independent.

(c) The coefficient of variation of damping obtained from different tests are all of the order of 0.50. Thus, $\delta_{\beta} = 0.50$ will be assumed for purposes of this study.

(d) By comparing the means and individual values of β obtained from different dynamic tests, it appears that average equivalent damping factors higher than about 4 or 5% of critical are difficult to obtain for reinforced concrete structures within the elastic range (unless the influence of non-structural elements or soil-structure interaction is important). Thus, $\bar{\beta} = 4\%$ of critical is assumed in the following. It is easy to see that there could be significant error in this value; to account

for this error, a prediction uncertainty of 0.25 is assumed,

(e) Information concerning damping in the second and third modes is reported in References [18, 39, 44, 45, 48, 73, 79, 84, 85, 97]. However, reliable estimates of the statistics of the damping factors for the higher modes could not be obtained from these data; thus, it is assumed in the following that the damping coefficients for the first mode are also applicable for the higher modes.

CHAPTER 4

ANALYSIS OF LOAD MODELS AND LOAD EFFECTS

4.1 Introductory Remarks

Structures are subjected to many types of loads; they may include permanent loads from the weight of the structure and permanent fixtures, live loads from occupancy and movable furnitures, lateral loads induced by wind and earthquakes, stresses due to temperature, differential settlement, creep, shrinkage, etc. The total load effect may be due to many possible combinations of such loads.

A statistical treatment of the problem of load combination requires a suitable definition of the loads under consideration. Loads are, in general, time and space dependent. For studying their combinations, the variability with time and space must be considered. (A general treatment of load combination is given by Borges and Castenheta [24].

In the following, dead, live, and earthquake loads are considered. It is assumed that the different loads are mutually statistically independent and also independent of the resistance. The uncertainty in the estimation of future earthquake intensities is not considered; i.e., the reliability analysis performed herein is for structures subjected to earthquakes of prescribed intensities.

4.2 Dead Load

The dead load consists of the weights of the structure and permanent installations. The weight of a structure is obtained from its geometry and depends on the unit weight of the elements and their dimensions.

The weight of a reinforced concrete member may be expressed as

$$W_D = \text{Length} (w_c A_c + w_{st} A_{st}) \quad (4.1)$$

where w_c and w_{st} are the unit weights of the concrete and the reinforcement, and $A_c = bh$ and A_{st} are their respective areas. The basic variability of W_D can be easily calculated from Eq. 4.1; however, with the typical reinforcement ratios found in modern reinforced concrete buildings, a small

error in the estimation of Ω_{W_D} is introduced if the variability in the weight of the reinforcement is neglected. Moreover, any uncertainty in the member length is negligible in comparison with those in w_c and A_c . Thus, an approximate expression for Ω_{W_D} is given by [33]

$$\Omega_{W_D} = \sqrt{\Omega_{w_c}^2 + \Omega_b^2 + \Omega_h^2} \quad (4.2)$$

With the values for Ω_b and Ω_h estimated in Ref. [33] (as shown in Table 2.1) and $\Omega_{w_c} = 0.03$ [23], we obtain $\Omega_{W_D} = 0.70$.

Additional uncertainties arise from the weight of non-structural elements such as partitions, etc. [23]. These uncertainties can only be estimated subjectively and must be combined with Ω_{W_D} to obtain the total uncertainty in the dead load intensity, Ω_D . These additional uncertainties could be of the order of 0.10 [33]. Then Ω_D is found to be = $\sqrt{(0.07)^2 + (0.10)^2} = 0.12$. The mean dead load can usually be estimated fairly accurately; thus, any bias would be negligible.

The theoretical dead load effect, S_D , is obtained by translating the dead load intensity, D , into the desired load effect through structural analysis. Conceptually, this may be expressed by

$$S_D = c_D D \quad (4.3)$$

where c_D is an influence coefficient. The mean value of S_D is then

$$\bar{S}_D = c_D \bar{D} \quad (4.4)$$

and its c.o.v. is

$$\Omega_{S_D} = \sqrt{(0.10)^2 + \Omega_D^2} = 0.16 \quad (4.5)$$

An uncertainty of 0.10 is assumed for possible error in the method of static analysis.

4.3 Live Load

4.3.1 Introduction -- Live loads are those arising from movable equipment and fixtures, and other non-permanent loads. A number of

studies concerning live loads have been performed. Surveys of these studies are available in the literature (e.g., Heaney [47] and Peir [75]).

The temporal variation of live loads has long been recognized. A typical representation of temporal variation is shown in Fig. 4.1 [75, 76]. This can be decomposed into two parts; namely, a sustained load which exists on the floor for a long time, and the extraordinary (transient) load which has a relatively high intensity but whose load duration is very short. The sustained live load consists of the normal working personnel, furniture, equipment, etc. This portion of the total live load may have abrupt changes from time to time due to changes in tenants of the floor area, or to changes in the use of the floor area. Examples of extraordinary loads include large groups of people occupying a floor area during special occasions, concentration of furniture in a room during remodeling, etc.; its duration could be only for a few hours or a few days.

The probability of simultaneous occurrence of a strong earthquake and high extraordinary load is small and, therefore, may be neglected; for this reason, only the sustained portion of the live load will be considered.

4.3.2 Live Load Models -- Denote the sustained live load [75, 76] as

$$\omega_L(x,y) = m_L + \gamma_{bld} + \gamma_{flr} + \epsilon(x,y) \quad (4.6)$$

where $\omega_L(x,y)$ is the load intensity at a location (x,y) in a given floor; m_L is the mean live load (e.g., office occupancy); γ_{bld} and γ_{flr} are zero-mean statistically independent random variables representing, respectively, the variation of the average load from one building to another, and from one floor to another (within a given building); whereas $\epsilon(x,y)$ is a zero-mean random variable, statistically independent of the γ terms, representing the spatial variation of the load intensity.

In general, $\epsilon(x,y)$ has a non-zero spatial correlation; i.e., $\text{COV}[\epsilon(x_0,y_0) \epsilon(x_1,y_1)] \neq 0$. Different forms of the covariance between $\epsilon(x_0,y_0)$ and $\epsilon(x_1,y_1)$ may be used; $\epsilon(x,y)$ may be assumed to be a "white noise" process, in which case the correlation between the values of ϵ at two different points is zero. In this latter case,

$$\text{COV} [\varepsilon(x_0, y_0) \varepsilon(x_1, y_1)] = \begin{cases} 0 & \text{for } (x_0, y_0) \neq (x_1, y_1) \\ \sigma_\varepsilon^2 & \text{for } (x_0, y_0) = (x_1, y_1) \end{cases} \quad (4.7)$$

Peir [75] proposed two forms for the covariance function. For two points (x_0, y_0) and (x_1, y_1) on the same floor

$$\text{COV} [\varepsilon(x_0, y_0) \varepsilon(x_1, y_1)] = \sigma_{sp}^2 e^{-r^2/d} \quad (4.8)$$

where d is a constant to be estimated, and r is the distance between the two points. For (x_0, y_0) and (x_2, y_2) located on different floors

$$\text{COV} [\varepsilon(x_0, y_0) \varepsilon(x_2, y_2)] = \rho_m \sigma_{sp}^2 e^{-r^2/d} \quad (4.9)$$

where ρ_m is the correlation between the spatially varying load intensities at two points that are one above the other.

Let $W_L(A_t)$ be the total live load acting over a given area, A_t , i.e., $W_L(A_t) = \int_{A_t} \omega_L(x, y) dA$, and $L(A_t)$ is the average unit load, or $L(A_t) =$

$W_L(A_t)/A_t = (1/A_t) \int_{A_t} \omega_L(x, y) dA$. The mean and variance of the unit load

are

$$\overline{L(A_t)} = E \left\{ \frac{1}{A_t} \int_{A_t} \omega_L(x, y) dA \right\} = \frac{1}{A_t} \int_{A_t} E [\omega_L(x, y)] dA \quad (4.10)$$

and

$$\begin{aligned} \sigma_{L(A_t)}^2 &= \text{VAR} \left\{ \frac{1}{A_t} \int_{A_t} \omega_L(x, y) dA \right\} = \\ &= \frac{1}{A_t^2} \iint_{A_t} \text{COV} [\omega_L(x_0, y_0) \omega_L(x_1, y_1)] dx_0 dy_0 dx_1 dy_1 \end{aligned} \quad (4.11)$$

The covariance of the two load intensities $\omega_L(x_0, y_0)$ and $\omega_L(x_1, y_1)$ may be obtained from the assumptions above. Furthermore, if the unit load comes from n different floors with equal areas, A , (i.e., $A_t = nA$) the mean and variance of $L(A_t) = L(nA)$, from Eqs. (4.10) and (4.11), are

$$\overline{L(nA)} = m_L \quad (4.12)$$

and

$$\begin{aligned} \sigma_{L(nA)}^2 = & \sigma_{\gamma_{bld}}^2 + \frac{\sigma_{\gamma_{flr}}^2}{n} + \frac{1}{nA^2} \iiint_{A_t} \iiint_{A_t} \text{COV} [\varepsilon(x_0, y_0) \varepsilon(x_1, y_1)] dx_0 dy_0 dx_1 dy_1 \\ & + \frac{(n-1)}{nA^2} \iiint_{A_t} \iiint_{A_t} \text{COV} [\varepsilon(x_0, y_0) \varepsilon(x_2, y_2)] dx_0 dy_0 dx_2 dy_2 \end{aligned} \quad (4.13)$$

where (x_0, y_0) and (x_1, y_1) are points located on the same floor; whereas (x_0, y_0) and (x_2, y_2) are points on different floors.

The value of Eq. 4.13 depends on the form of the covariance function. Thus, for the "white noise" model (substituting Eq. 4.7 into 4.13)

$$\sigma_{L(nA)}^2 = \sigma_{\gamma_{bld}}^2 + \frac{\sigma_{\gamma_{flr}}^2}{n} + \frac{\sigma_{\varepsilon}^2}{nA} \quad (4.14)$$

If the covariance functions of Peir [75] are used

$$\sigma_{L(nA)}^2 = \sigma_{\gamma_{bld}}^2 + \frac{\sigma_{\gamma_{flr}}^2}{n} + \frac{\sigma_{sp}^2 \pi d K(A)}{nA} \left[1 + \frac{(n-1)}{n} \rho_m \right] \quad (4.15)$$

in which

$$K(A) = \left[\text{erf} \left(\sqrt{\frac{A}{d}} \right) - \sqrt{\frac{d}{A\pi}} (1 - e^{-A/d}) \right]^2 \quad (4.16)$$

and $\text{erf}(-)$ is the error function.

Peir [75] used the data from the load survey of Mitchell and Woodgate [68] to estimate the parameters of the sustained load model. McGuire and Cornell [65, 66] estimated the value of σ_{ε} , to be used with the white noise model, so as to fit the more accurate Peir's model. The results are as follows:

$$\begin{aligned} m_L &= 11.8 \text{ (psf)} \\ \sigma_{\gamma_{bld}}^2 &= 3 \text{ (psf)}^2 \\ \sigma_{\gamma_{flr}}^2 &= 17.25 \text{ (psf)}^2 \end{aligned}$$

$$\sigma_{sp}^2 = 260 \text{ (psf)}^2$$

$$\rho_m = 0.7$$

$$\sigma_\varepsilon^2 = 8230 \text{ (psf)}^2$$

$$d = 9 \text{ (ft)}^2$$

The coefficient of variation of the live load intensity obtained from the above formulation is shown in Fig. 4.2 as a function of the floor area A . It is apparent from this figure that the results of the white noise model and that of the Peir's model are very close to each other, except for very small floor areas.

4.3.3 Arbitrary-Point-in-Time Load -- As mentioned earlier, the sustained load will change from time to time (due to functional or occupancy changes of the area). The unit load intensity, as defined previously, should be understood to be the unit load at time t ; i.e., the "arbitrary-point-in-time" load. Under the assumption that the process is stationary, i.e.,

$$f_{L(A,t)}(\ell) = f_{L(A)}(\ell) \quad \text{for all } t$$

(where $f_{L(A)}(\ell)$ is the probability density function of $L(A)$), the distribution of the lifetime maximum sustained load may be found for known or assumed distributions [65, 75].

Because of the rare occurrence, and short duration, of earthquakes it is believed that the use of the arbitrary-point-in-time load in investigating the combined effect of dead, live, and earthquake loads should yield meaningful measures of the risk involved in current earthquake-resistant designs. For this reason, only this portion of the live load is considered in the sequel.

4.3.4 Live Load Effects -- To translate the live load intensity, $\omega_L(x,y)$, into load effects, the concept of influence surfaces is necessary

[86]. The ordinate, $I(x,y)$, of the influence surface is equal to the desired load effect on a given member of a structure resulting from the application of a unit load at floor location (x,y) . The total live load effect, S_L , is then found by integrating the product of the load intensity and $I(x,y)$ over the entire floor area; or

$$S_L = \iint_A \omega_L(x,y) I(x,y) dx dy \quad (4.17)$$

For the mid-span bending moment in a beam in framed buildings, the influence area can be considered as the length of the beam times twice the distance to an adjacent beam in a parallel frame; whereas, for the axial load in a single-story column, this is twice the beam length in one frame times twice the distance between frames [75]. Other load effects have similar influence areas.

The mean and variance of S_L may be found with Eq. 4.17 and the basis of the assumption stated in Sect. 4.3.2 [75]. Consider first the case in which the load effects are due mainly to the load acting on only one floor (i.e., beam moments and shear, axial load in a column supporting one floor, etc.). Then, the mean and variance of S_L are given by

$$\bar{S}_L = c_L m_L \quad (4.18)$$

and

$$\begin{aligned} \text{VAR} [S_L] = & \sigma_{\gamma_{bld}}^2 c_L^2 + \sigma_{\gamma_{flr}}^2 c_L^2 + \\ & + \iiint_A \iiint_A \text{COV}[\epsilon(x_0, y_0) \epsilon(x_1, y_1)] I(x_0, y_0) I(x_1, y_1) dx_0 dy_0 dx_1 dy_1 \end{aligned} \quad (4.19)$$

where $c_L = \int_A I(x,y) dA$ is an influence coefficient that translates the unit load intensity into the desired load effect.

McGuire and Cornell [65,66] showed that, as in the case of unit load intensities, the coefficient of variation for different load effects obtained from the "white-noise" and Peir's models are very close (see Sect. 4.3.2). On this basis, the "white-noise" model will be adopted in the sequel. From Eqs. 4.7 and 4.19, the variance of S_L may be expressed as

$$\text{VAR } [S_L] = \sigma_{\gamma_{bld}}^2 c_L^2 + \sigma_{\gamma_{flr}}^2 c_L^2 + \sigma_{\epsilon}^2 \int_A I(x,y)^2 dA \quad (4.20)$$

and its coefficient of variation is

$$\Omega_{S_L} = \left[\frac{1}{m_L^2} (\sigma_{\gamma_{bld}}^2 + \sigma_{\gamma_{flr}}^2 + \frac{\sigma_{\epsilon}^2 u^2}{A}) + (0.10)^2 \right]^{1/2} \quad (4.21)$$

where,

$$u^2 = \frac{\int_0^1 I(x,y)^2 dA}{\left[\int_0^1 I(x,y) dA \right]^2} \quad (4.22)$$

and (0.10) represents the uncertainty associated with the method of static analysis. The value of u^2 depends on the type of load effect (i.e., bending, shear, axial load, etc.). Based on theoretical forms of the influence functions, McGuire and Cornell [65] calculated the values of u^2 to be 2.20 for axial load, 2.04 for beam end-moments and 2.76 for beam mid-span moment. A plot of Ω_{S_L} as a function of the influence area, obtained with the first three terms of Eq. 4.21, is shown in Fig. 4.3. Also shown, for comparison purposes, is the c.o.v. for the load effects obtained by Rosenblueth and Esteva [86] based on the data of Mitchell and Woodgate [68]. It can be observed that Ω_{S_L} is not very sensitive to u^2 , except for very small areas. This and the relative insensitivity of u^2 to the different load effects, allows the use of a single value of u^2 for all load effects [65]. In the following, a value of $u^2 = 2.20$ (corresponding to axial load and very close to the end-of-span shear) is used for all load effects. This results in coefficients of variation that are slightly conservative for the end-of-span moment and slightly unconservative for mid-span moment and shear.

The c.o.v. of a column supporting n floors may be found as follows. Let $S_{L(n)}$ be the total load in the column under consideration. Then, according to Eq. 4.17,

$$S_{L(n)} = \sum_{i=1}^n \iint_{A_i} \omega_L(x,y) I_i(x,y) dx dy \quad (4.23)$$

where $I_i(x,y)$ is the influence function for the i^{th} floor, and A_i is the corresponding influence area. If the areas and the influence surfaces are equal for all floors, the mean and c.o.v. of $S_{L(n)}$ are given by

$$\overline{S_{L(n)}} = n c_L m_L \quad (4.24)$$

and

$$\Omega_{S_{L(n)}} = \left[\frac{1}{m_L^2} \left(\sigma_{\gamma_{bld}}^2 + \frac{\sigma_{\gamma_{flr}}^2}{n} + \frac{\sigma_{\epsilon}^2 u^2}{nA} \right) + (0.10)^2 \right]^{1/2} \quad (4.25)$$

A plot of $\Omega_{S_{L(n)}}$ as a function of the influence area, obtained from Eq. 4.25 (excluding the uncertainty of 0.10 in the method of structural analysis) is shown in Fig. 4.4 for various values of n . It may be seen that as the number of floors supported by a column increases, the c.o.v. of the axial load decreases. This is better observed also from Fig. 4.5 where the ratio $\Omega_{S_{L(n)}}/\Omega_{S_{L(1)}}$ is presented.

4.4 Earthquake Load

4.4.1 Introduction -- The description of seismic ground motions at a site involves two main steps: (1) the prediction of future earthquake intensities expected at the site ("intensity" is any measure of the motion that is important to the response of the structure); and (2) modeling and analysis of the ground shaking effects corresponding to the intensity estimated in step one.

The prediction of future earthquake intensities is the object of seismic risk analysis [30, 31]; this topic is outside the scope of this study. Only the second step is considered here; i.e., the analysis and assessment of the uncertainties underlying the determination of the response and earthquake load effects corresponding to a prescribed intensity. In doing this, it is assumed that the response of structures can be evaluated through linear methods of analysis, and that the structural properties of the systems are random.

4.4.2 Methods of Earthquake Response Analysis -- The earthquake loading may be described in various ways; by equivalent static lateral force, time-history (of past or artificial earthquakes), response spectrum, and stochastic process models. The first of these is found in construction codes as a design-aid, but the true dynamic nature of the earthquake forces is ignored.

The use of time-histories to evaluate the statistics of the response of a multi-degree-of-freedom system requires repeated analysis of the system for many earthquake records. Because of the excessive amount of computation required to cover a sufficient range of random properties in the system, this method will not be pursued.

The response spectrum approach is a simple way of including the dynamic effects. With this method, as will be shown later, the uncertainties of the structural properties can be treated systematically through first-order approximation. The method requires the combination of the maximum modal components to predict the peak responses of MDOF systems; the square-root-of-the-sum-of-squares of the modal peaks (SRSS method) is commonly used.

Random vibration recognizes the probabilistic nature of earthquake ground motions; however, a practical method for systems with random structural properties has yet to be developed.

The response statistics obtained by these methods are examined in the following. A four-degree-of-freedom system was analyzed in Ref. [17] for 39 real accelerograms normalized to the peak ground acceleration. The statistics of the maximum response, expressed in the form of peak inter-story displacements, were first obtained from a time-history analysis. Then the mean response spectrum and its variance were calculated, and the inter-story displacements were evaluated from the mean and mean + σ response spectrum (using the SRSS method). When the mean response spectrum is used, the results agree very closely with the mean of the 39 time-history analysis. The same is true for the mean plus one standard deviation, or at any other probability levels. Similar results were obtained by McGuire [64], who used linear regression analysis techniques in the analysis of 47 close-coupled 2 d.o.f. systems, subjected to 68 (unscaled) time-histories of 34 earthquakes.

Gungor [41] compared the response statistics obtained by random vibration and the response spectrum method (using the SRSS), with the response spectrum generated from the same power spectral density of the random vibration analysis. The agreement in the results for a 10 d.o.f. system was also very close.

A five degree-of-freedom system was analyzed in this study to compare the response statistics obtained from random vibration theory and those of the response spectrum method, when the response spectrum is obtained from a set of real earthquake records. A stationary Gaussian excitation process, with the power spectral density of Kanai [54] and Tajimi [96], was used in the random vibration analysis. The mean and mean + σ responses were obtained by a method described in Ref. [41]. The results are shown in Table 4.1,

TABLE 4.1 5 DOF SYSTEM: RELATIVE DISPLACEMENT OF THE FLOORS

Level	$E[X_{\max}]$	c.o.v.
Random Vibration Theory		
1	1.00	0.16
2	2.20	0.16
3	3.59	0.16
4	4.69	0.16
5	5.27	0.16
Response Spectrum (MHN)		
1	1.00	0.38
2	2.20	0.38
3	3.60	0.38
4	4.70	0.38
5	5.29	0.38

where the relative displacements of the floors with respect to the base are tabulated (these are normalized to the relative displacement of the first floor). The mean and mean + σ values of a response spectrum

obtained by Mohraz, et al. [69] from 28 records normalized to peak ground acceleration were used for the response spectrum analysis. Its results are also shown in Table 4.1. Close agreement in the mean-value estimates is obtained. This is mainly due to the fact that the mean response spectrum obtained by Mohraz, et al. can be approximated very closely with the power spectral density proposed by Kanai, for the frequency range at which the structure is located (the fundamental period of the system is 0.5 seconds). For other systems, wider differences may be expected. However, the mean + σ response obtained by random vibration lies below the corresponding response calculated with the response spectrum method. Assuming that the c.o.v. of the response can be approximated by $[(\mu + \sigma)_{RS} - \mu_{RS}]/\mu_{RS}$, where $(-)_RS$ are the mean or mean plus one standard deviation obtained by the response spectrum approach, it is observed that these values are more than twice those obtained through stationary random vibration analysis.

On the basis of the results described above, it is concluded that the response spectrum approach can be used to obtain reliable predictions of the effect of ground motions at a site. The c.o.v. of the response depends on the procedure used to generate the mean and standard deviation of the response spectrum. In particular, stochastic process models yield c.o.v.'s that are only about half as large as those obtained on the basis of real earthquake records. The c.o.v. obtained from the random vibration analysis, of course, does not include uncertainties associated with the nonstationarity of the ground motions and local site conditions, whereas the c.o.v. obtained through the response spectrum approach for a set of real earthquake records may be too high since the available records are not from the same site. In the sequel, the response c.o.v. based on available earthquake records will be used, recognizing that it may be on the conservative side.

4.4.3 Statistics of Maximum Response -- There are various procedures to generate response spectral shapes for given probability levels. These include the analysis of normalized earthquake records [21, 50, 69, 71], linear regression analysis techniques [36, 64], and random vibration

analysis [41]. For the purpose of this work, the response spectrum proposed by Mohraz, Hall and Newmark [69] is used. In this study [69], a statistical analysis of the data from 9 strong earthquakes (28 records in the horizontal direction and 14 in the vertical direction) was performed. The records were normalized with respect to the maximum ground acceleration, a , in the high-frequency range (2 to 4 Hz in the horizontal direction, and 3 to 10 Hz in the vertical direction), to the maximum ground velocity, v , in the middle-frequency range (0.4 to 2 Hz in the horizontal direction and 0.3 to 3 Hz in the vertical direction), and to the maximum ground displacement, d , in the low-frequency range (0.2 to 0.4 and 0.1 to 0.3 Hz in the horizontal and vertical directions, respectively). By normalizing the earthquake records to different ground parameters, as indicated above, it is intended to minimize the variance of the response spectrum at different natural frequencies.

The mean and standard deviations of the amplification factors (i.e., the ratio of the computed maximum response to the maximum ground motion) for prescribed damping values, were evaluated from these data for 38 frequencies. On the basis of these results, the amplification factors for displacement and velocity may be considered to be constant over the low and intermediate-frequency ranges, whereas the amplification factor for acceleration may be assumed to be constant up to a frequency of about 6 to 10 Hz and then to decrease exponentially to a value of 1.0 at frequencies of 20 to 50 Hz (the values of these frequencies depend on the damping and on the direction of the motion). Plotted on a tripartite logarithmic paper, the response spectral shape is as shown in Fig. 4.6. As can be seen in this figure, a response spectrum is defined by straight lines between the control frequencies f_1 through f_4 , defining ranges of constant displacement, velocity and acceleration, and a transition region between f_3 and f_4 . The conditional means and standard deviations of the amplification factors for the constant displacement, velocity and acceleration ranges (denoted hereafter by α_d , α_v and α_a), as obtained in Ref. [69], are summarized in Table 4.2, and Figs. 4.7 and 4.8.

TABLE 4.2 STATISTICS OF THE AMPLIFICATION FACTORS

DAMPING		MEAN (STD. DEV.)			
%	α_d	α_v	α_a	f_3	f_4
HORIZONTAL DIRECTION					
0.5	1.97(1.02)	2.58(1.23)	3.67(1.45)	6	40
2.0	1.68(0.83)	2.06(0.92)	2.76(0.89)	6	30
5.0	1.40(0.64)	1.66(0.66)	2.11(0.56)	6	20
10.0	1.15(0.47)	1.34(0.47)	1.65(0.36)	6	20
VERTICAL DIRECTION					
0.5	1.86(0.92)	2.52(1.29)	4.02(2.13)	10	50
2.0	1.65(0.76)	1.97(0.94)	2.80(1.33)	10	50
5.0	1.40(0.61)	1.51(0.67)	2.05(0.77)	10	50
10.0	1.16(0.46)	1.17(0.47)	1.59(0.49)	10	50

The amplification factors for acceleration in the transition range ($f_3 < f < f_4$) may be expressed, with reference to Fig. 4.6, as

$$\alpha_a(\omega) = \exp \left[\frac{\ln \alpha_a \ln (f_4/f)}{\ln(f_4/f_3)} \right] \quad (4.26)$$

from which its statistics may be obtained. Also shown in Table 4.2 are the estimated values of f_3 and f_4 [69].

An attempt has been made [69] to include the local soil properties by treating the data from rock and alluvium separately. However, no really valid statistical inference could be made from the available information although separate design spectra for alluvium and rock have been suggested [69]. On the basis of the data considered, the response spectrum proposed by Mohraz, et al. is probably representative of stiff soil conditions [89], and of sites located at moderate distances to the epicenter [31, 64, 89]. Thus, reliable results can only be obtained for similar type of soils and epicentral distances.

In examining the response amplifications, especially in the ranges of constant velocity and acceleration, Mohraz, et al. [69] inferred that earthquakes with low ground acceleration have greater amplifications than those with high ground acceleration. It was also observed [69] that the presence of sharp peaks in the acceleration record reduces the amplification for high frequencies. This observation is important in deciding what earthquake records should be considered to obtain valid statistical estimates.

Also investigated were the ratios ad/v^2 and v/a of the earthquake records referred to above (only the results for the horizontal direction are reported here). These quantities are useful in constructing response spectra curves when only one or two of the peak ground motion components can be obtained. The mean and c.o.v. of ad/v^2 and v/a in the horizontal direction are shown in Table 4.3. Also shown are the mean and c.o.v. of

TABLE 4.3 SUMMARY OF v/a AND ad/v^2 (HORIZONTAL DIRECTION)

SITE	No. Rec.	ad/v^2		v/a	
		mean	c.o.v.	mean	c.o.v.
Alluvium & rock	28	5.6	0.65	45	0.51
Alluvium & rock*	26	-	-	48	0.45
Alluvium	22	5.7	0.72	52	0.41
Rock	6	5.4	0.24	22	0.55
Rock*	4	-	-	28	0.36
Alluvium & rock ($a > 0.1$ g)	20	5.7	0.72	39	0.53
Alluvium & rock* ($a > 0.1$ g)	18	-	-	43	0.45
Alluvium $a > 0.1$ g	14	5.9	0.84	47	0.41
Alluvium $a < 0.1$ g	8	5.3	0.40	60	0.39
San Fernando	118	5.1	0.43	45	0.40

* Not including the extreme ratios of the San Francisco Golden Gate Park earthquake.

these quantities as estimated in this study based on 60 records of the San Fernando earthquake [52]. The mean values of both ad/v^2 and v/a , and the c.o.v. of v/a , obtained from the two sets of data are in reasonable agreement, as shown in Table 4.3. The coefficient of variation of ad/v^2 obtained from the San Fernando data, however, is significantly smaller than those from the Mohraz, et al. [69] study. It must be emphasized that these ratios are, at least in part, function of the focal distance, soil conditions, attenuation of motion in the ground, earthquake magnitude, etc. [72]. Thus, by ignoring these factors, it is not surprising to obtain discrepancies, such as those shown in Table 4.3, in the estimation of ad/v^2 and v/a when data from different sources are considered together.

4.4.4 Maximum Earthquake Load Effects -- The earthquake load effect on any given member of a structure can be expressed, as a function of the relative displacement of the floors with respect to the base, as

$$S_E = \left[\sum_{i=1}^n \{c_E \gamma_i \{\phi_i\} D_i\}^2 \right]^{1/2} \quad (4.27)$$

where D_i is the spectral displacement corresponding to the i^{th} mode, and c_E is an influence coefficient that translates the relative displacement of the floors into the desired load effects.

Alternatively, the same load effect may be determined on the basis of the inertial forces acting on each floor; i.e.,

$$S_E = \left[\sum_{i=1}^n \{c_E' \gamma_i [\bar{M}] \{\phi_i\} M^* \omega_i^2 D_i\}^2 \right]^{1/2} \quad (4.28)$$

In a deterministic analysis these two approaches are equivalent; however, some differences could arise in the corresponding probabilistic problem. In particular, the c.o.v. of S_E obtained with Eq. 4.27 may be different from that obtained through Eq. 4.28.

For purposes of this study, the statistics of the earthquake load effects will be estimated with Eq. 4.27, except in the case of very rigid structures, in which Eq. 4.28 may be preferable. In Sect. 3.3.3, it was shown that the modal shapes and the participation factors may be assumed to be deterministic quantities. On this basis, the mean and c.o.v. of S_E may be expressed as

$$\bar{S}_E = \left[\sum_{i=1}^n \{S'_{E_i} \bar{D}_i\}^2 \right]^{1/2} \quad (4.29)$$

and

$$\Omega_{S_E} = \left[\frac{1}{\bar{S}_E^4} \left\{ \sum_{i=1}^n (S'_{E_i} \bar{D}_i)^4 \Omega_{D_i}^2 + \sum_{i=1}^n \sum_{\substack{j=1 \\ i \neq j}}^n (S'_{E_i} \bar{D}_i)^2 (S'_{E_j} \bar{D}_j)^2 \rho_{D_i, D_j} \Omega_{D_i} \Omega_{D_j} \right\} + (0.15)^2 \right]^{1/2} \quad (4.30)$$

in which $S'_{E_i} = c_{E_i} \gamma_i \{\phi_i\}$, and a prediction uncertainty of 0.15 is ascribed to the imperfection in the method of dynamic analysis.

For simplicity, D_i and D_j are assumed to be perfectly correlated; then

$$\Omega_{S_E} = \left[\frac{1}{\bar{S}_E^4} \left\{ \sum_{i=1}^n (S'_{E_i} \bar{D}_i)^2 \Omega_{D_i} \right\}^2 + (0.15)^2 \right]^{1/2} \quad (4.31)$$

This yields conservative Ω_{S_E} ; also, any error would be small since the first mode usually contributes the major part of Ω_{S_E} (see Chapter 5). However, if desired, the correlation coefficient between D_i and D_j can be evaluated using the procedure shown in Appendix A.

In order to find the statistics of S_E from Eqs. 4.29 and 4.31, the statistics of D_i must first be determined. For this purpose, expressions for D_i may be obtained with reference to Fig. 4.6, depending on the natural frequency of the structure under consideration; i.e.,

- in the constant displacement range: $2\pi\omega_i < f_1$

$$D_i = \alpha_{d_i} d \quad (4.32)$$

- in the constant velocity range: $f_1 < 2\pi\omega_i < f_2$

$$D_i = \frac{\alpha_{v_i} v}{\omega_i} \quad (4.33)$$

- in the constant acceleration range: $f_2 < 2\pi\omega_i < f_3$

$$D_i = \frac{\alpha_{a_i} a}{\omega_i^2} \quad (4.34)$$

- in the transition range: $f_3 < 2\pi\omega_i < f_4$

$$D_i = \frac{\alpha_{a_i}(\omega) a}{\omega_i^2} \quad (4.35)$$

The natural frequency, ω_i , as well as f_1 and f_2 are random variables; therefore, it is not possible to state a priori which of these equations is applicable. This is especially true when ω_i is close to one of the control frequencies. However, in Sect. 4.4.2, it was shown that in the case of systems with known properties, the mean response obtained from a set of real earthquake records through time-history analysis agrees very closely with the response obtained from the mean response spectrum (of the same set of records). This implies that in calculating the mean value of the response, the governing equation for D_i may be established on the basis of the mean value of ω_i , f_1 and f_2 ; that is, if $2\pi\bar{\omega}_i < \bar{f}_1$ then $D_i = \alpha_{d_i} d$ (Eq. 4.32); if $\bar{f}_1 < 2\pi\bar{\omega}_i < \bar{f}_2$, $D_i = \alpha_{v_i} v/\omega_i$ (Eq. 4.33); etc.

The c.o.v. of D_i may be estimated also on the same basis; however, for systems whose frequencies are in the neighborhood of the control frequencies f_1 , f_2 , or f_3 , the c.o.v. may be evaluated using either of two equations. The difference in the calculated coefficient of variation

of the total load effects is small (as has been verified numerically) and for practical purposes may be neglected.

The mean and c.o.v. of D_i , therefore, can be obtained as follows:

For $2\pi\bar{\omega}_i < \bar{f}_1$:

$$\bar{D}_i = \bar{\alpha}_{d_i} \bar{d} \quad (4.36)$$

$$\Omega_{D_i}^2 = \Omega_{\alpha_{d_i}}^2 + \Omega_d^2 \quad (4.37)$$

For $\bar{f}_1 < 2\pi\bar{\omega}_i < \bar{f}_2$:

$$\bar{D}_i = \frac{\bar{\alpha}_{v_i} \bar{v}}{\bar{\omega}_i} \quad (4.38)$$

$$\Omega_{D_i}^2 = \Omega_{\alpha_{v_i}}^2 + \Omega_v^2 + \Omega_{\omega_i}^2 \quad (4.39)$$

For $\bar{f}_2 < 2\pi\bar{\omega}_i < \bar{f}_3$:

$$\bar{D}_i = \frac{\bar{\alpha}_{a_i} \bar{a}}{\bar{\omega}_i^2} \quad (4.40)$$

$$\Omega_{D_i}^2 = \Omega_{\alpha_{a_i}}^2 + \Omega_a^2 + 4\Omega_{\omega_i}^2 \quad (4.41)$$

and for $\bar{f}_3 < 2\pi\bar{\omega}_i < \bar{f}_4$:

$$\bar{D}_i = \frac{\bar{\alpha}_{a_i(\omega)} \bar{a}}{\bar{\omega}_i^2} \quad (4.42)$$

$$\Omega_{D_i}^2 = \left[\frac{\ln(\bar{f}_4/2\pi\bar{\omega}_i)}{\ln(\bar{f}_4/\bar{f}_3)} \right]^2 (\Omega_{\alpha_{a_i}}^2 + 4\omega_1^2 - \Omega_{M^*}^2) + \Omega_a^2 + \Omega_{M^*}^2 \quad (4.43)$$

Eq. 4.43 was obtained by using an interpolating procedure between the c.o.v.'s of S_E at $2\pi\bar{\omega}_i = \bar{f}_3$ and $2\pi\bar{\omega}_i = \bar{f}_4$, determined as follows: (1) in

the case of very rigid structures, the maximum floor accelerations tend to be the same as the maximum ground acceleration and, therefore, the load effects may be estimated with greater accuracy based on the inertial forces; in particular, it may be shown that for single-degree-of-freedom systems with $2\pi\bar{\omega}_i \geq \bar{f}_4$, Ω_{SE} , as obtained from Eq. 4.28, is $\Omega_{SE}^2 = (0.15)^2 + \Omega_a^2 + \Omega_{M*}^2$; and (2) from Eqs. 4.31 and 4.41, $\Omega_{SE}^2 = (0.15)^2 + \Omega_{\alpha a i}^2 + \Omega_a^2 + 4\Omega_{\omega i}^2$ at $2\pi\bar{\omega}_i = \bar{f}_3$.

When only one or two of the peak ground motion components is available, information on v/a and/or ad/v^2 may be used to estimate the statistics of D_i . For example, suppose that only the value of the maximum ground acceleration is available, and that $\bar{f}_1 < 2\pi\bar{\omega}_i < \bar{f}_2$; then

$$v = \left(\frac{v}{a} \right) a$$

and assuming v/a and a to be statistically independent, it follows from Eq. 4.33 that

$$\bar{D}_i = \frac{\bar{\alpha}_{v i} \left(\frac{\bar{v}}{a} \right) \bar{a}}{\bar{\omega}_i}$$

and

$$\Omega_{D_i}^2 = \Omega_{\alpha_{v i}}^2 + \Omega_{v/a}^2 + \Omega_a^2 + \Omega_{\omega_i}^2$$

in which $\left(\frac{\bar{v}}{a} \right)$ and $\Omega_{v/a}$ can be obtained from Sect. 4.4.3.

In the present study, it is assumed that the ground spectrum is given; thus, the uncertainty in the peak ground motions is not considered. In more general cases, this uncertainty must be included which may be determined through a seismic risk analysis [30, 31, 32].

So far, all but the statistics of the amplification factors have been defined. To determine these, it should be recognized that the amplification factor for the p^{th} ground motion component in the i^{th} mode $\alpha_{p i}$, and the damping coefficient in the i^{th} mode β_i , are jointly distributed random variables. Thus, the mean and variance of $\alpha_{p i}$ are

$$E[\alpha_{p_i}] = E\{E[\alpha_{p_i} | \beta_i]\} \quad (4.44)$$

and

$$\text{Var}[\alpha_{p_i}] = E\{\text{Var}[\alpha_{p_i} | \beta_i]\} + \text{Var}\{E[\alpha_{p_i} | \beta_i]\} \quad (4.45)$$

where $E[\alpha_{p_i} | \beta_i]$ and $\text{Var}[\alpha_{p_i} | \beta_i]$ are, respectively, the conditional mean and conditional variance of the amplification factor.

Letting

$$f_{p_1}(\beta_i) = E[\alpha_{p_i} | \beta_i] \quad (4.46)$$

and

$$f_{p_2}^2(\beta_i) = \text{Var}[\alpha_{p_i} | \beta_i] \quad (4.47)$$

it follows from Eqs. 4.46 and 4.47 that (on the basis of first-order approximation);

$$\bar{\alpha}_{p_i} = f_{p_1}(\bar{\beta}_i) \quad (4.48)$$

and

$$\Omega_{\alpha_{p_i}} = \frac{1}{f_{p_1}(\bar{\beta}_i)} \left[f_{p_2}^2(\bar{\beta}_i) + \left(\frac{\partial f_{p_1}(\beta_i)}{\partial \beta_i} \right)^2_{\bar{\beta}_i} \bar{\beta}_i^2 \Omega_{\beta_i}^2 \right]^{1/2} \quad (4.49)$$

Values of $f_{p_1}(\beta_i)$ and $f_{p_2}(\beta_i)$ are given in Table 4.2 and Figs. 4.7 and 4.8, whereas $\bar{\beta}$ and Ω_{β} are given in Sect. 3.3.4.

In evaluating $\Omega_{\alpha_{p_i}}$ with Eq. 4.49, it is convenient to have a mathematical expression for $f_{p_1}(\beta_i)$. For this purpose, an expression of the form

$$f_{p_1}(\beta_i) = a_1[1 + a_2\beta]^a \quad (4.50)$$

was assumed, and the parameters a_1 , a_2 , and a_3 were determined using the data of Table 4.2. The resulting values of these parameters are summarized

in Table 4.4 (for β in percent); their applicability is limited to damping values in the range $0.5 < \beta < 10\%$ of critical.

TABLE 4.4 SUMMARY OF COEFFICIENTS IN EQ. 4.50

	a_1	a_2	a_3
ACCEL.	4.40	1.30	-0.365
VELOC.	2.98	1.20	-0.300
DISPL.	2.13	0.58	-0.310

With Eq. 4.50, Eq. 4.49 then yields

$$\Omega_{\alpha_{p_1}} = \frac{\left[f_{p_2}^2(\bar{\beta}_i) + f_{p_3}^2(\bar{\beta}_i) \bar{\beta}_i^2 \Omega_{\beta_i}^2 \right]^{1/2}}{f_{p_1}(\bar{\beta}_i)} \quad (4.51)$$

in which,

$$f_{p_3}(\beta_i) = a_1 a_2 a_3 [1 + a_2 \beta_i]^{a_3 - 1} \quad (4.52)$$

Table 4.5 summarizes the c.o.v. of the amplification factors in the constant displacement, velocity, and acceleration ranges, as obtained from Eqs. 4.51 and 4.52.

TABLE 4.5 COEFFICIENTS OF VARIATION OF AMPLIFICATION FACTORS

$\bar{\beta}(\%)$	Ω_{α_d}	Ω_{α_v}	Ω_{α_a}
4	0.47	0.43	0.34
5	0.47	0.42	0.32

Similarly, the c.o.v. of D_i (assuming Ω_a , Ω_v and $\Omega_d = 0$) for the constant displacement, velocity, and acceleration ranges, obtained

from Eqs. 4.37, 4.39 and 4.41, respectively, are summarized in Table 4.6 below.

TABLE 4.6 COEFFICIENT OF VARIATION OF D_i

$\bar{\beta}$ (%)	$2\pi\bar{\omega}_i \leq \bar{f}_1$	$\bar{f}_1 \leq 2\pi\bar{\omega}_i \leq \bar{f}_2$	$\bar{f}_2 \leq 2\pi\bar{\omega}_i \leq \bar{f}_3$
4.0	0.47	0.48	0.54
5.0	0.47	0.47	0.53

4.5 Total Load Effect

The total load effect, due to the combined action of dead, live, and earthquake loads is

$$S = S_D + S_L + S_E \quad (4.55)$$

The load effects, S_D , S_L and S_E are generally statistically independent. Recognizing that the same method of analysis is used in transforming the dead and live load intensities into load effects, it is easily shown that the mean and c.o.v. of S are

$$\bar{S} = \bar{S}_D + \bar{S}_L + \bar{S}_E \quad (4.56)$$

and

$$\Omega_S = \frac{1}{\bar{S}} \left[\bar{S}_D^2 \Omega_{S_D}^2 + \bar{S}_L^2 \Omega_{S_L}^2 + 2(0.10)^2 \bar{S}_D \bar{S}_L + \bar{S}_E^2 \Omega_{S_E}^2 \right]^{1/2} \quad (4.57)$$

CHAPTER 5

RELIABILITY OF CURRENT DESIGNS

5.1 Introductory Remarks

On the basis of the results obtained in the previous chapters, the safety of specific reinforced concrete structures, designed in accordance with the provisions of the 1974 edition of the SEAOC code [90], is evaluated in terms of the calculated probability of failure. The primary objective is to determine the levels of risk in different failure modes and in different members of a structure, implicit in current earthquake-resistant designs.

Uncertainties in the prediction of the ground motions at a site are not considered; thus, the probabilities of failure calculated herein are really conditional probabilities, i.e., the probabilities of failure when subjected to a specified intensity of ground motion. The total failure probabilities during the lifetime of a structure may be obtained by combining these conditional probabilities with the results of a seismic risk analysis for the site in which the structure is located (see for example [10]).

An earthquake is assumed to act in only one horizontal direction; no interaction with the other horizontal direction, nor with the vertical direction is considered. The influence of soil-structure interaction and accidental torsion are also disregarded.

5.2 Risk Implicit in Current Designs

To determine the seismic safety underlying structures designed according to current codes, it is necessary to examine specific structures. For this purpose, a ten-story building was designed with the seismic provisions of the 1974 SEAOC Code.

The typical plan and elevation of the structure considered are shown in Fig. 5.1. In designing the structure according to the SEAOC code, uniformly distributed loads equal to 50 psf for live load, 20 psf for

partitions, and 10 psf for mechanical equipment and ceiling, were assumed for all floors; except for the roof, in which only the load corresponding to the mechanical equipment was used. The floor weights, obtained from a preliminary analysis, are shown in Table 5.1. Also shown are the equivalent lateral forces calculated through Eq. 1.1 of the SEAOC code [90] (in which $Z = 1.0$, $I = 1.0$, $K = 0.67$, $C = 0.067$, and $S = 1.5$). The load effects due to dead,

TABLE 5.1 DESIGN LATERAL FORCES

Floor Level (from base)	Height h_x (in ft)	Story Weight w_x (k)	$w_x h_x$	Lateral Force	Story Shear
10	120	230	27600	40.15	40.15
9	108	270	29160	28.50	68.65
8	96	270	25920	25.34	93.99
7	84	270	22680	22.16	116.15
6	72	290	20880	20.41	136.56
5	60	290	17400	17.00	153.56
4	41	290	13920	13.60	167.16
3	36	300	10800	10.55	177.71
2	24	300	7200	7.04	184.75
1	12	300	3600	3.51	188.26

live, and earthquake loads for each member were determined using a STRUDL analysis and combined according to Eqs. (2.1) and (2.2) of the SEAOC code, from which the design member forces were obtained.

On the basis of the above information and the design requirements given in the SEAOC and ACI codes, member dimensions and flexural and shear reinforcements were determined. Two different structures were examined: Structure 1 (as designed according to the SEAOC provisions) has a fundamental period of 1.27 sec., in which the period is based on the gross moments of inertia of the members. The second structure

(Structure 2), with stiffer members than those of Structure 1, has a period of 1.0 sec. Based on the fully-cracked sections, the corresponding periods of these structures are 1.75 and 1.5 sec, respectively. The member dimensions for the two structures are shown in Fig. 5.2.

Modal analyses of the two structures were performed and the statistics of the total load effects for various ground spectra were calculated by the method described in Chapter 4. In doing this, the axial deformations of the elements were neglected, and their effective lengths were taken equal to the distance between the center lines of the supports. The ground spectrum was assumed to have v/a and ad/v^2 ratios equal to 47 in./sec/g and 6, respectively.

The coefficient of variations of the live load effects, were obtained from Fig. 4.4, in which the influence areas for the beams and columns were taken as follows:

Beams: 1056 ft² (all load effects)
 Exterior Columns: 1056 ft² (all load effects)
 Interior Columns: 1056 ft² (for shear and moments)
 2112 ft² (for axial load)

The total load effects in the members of Structure 1, and the respective resistances and failure probabilities for $a = 0.1$ g, are summarized in Table 5.2. Beams and columns are examined with regard to their adequacy in flexure and shear.

The probability of failure in flexure and shear for the members of the two structures, when subjected to a ground acceleration of 0.1 g, is shown in Figs. 5.3 and 5.4. From these figures it may be observed that the probability of a flexural failure in the beams is practically constant at all story levels, except at the roof which is designed on the basis of the minimum reinforcement limitations. The probability of flexural failures in the columns, however, increases for the upper stories, indicating that the code equivalent lateral forces tend to produce "weaker" columns for the upper stories. This observation agrees with the results of other investigations; for example [28]. The comparison between the risk levels for beams and columns (failing in flexure) is

TABLE 5.2 FAILURE PROBABILITIES OF THE MEMBERS OF STRUCTURE 1 FOR $a = 0.1 g$

Member	Story Level	BENDING (kips-in)					SHEAR (kips)				
		\bar{S}_M	Ω_{S_M}	\bar{M}_t	Ω_{M_t}	P_f	\bar{S}_V	Ω_{S_V}	\bar{V}_t	Ω_{V_t}	P_f
Ext. Beam	1	4227	0.42	9038	0.17	2.99E-2	38	0.36	139	0.24	8.01E-4
	2	4637	0.42	9889	0.18	2.96E-2	41	0.36	148	0.23	8.40E-4
	3	4321	0.42	9496	0.18	2.52E-2	39	0.36	146	0.23	5.75E-4
	4	3867	0.42	8776	0.17	2.13E-2	36	0.35	139	0.24	4.02E-4
	5	3622	0.40	8185	0.17	1.98E-2	34	0.34	132	0.24	3.11E-4
	6	3318	0.40	7398	0.17	2.07E-2	34	0.31	129	0.24	2.17E-4
	7	2871	0.39	6172	0.17	2.32E-2	31	0.29	112	0.24	1.99E-4
	8	2531	0.37	5282	0.17	2.39E-2	28	0.27	111	0.24	4.31E-5
	9	1950	0.33	4089	0.17	1.58E-2	23	0.23	95	0.23	6.55E-6
	10	1297	0.22	2792	0.17	2.48E-3	16	0.17	92	0.24	5.11E-10
Int. Beam	1	4872	0.40	9823	0.18	3.67E-2	42	0.36	144	0.23	1.15E-3
	2	5182	0.41	10609	0.18	3.53E-2	44	0.37	154	0.23	1.13E-3
	3	5033	0.41	10478	0.18	3.17E-2	43	0.36	152	0.23	9.54E-4
	4	4780	0.40	10019	0.18	2.97E-2	41	0.36	146	0.23	8.24E-4
	5	4448	0.40	9364	0.17	2.77E-2	39	0.35	139	0.23	6.76E-4
	6	4210	0.39	8709	0.17	2.91E-2	37	0.34	130	0.24	7.37E-4
	7	3602	0.37	7256	0.17	3.06E-2	33	0.31	111	0.24	6.87E-4
	8	3184	0.36	6270	0.17	3.11E-2	30	0.30	110	0.24	1.92E-4
	9	2491	0.32	5083	0.17	1.82E-2	25	0.26	94	0.24	4.27E-5
	10	1469	0.26	2792	0.17	1.46E-2	16	0.20	91	0.24	4.25E-9
Ext. Column	1	2614	0.48	9588	0.17	2.07E-3	30	0.46	393	0.20	1.58E-8
	2	2360	0.42	6421	0.18	7.83E-3	34	0.42	361	0.20	3.47E-8
	3	2419	0.41	5709	0.18	1.59E-2	33	0.41	356	0.20	1.43E-8
	4	1933	0.43	5809	0.16	3.89E-3	27	0.43	297	0.20	3.26E-8
	5	1910	0.41	4359	0.16	1.79E-2	26	0.41	279	0.20	2.01E-8
	6	1801	0.40	3323	0.16	5.25E-2	25	0.40	260	0.20	9.37E-9
	7	1553	0.41	2741	0.16	6.66E-2	21	0.40	151	0.18	1.16E-6
	8	1442	0.38	2186	0.15	1.19E-1	20	0.38	113	0.18	6.07E-6
	9	1199	0.37	1732	0.15	1.36E-1	16	0.36	131	0.18	3.44E-8
	10	896	0.29	1423	0.15	6.22E-2	12	0.28	111	0.18	2.24E-12
Int. Column	1	6209	0.49	19912	0.15	4.59E-3	65	0.49	527	0.22	8.72E-6
	2	4215	0.49	12732	0.15	6.44E-3	60	0.49	508	0.22	6.57E-6
	3	3956	0.49	12071	0.14	5.86E-3	56	0.49	488	0.22	4.30E-6
	4	3837	0.49	13765	0.15	2.30E-3	53	0.49	440	0.20	4.93E-6
	5	3495	0.49	10474	0.14	6.76E-3	48	0.49	438	0.19	1.99E-6
	6	3152	0.49	8905	0.14	9.35E-3	43	0.49	406	0.19	1.53E-6
	7	2910	0.49	7407	0.14	1.63E-2	39	0.49	348	0.19	2.39E-6
	8	2484	0.49	5695	0.14	2.72E-2	33	0.49	300	0.19	2.40E-6
	9	2003	0.49	3356	0.14	1.02E-1	26	0.49	235	0.18	2.00E-6
	10	1194	0.50	2482	0.14	4.49E-2	14	0.50	185	0.18	6.36E-7

of significance. The Code is presumably intended to give structures with strong columns and weak beams, so that yielding will occur first in the beams. However, the results of Figs. 5.3 and 5.4 would suggest that this may not always be fulfilled by the provisions of the SEAOC Code; the columns may yield before the beams, especially those in the upper stories.

It may also be observed from Figs. 5.3 and 5.4 that the probability of shear failure is lower than the probability of flexural failures. On these bases, the SEAOC Code appears to give sufficiently conservative designs for shear as to avoid premature shear failures.

Figure 5.5 shows the probability of failure in flexure and shear for the interior and exterior columns, and for the interior beam at story level 5 of Structure 1, as a function of the maximum ground acceleration. In calculating these probabilities it is assumed that Ω_p is less than or equal to the c.o.v. of the axial load induced by the earthquake load alone (this avoids the problem of unlimited Ω_p when $\bar{P} = 0$). The discontinuities in the shear failure probability curves for the columns (Fig. 5.5) are due to the change in the governing equation for the determination of v_c (i.e., from Eq. 2.12 to Eq. 2.14). These curves are typical of most of the members of the two structures. The sensitivity of the calculated probability to the maximum ground acceleration is apparent from Fig. 5.5.

Figures 5.6 through 5.9 compare the failure probability of Structure 1 for different values of the natural periods and damping. As expected, these results show that the probability of failure decreases for structures with higher natural periods (see Figs. 5.6 and 5.7) or higher damping values (see Figs. 5.8 and 5.9).

The influence on the failure probability of the number of modes considered in the analysis is shown in Figs. 5.10 and 5.11. Calculations based on only the fundamental mode gives a good approximation for the failure probability in the lower stories; however, it underestimates the risk for the upper stories. The use of the first 2 modes gives a good approximation for most cases.

CHAPTER 6

SUMMARY AND CONCLUSIONS

6.1 Summary of Study

A model is developed that provides the basis for the determination of the levels of risk implicit in current earthquake-resistant design procedures. The basic variabilities in the loads and structural properties, as well as the errors in the mathematical models used to predict these quantities in design, are carefully examined and assessed from available information. These uncertainties lead to risk estimates that are consistent with the present state of knowledge.

Only linear structures are considered; thus the failure probabilities calculated herein must be regarded as an indication of the likelihood of a structure (or a structural member) being stressed beyond the elastic range, and not necessarily that collapse, or even serious structural damage, will occur.

The levels of risk implicit in the 1974 SEAOC Code for bending, shear, and axial load, are evaluated. This is accomplished by examining specific typical structures designed according to the Code.

On the basis of the calculations performed for a 10-story building designed according to the SEAOC Code, failure probabilities of the major structural components to specified earthquake intensities are presented in Figs. 5.3 to 5.11; the main results are summarized in Table 6.1 for three intensities of ground acceleration.

TABLE 6.1 CALCULATED FAILURE PROBABILITY

FAILURE MODE	FAILURE PROBABILITY		
	a = 0.1 g	a = 0.2 g	a = 0.3 g
Beams in Flexure	0.020-0.035	0.25-0.34	0.50-0.63
Beams in Shear	10^{-3} - 10^{-4}	0.02-0.05	0.15-0.20
Ext. Col. in Flexure and Axial Load			
lower stories	0.002-0.016	0.13-0.39	0.54-0.85
upper stories	0.06-0.14	0.44-0.64	0.72-0.90
Int. Col. in Flexure and Axial Load			
lower stories	0.002-0.006	0.08-0.14	0.28-0.40
upper stories	0.016-0.100	0.25-0.57	0.57-0.85
Columns in Shear and Axial Load	10^{-8} - 10^{-4}	0.001-0.010	0.015-0.20

6.2 Main Conclusions

On the basis of the results developed in this study, the following conclusions may be drawn:

1. Current earthquake-resistant design provisions can be appraised in terms of risk measures. The basic variabilities and prediction errors (bias and prediction uncertainty) in the variables involved, as well as those underlying the mathematical models, must be included.
2. As expected, the probabilities of failure to specified ground motion intensity depend on the structural members and the mode of failure. On the basis of a 10-story building designed according to the SEAOC Code, the failure probabilities of the beams under bending and axial load are fairly constant for all story levels, whereas for the columns the corresponding probabilities increase with the story level.
3. The comparison between failure probabilities for the beams and columns of the structure examined indicates that the SEAOC Code may not necessarily give columns that are stronger than the beams (especially in the upper stories); that is, yielding may occur first in the columns.
4. In code-designed structures, shear failures have lower probability of occurrence than flexural failures. This is mainly due to the limitations in the shear design and minimum reinforcement. Therefore, the SEAOC Code provides sufficiently conservative designs for shear as to avoid premature shear failures.
5. As expected, the mean values of the natural frequencies and damping have an important effect in the risk levels of the structure. In particular, higher natural frequencies and damping tend to decrease the probability of failure.

LIST OF REFERENCES

1. ACI-ASCE, Committee 326, "Shear and Diagonal Tension", ACI Journal, Proc., Vol. 59, January, February and March 1962.
2. ACI Committee 435, "Variability of Deflections of Simply Supported Reinforced Concrete Beams", ACI Journal, Proc., Vol. 69, January 1972.
3. ACI Task Committee on Structural Safety, "Structural-Safety - A Literature Review", Journal of the Structural Division, ASCE, No. ST4, April 1972.
4. ACI Standard 318-71, "Building Code Requirements for Reinforced Concrete and Commentary", 1971.
5. Alatorre, G. and Casillas, J., "Shear Strength Behavior of Reinforced Concrete Beams Subjected to Alternate Loads", International Symposium on the Effects of Repeated Loading of Materials and Structures, RILEM, Mexico, September 1966.
6. Alford, J. and Housner, G., "A Dynamic Test of a Reinforced Concrete Building", Bull. Seism. Soc. of America, 43(7), 1953.
7. Amin, M. and Ang, A. H.-S., "A Nonstationary Stochastic Model for Strong-Motion Earthquake", Structural Research Series No. 306, University of Illinois, April 1966.
8. Ang, A. H.-S., "Structural Risk Analysis and Reliability Based Design", Journal of the Structural Division, ASCE, No. ST9, September 1973.
9. Ang, A. H.-S., "Probability Concepts in Earthquake Engineering", Applied Mechanics in Earthquake Engineering, The Winter Annual Meeting of ASME, New York, November 1974.
10. Ang, A. H.-S., "Risk and Reliability Analysis in Engineering Design", Symposium on Structural and Geotechnical Mechanics, Urbana, Ill., October 1975.
11. Ang, A. H.-S. and Cornell, C., "Reliability Basis of Structural Safety and Design", Journal of the Structural Division, ASCE, No. ST9, September 1974.
12. Aoyama, H., "Moment-Curvature Characteristics of Reinforced Concrete Members Subjected to Axial Load and Reversal Bending", Flexural Mechanics of Reinforced Concrete, Proc. of the International Symposium, Miami, Fla., November 1964.
13. Aoyama, H., Endo, T. and Minami, T., "Behavior of Reinforced Concrete Frames Subjected to Reversals of Horizontal Forces", Proc. of Japan Earthquake Engineering Symposium, Tokyo, Japan, October 1966.

14. ASCE-ACI, Committee 426, "The Shear Strength of Reinforced Concrete Members", Journal of the Structural Division, ASCE, No. ST6, June 1973.
15. Beaufait, F. and Williams, R., "Experimental Study of Reinforced Concrete Frames Subjected to Alternating Sway Forces", ACI Journal, Proc., Vol. 65, November 1968.
16. Bertero, V. and McClure, G., "Behavior of Reinforced Concrete Frames Subjected to Repeated Reversible Loads", ACI Journal, Proc., Vol. 66, October 1964.
17. Biggs, J., Hansen, R. and Holley, M., "On Methods of Structural Analysis and Design for Earthquake", Symposium on Structural and Geotechnical Mechanics, Urbana, Ill., October 1975.
18. Blume, J., "The Motion and Damping of Buildings Relative to Seismic Response Spectra", Bull. Seism. Soc. of America, 60 (1), February 1970.
19. Blume, J. and Meehan, J., "A Structural Dynamic Research Program on Actual School Buildings", Proc. 2nd World Conf. in Earthquake Eng., Tokyo, Japan, 1960.
20. Blume, J., Newmark, N. and Corning, L., "Design of Multistory Reinforced Concrete Buildings for Earthquake Motions", Portland Cement Association, Skokie, 1961.
21. Blume, J., Sharpe, R. and Dalal, J., "Evaluation and Recommendations for Shape of Earthquake Ground Motion Response Spectra Based on Statistical Analysis of 33 Records", John A. Blume and Associates, Engineers, San Francisco, Cal., 1972.
22. Bolotin, V., "Statistical Methods in Structural Mechanics", Holden-Day Series in Mathematical Physics, Holden-Day Inc., 1969.
23. Borges, J. and Castenheta, M., "Structural Safety", 2nd ed., National Civil Engineering Laboratory, Lisbon, Portugal, March 1971.
24. Borges, J. and Castenheta, M., "Statistical Definition and Combination of Loads", Probabilistic Design of Reinforced Concrete Buildings, ACI-SP-31, 1972.
25. Branson, D., "Design Procedures for Computing Deflections", ACI Journal, Proc., Vol. 65, September 1968.
26. Burns, N. and Siess, C., "Load-Deformation Characteristics of Beam-Column Connections in Reinforced Concrete", Structural Research Series No. 234, University of Illinois, Urbana, Ill., January 1962.
27. Burns, N. and Siess, C., "Repeated and Reversed Loading in Reinforced Concrete", Journal of the Structural Division, ASCE, No. ST10, October 1966.

28. Clough, R. and Benuska, K., "FHA Study of Seismic Design Criteria for High Rise Buildings", Report HUD, TS-3, Washington, D.C.: Federal Housing Administration, 1966.
29. Corley, W., "Rotational Capacity of Reinforced Concrete Beams", Journal of the Structural Division, ASCE, No. ST5, October 1966.
30. Cornell, C., "Engineering Seismic Risk Analysis", Bull. Seism. Soc. of America, Vol. 58, No. 5, October 1968.
31. Der-Kiureghian, A. and Ang, A. H.-S., "A Line-Source Model for Seismic Risk Analysis", Structural Research Series No. 419, University of Illinois, Urbana, Ill., October 1975.
32. Donovan, N., "Earthquake Hazards for Buildings", Building Practices for Disaster Mitigation, Building Science Series No. 46, U.S. Department of Commerce, National Bureau of Standards, February 1973.
33. Ellingwood, B. and Ang, A. H.-S., "A Probabilistic Study of Safety Criteria for Design", Structural Research Series No. 387, University of Illinois, Urbana, Ill., June 1972.
34. Englekirk, R. and Matthiesen, R., "Forced Vibration of an Eight Story Reinforced Concrete Building", Bull. Seism. Soc. of America, Vol. 57 (3), June 1967.
35. Esteva, L., "Seismic Risk and Seismic Design Decisions", Seismic Design of Nuclear Power Plants, The M.I.T. Press, Cambridge, Mass., 1971.
36. Esteva, L. and Villaverde, R., "Seismic Risk, Design Spectra and Structural Reliability", Proc. 5th World Conf. in Earthquake Eng., Rome, Italy, 1973.
37. Freudenthal, A., "Safety of Structures", Transactions, ASCE, Vol. 112, 1947.
38. Funahashi, I. and Kinoshita, K., "The Vibrational Analysis of the Tower Building", Proc. 3rd World Conf. in Earthquake Eng., New Zealand, 1965.
39. The Group for Dynamic Tests of High-Rise Buildings, "Summarized Report on Dynamic Tests of High-Rise Buildings and Cooperative Plan for Large-Scale Vibration Tests in Japan", Proc. 4th World Conf. in Earthquake Eng., Santiago, Chile, 1969.
40. Gulkan, P. and Sozen, M., "Response and Energy-Dissipation of Reinforced Concrete Frames Subjected to Strong Base Motions", Structural Research Series No. 377, University of Illinois, Urbana, Ill., May 1971.
41. Gungor, I., "A Study of Stochastic Models for Predicting Maximum Earthquake Structural Response", Ph.D. Thesis, Civil Engineering Department, University of Illinois, Urbana, Ill., 1971.

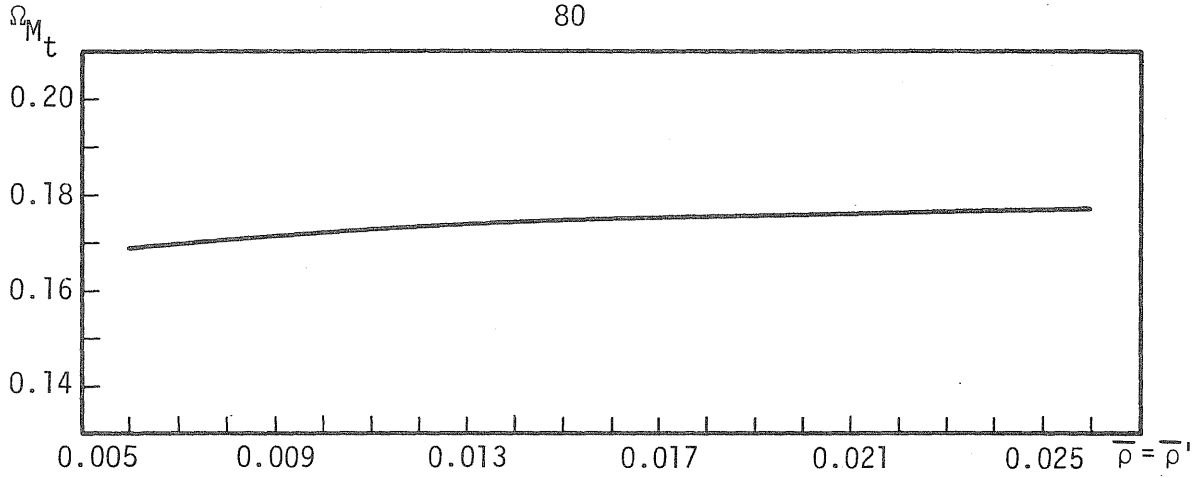
42. Haddadin, M., Hong, S. and Mattock, A., "Stirrup Effectiveness in Reinforced Concrete Beams with Axial Force", Journal of the Structural Division, ASCE, No. ST9, September 1971.
43. Hart, G., "Eigenvalue Uncertainty in Stressed Structures", Journal of the Engineering Mechanics, ASCE, No. EM3, June 1973.
44. Hart, G., Lew, M. and DiJulio, R., "High-Rise Building Response: Damping and Period Non-Linearities", Proc. 5th World Conf. in Earthquake Eng., Rome, Italy, 1973.
45. Hart, G. and Vasudevan, R., "Earthquake Design of Buildings: Damping", Journal of the Structural Division, ASCE, No. ST1, January 1975.
46. Hasselman, T. and Hart, G., "Modal Analysis of Random Structural Systems", Journal of the Engineering Mechanics Division, ASCE, No. EM3, June 1972.
47. Heaney, A., "A Reliability-Based Study Concerning Live Loads and Codified Structural Design", Ph.D. Thesis, Department of Civil Engineering, University of Waterloo, March 1971.
48. Hidalgo, P. and Clough, R., "Earthquake Simulator Study of a Reinforced Concrete Frame", Earthquake Engineering Research Center, University of California, Berkeley, December 1974.
49. Hognestad, E., Hanson, N. and McHenry, D., "Concrete Stress Distribution in Ultimate Strength Design", ACI Journal, Proc. Vol. 52, December 1955.
50. Housner, G., "Behavior of Structures during Earthquakes", Journal of the Engineering Mechanical Division, ASCE, No. EM4, October 1959.
51. Hudson, D., "Dynamic Tests of Full-Scale Structures", Earthquake Engineering, Chapter 7, Wiegel, R., editor, Prentice-Hall, 1970.
52. Hudson, D., "Destructive Earthquake Ground Motions", The Winter Annual Meeting of the American Society of Mechanical Engineering, New York, N.Y., November 1974.
53. Jennings, P., Housner, G. and Tsai, N., "Simulated Earthquake Motions", Earthquake Engineering Research Laboratory, Pasadena, Cal., April 1968.
54. Kanai, K., "Semi-empirical Formula for the Seismic Characteristics of the Ground", Bull. of the Earthquake Research Inst., Univ. of Tokyo, 35, 1957.
55. Kuroiwa, J., "Vibration Test of a Multistory Building", Earthquake Engineering Research Laboratory, Calif. Inst. of Technology, June 1967.
56. Lin, Y., "Probabilistic Theory of Structural Dynamics", McGraw-Hill Book Co., Inc., New York, 1969.

57. Lutes, L., "Equivalent Linearization for Random Vibration", Journal of the Engineering Mechanics Division, ASCE, No. EM3, June 1970.
58. M.I.T. Department of Civil Engineering, "Statistical Studies of Response of MDOF Systems to Real and Artificial Ground Motions", Internal Study Reports No. 4 and 6, M.I.T. Dept. of Civil Eng., January and August 1975.
59. Mattock, A., "Rotational Capacity of Hinging Regions in Reinforced Concrete Beams", Flexural Mechanics of Reinforced Concrete, Proc. of the International Symposium, Miami, Fla., November 1964.
60. Mattock, A., "Diagonal Tension Cracking in Concrete Beams with Axial Forces", Journal of the Structural Division, ASCE, No. ST9, September 1969.
61. Mattock, A., Kriz, L. and Hognestad, E., "Rectangular Concrete Stress Distribution in Ultimate Strength Design", ACI Journal, Proc., Vol. 57, February 1961.
62. McCafferty, R. and Moody, M., "Dynamic Characteristics of Reinforced Concrete Beam-Column Specimens for Various Levels of Cracking", Proc. 5th World Conf. in Earthquake Eng., Rome, Italy, 1973.
63. McCollister, H., Siess, C. and Newmark, N., "Load-Deformation Characteristics of Simulated Beam-Column Connections in Reinforced Concrete", Structural Research Series No. 76, University of Illinois, Urbana, Ill., June 1954.
64. McGuire, R., "Seismic Structural Response Risk Analysis, Incorporating Peak Response Regressions on Earthquake Magnitude and Distance", M.I.T. Dept. of Civil Eng., R74-51-Structures Publication No. 399, August 1974.
65. McGuire, R. and Cornell, C., "Live Load Effects in Office Buildings", M.I.T. Dept. of Civil Eng., R73-28 Structures Publication No. 365, July 1973.
66. McGuire, R. and Cornell, C., "Live Load Effects in Office Buildings", Journal of the Structural Division, ASCE, No. ST7, July 1974.
67. Milne, W. and Davenport, A., "Distribution of Earthquake Risk in Canada", Bull. Seism. Soc. of America, Vol. 59, (2), April 1969.
68. Mitchell, G. and Woodgate, R., "Floor Loadings in Office Buildings. The Result of a Survey", CP3/71 Building Design Station, Garston, United Kingdom, January 1971.
69. Mohraz, B., Hall, W. and Newmark, N., "A Study of Vertical and Horizontal Earthquake Spectra", Division of Reactor Standards, U.S. Atomic Energy Commission, Washington, D.C., December 1972.

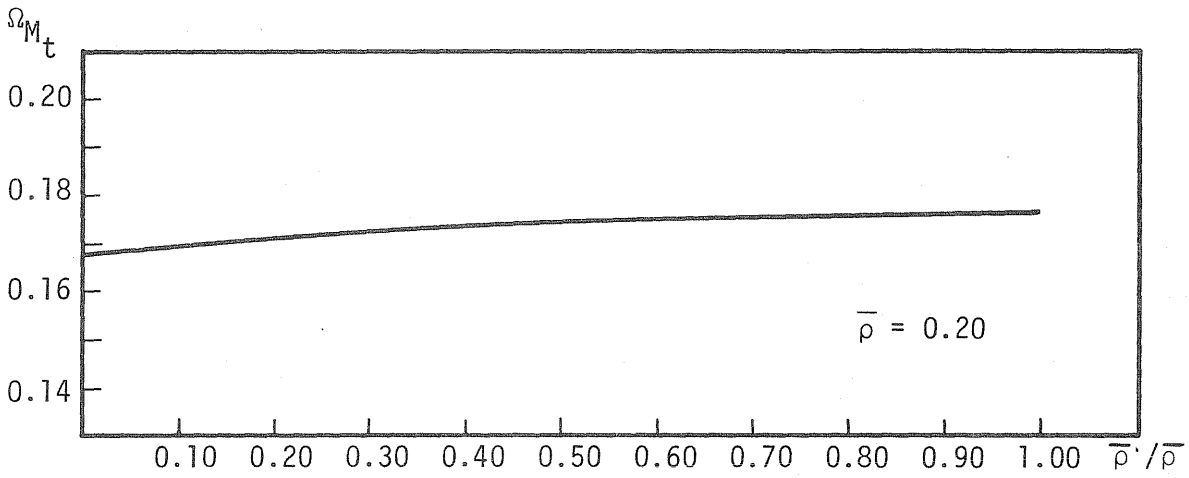
70. Nakagawa, K., "Vibrational Characteristics of Buildings Part II. Vibrational Characteristics of Reinforced Concrete Buildings Existing in Japan", Proc. 2nd World Conf. in Earthquake Eng., Tokyo, Japan, 1960.
71. Newmark, N., Blume, J. and Kapur, K., "Design Response Spectra for Nuclear Power Plants", Paper presented at the Structural Engineers ASCE Conference, San Francisco, Calif., April 1973.
72. Newmark, N. and Rosenbleuth, E., "Fundamentals of Earthquake Engineering", Prentice-Hall Inc., 1971.
73. Nielsen, N., "Dynamic Response of Multistory Buildings", Earthquake Engineering Research Laboratory, Calif. Inst. of Technology, 1964.
74. Park, R. and Paulay, T., "Reinforced Concrete Structures", Wiley-Interscience, 1975.
75. Peir, J., "A Stochastic Live Load Model for Buildings", Research Report R71-35, M.I.T. Dept. of Civil Eng., October 1971.
76. Peir, J. and Cornell, C., "Spatial and Temporal Variability of Live Loads", Journal of the Structural Division, ASCE, No. ST5, May 1973.
77. Penzien, J., "Applications of Random Vibration Theory", Earthquake Engineering, Chapter 13, Wiegel, R., editor, Prentice-Hall, 1970.
78. Penzien, J. and Liu, S.-C., "Nondeterministic Analysis of Nonlinear Structures Subjected to Earthquake Excitations", Proc. 4th World Conf. in Earthquake Eng., Santiago, Chile, 1969.
79. Petrovski, J., Jurukovski, D. and Paskalov, T., "Dynamic Properties of Fourteen Story R.C. Frame Building from Full Scale Forced Vibration Study and Formulation of Mathematical Model", Proc. 5th World Conf. in Earthquake Eng., Rome, Italy, 1973.
80. Pfrang, E., Sozen, M. and Siess, C., "Load-Moment-Curvature Characteristics of Reinforced Concrete Cross Sections", ACI Journal, Proc., Vol. 61, July 1964.
81. Rajagopalan, K. and Ferguson, P., "Exploratory Shear Tests Emphasizing Percentage of Longitudinal Steel", ACI Journal, Proc., Vol. 65, August 1968.
82. Ragan, B., "A Comparison of Code Requirements for Shear Strength of Reinforced Concrete Beams", Shear in Reinforced Concrete, ACI-SP-42, 1974.
83. Rascon, O. and Cornell, C., "A Physically Based Model to Simulate Strong Earthquake Records on Firm Ground", Proc. 4th World Conf. in Earthquake Eng., Santiago, Chile, 1969.

84. Reay, A. and Shepherd, R., "Steady State Vibration Tests of a Six-Story Reinforced Concrete Building", Bull. New Zealand Soc. for Earthquake Engineers 4, 1, March 1971.
85. Reay, A. and Shepherd, R., "Dynamic Characteristics of Three Adjacent Reinforced Concrete Buildings", Proc. The Institution of Civil Engineers, Paper No. 7388, September 1971.
86. Rosenblueth, E. and Esteva, L., "Reliability Bases for Some Mexican Codes", Probabilistic Design of Reinforced Concrete Buildings, ACI-SP-31, 1972.
87. Ruiz, W. and Winter, G., "Reinforced Concrete Beams under Repeated Loads", Journal of the Structural Division, ASCE, No. ST6, June 1969.
88. Schitf, A. and Bogdanoff, J., "An Estimation of the Standard Deviation of Natural Frequencies", Journal of Applied Mechanics Parts 1 and 2, 39, Series E, June 1972.
89. Seed, H., Ugas, C. and Lysmer, J., "Site Dependent Spectra for Earthquake-Resistant Design", Report No. EERC-74-12, College of Engineering, University of California, Berkeley, Cal., 1974.
90. Seismology Committee, Structural Engineers Association of California, "Recommended Lateral Force Requirements and Commentary", 1974.
91. Shiga, T. and Ogawa, J., "An Experimental Study on Dynamical Behavior of Reinforced Concrete Frames", Proc. of Japan Earthquake Engineering Symposium, Tokyo, Japan, October 1966.
92. Shiga, T., Ogawa, J., Shibata, A. and Shibuya, J., "The Dynamic Properties of Reinforced Concrete Members", Proc. U.S.-Japan Seminar on Earthquake Engineering with Emphasis on the Safety of School Buildings, Sendai, Japan, September 1970.
93. Shiga, T., Shibata, A. and Shibuya, J., "Dynamic Properties and Earthquake Response of a 9-story Reinforced Concrete Building", Proc. 5th World Conf. in Earthquake Eng., Rome, Italy, 1973.
94. Shinozuka, M., "Probability of Structural Failure under Random Loading", Journal of the Engineering Mechanics Division, ASCE, No. EM5, October 1964.
95. Shinozuka, M., "Dynamic Safety Analysis of Multistory Buildings", Journal of the Structural Division, ASCE, No. ST1, January 1968.
96. Tajimi, H., "A Statistical Method of Determining the Maximum Response of a Building Structure during an Earthquake", Proc. 2nd World Conf. in Earthquake Eng., Tokyo, Japan, 1960.

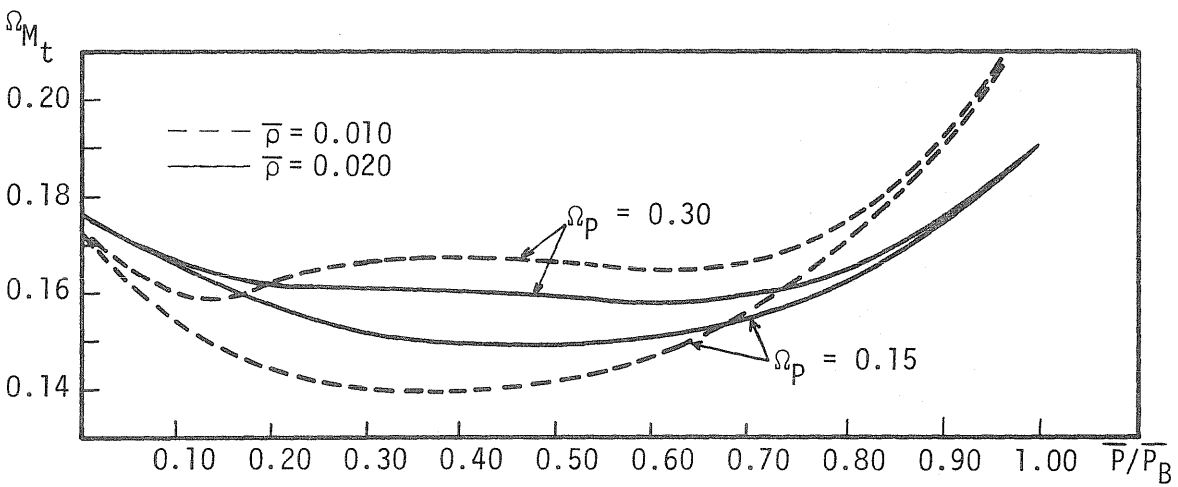
97. Tajimi, H., "Dynamic Behavior of a Multistory Building during the Matsushiro Earthquake", Recent Researches of Structural Mechanics, Tokyo, Japan, 1968.
98. Tanaka, T., Yoshizawa, S. and Osawa, Y., "Period and Damping of Vibration in Actual Buildings during Earthquakes", Bull. of the Earthquake Research Institute, University of Tokyo, Vol. 47, November 1969.
99. Tang, W. and Ang, A. H.-S., "Modeling, Analysis and Updating of Uncertainties", ASCE, National Structural Engineering Meeting, San Francisco, Cal., April 1973.
100. Taoka, G., Furumato, A. and Chiu, A., "Dynamic Properties of Tall Shear-Wall Buildings", Journal of the Structural Division, ASCE, No. ST2, February 1974.
101. U.S. Department of Commerce, "San Fernando, California Earthquake of February 9, 1971", National Oceanic and Atmospheric Administration, Washington, 1973.
102. Ward, H. and Crawford, R., "Wind-Induced Vibration and Buildings Modes", Bull. Seism. Soc. of America, 56 (4), August 1966.
103. Yamashiro, R. and Siess, C., "Moment Rotation Characteristics of Reinforced Concrete Members Subjected to Bending, Shear and Axial Load", Structural Research Series No. 260, University of Illinois, Urbana, Ill., December 1962.
104. Yu, W. and Winter, G., "Instantaneous and Long-Time Deflections of Reinforced Concrete Beams under Working Loads", ACI Journal, Proc., Vol. 57, July 1960.
105. Yucemen, M., Tang, W. and Ang, A. H.-S., "A Probabilistic Study of Safety and Design of Earth Slopes", Structural Research Series No. 402, Univ. of Illinois, Urbana, Ill., July 1973.
106. Zsutty, T., "Beam Shear Strength Prediction by Analysis of Existing Data", ACI Journal, Proc. Vol. 65, November 1968.



SYMMETRICALLY REINFORCED BEAM



DOUBLY REINFORCED BEAM



SYMMETRICALLY REINFORCED COLUMN

FIG. 2.1 COEFFICIENT OF VARIATION IN FLEXURAL CAPACITY

$$\bar{f}_c = 4.7 \text{ ksi}, \bar{f}_y = 47.7 \text{ ksi}$$

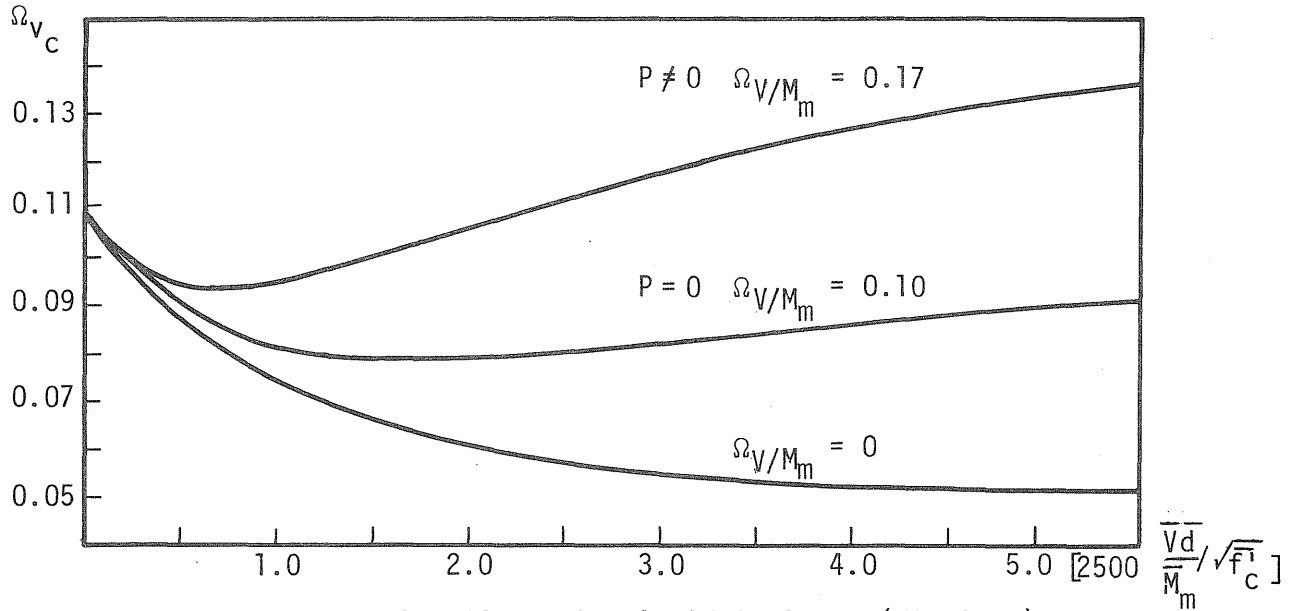
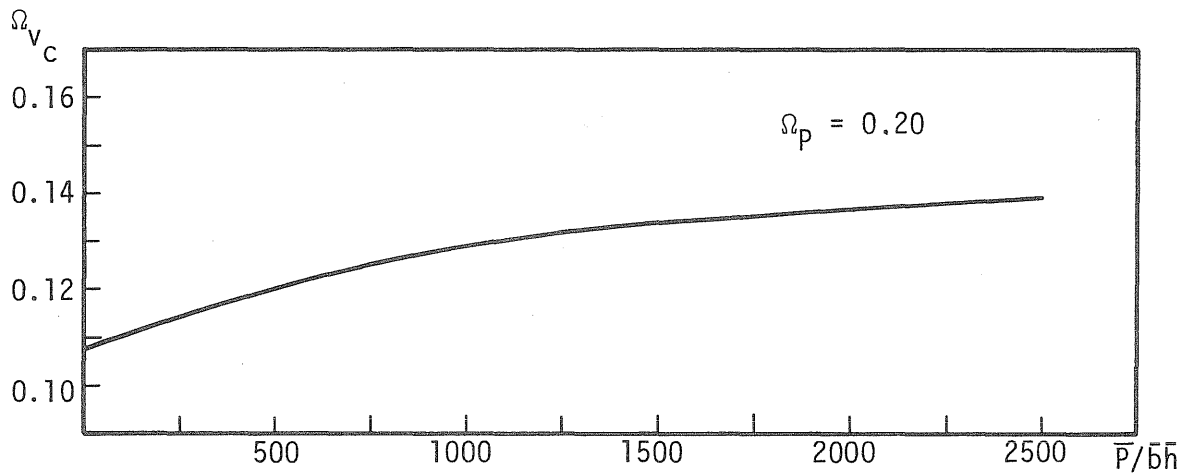
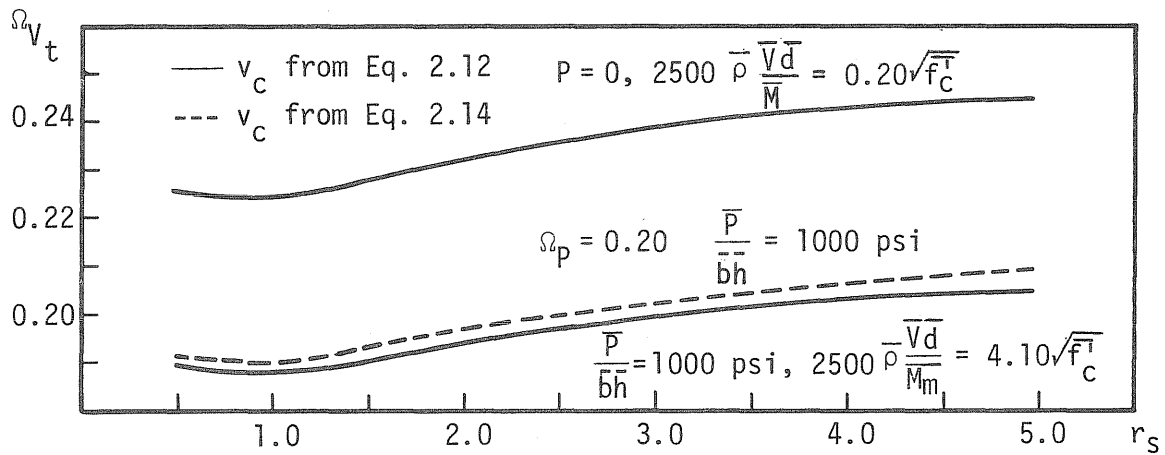
FIG. 2.2 COEFFICIENT OF VARIATION OF v_c (EQ. 2.14)FIG. 2.3 COEFFICIENT OF VARIATION OF v_c (EQ. 2.18)

FIG. 2.4 COEFFICIENT OF VARIATION IN SHEAR CAPACITY

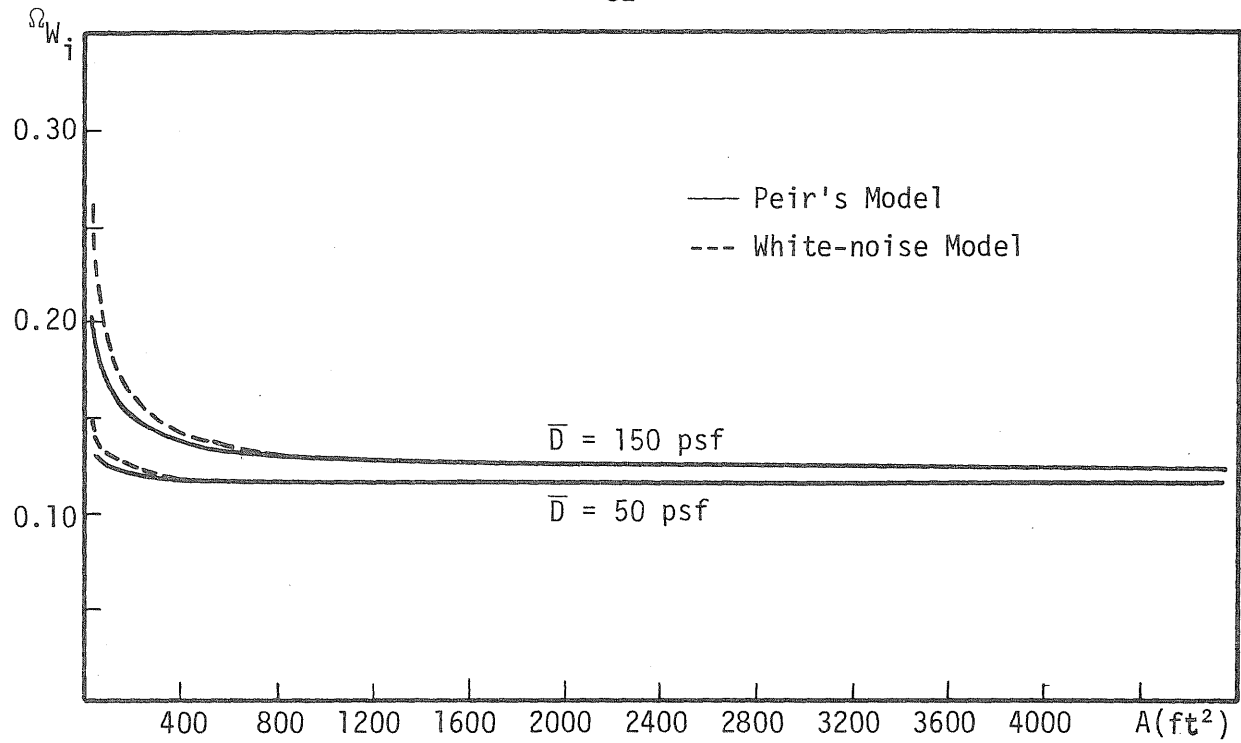


FIG. 3.1 COEFFICIENT OF VARIATION OF TOTAL DEAD AND LIVE LOAD ON A FLOOR

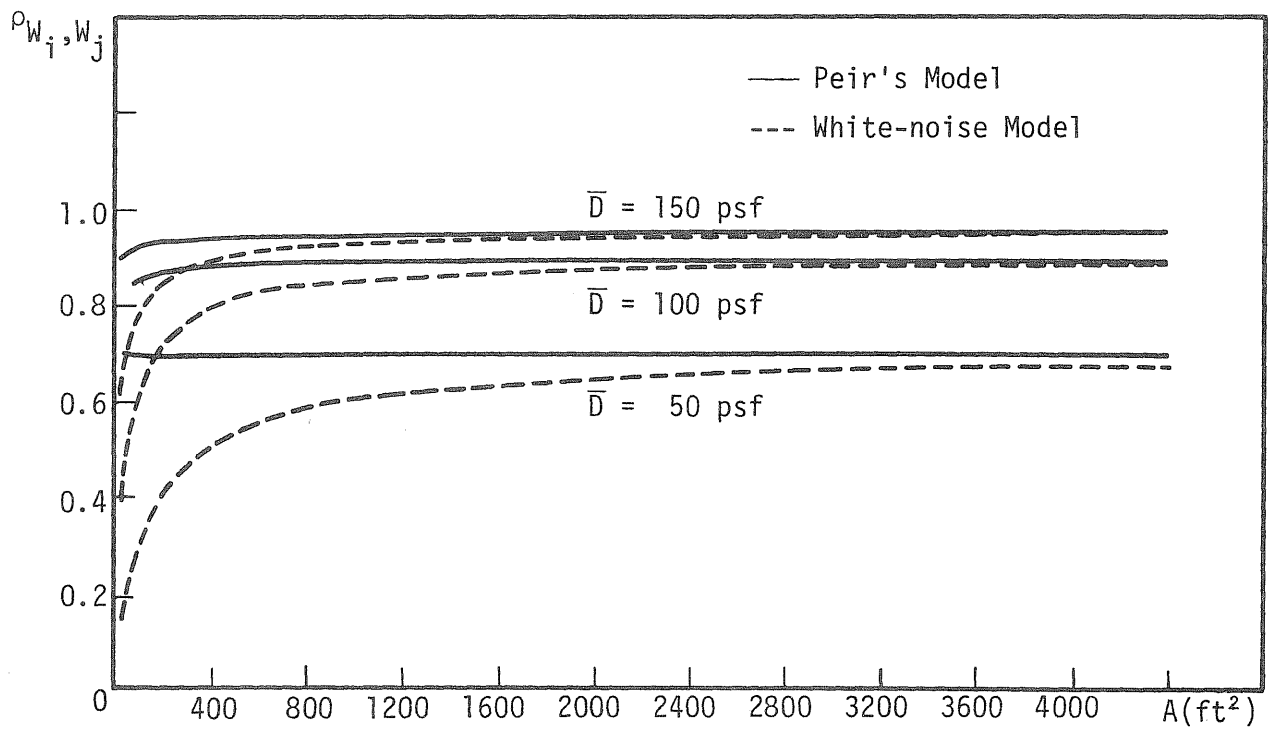


FIG. 3.2 CORRELATION COEFFICIENT BETWEEN TOTAL LOADS ON TWO FLOORS

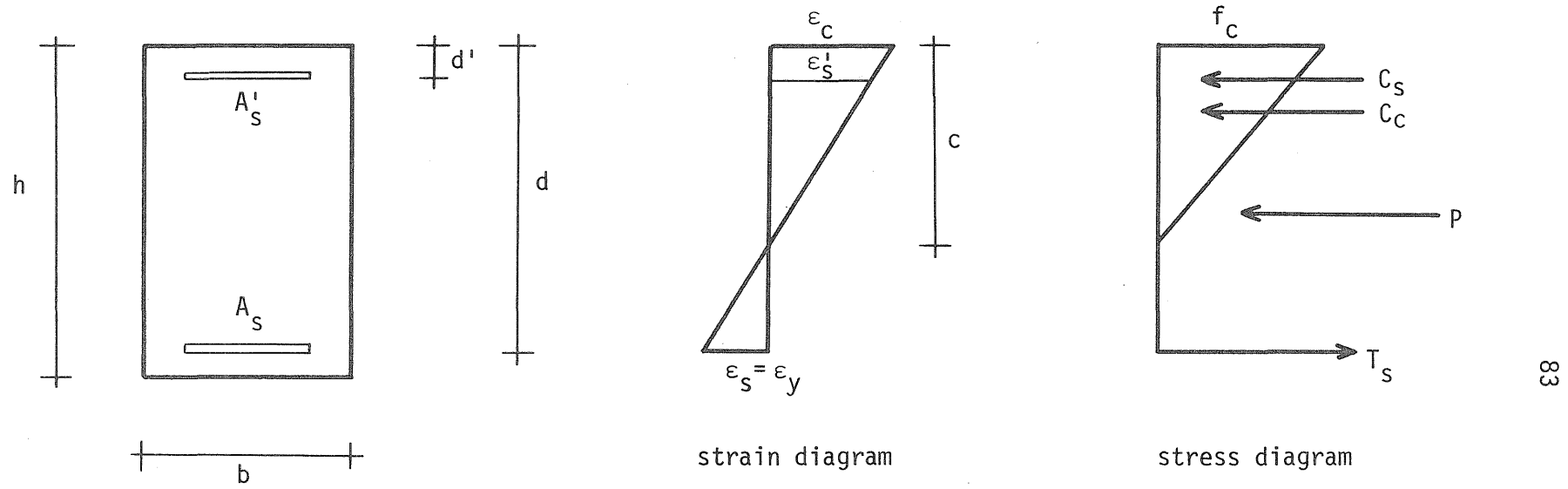


FIG. 3.3 ASSUMED STRAIN AND STRESS DISTRIBUTION FOR CALCULATION OF EI

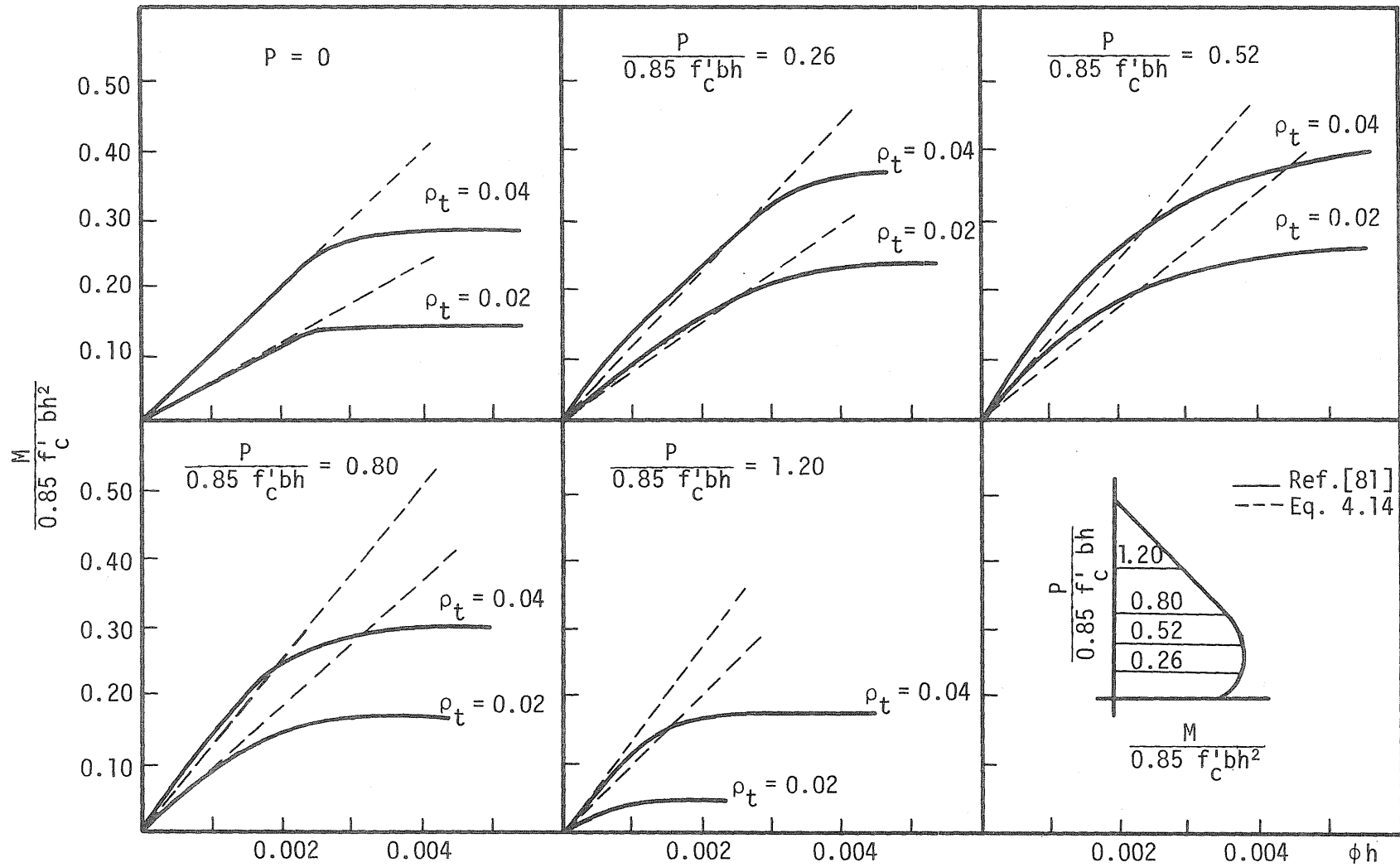


FIG. 3.4 MOMENT-CURVATURE RELATIONSHIP OF REINFORCED CONCRETE MEMBERS

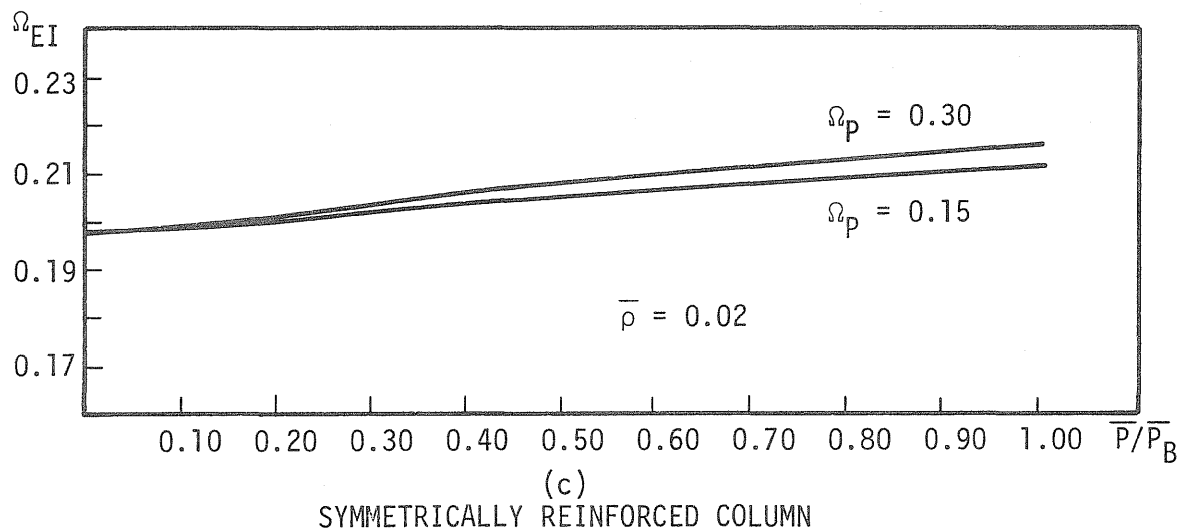
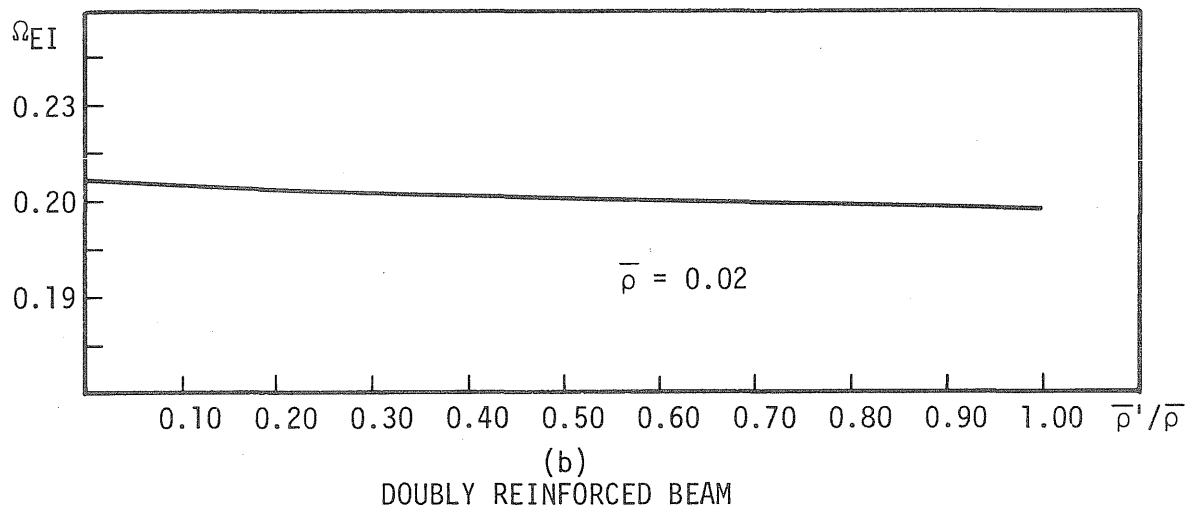
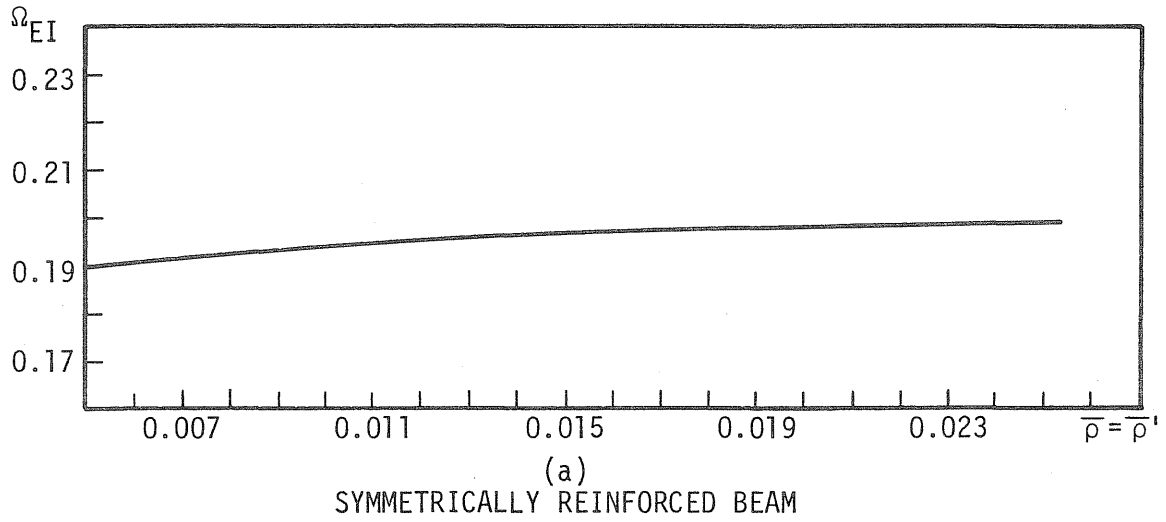


FIG. 3.5 COEFFICIENT OF VARIATION OF EI
 $\bar{f}'_c = 4.7$ ksi, $\bar{f}_y = 47.7$ ksi

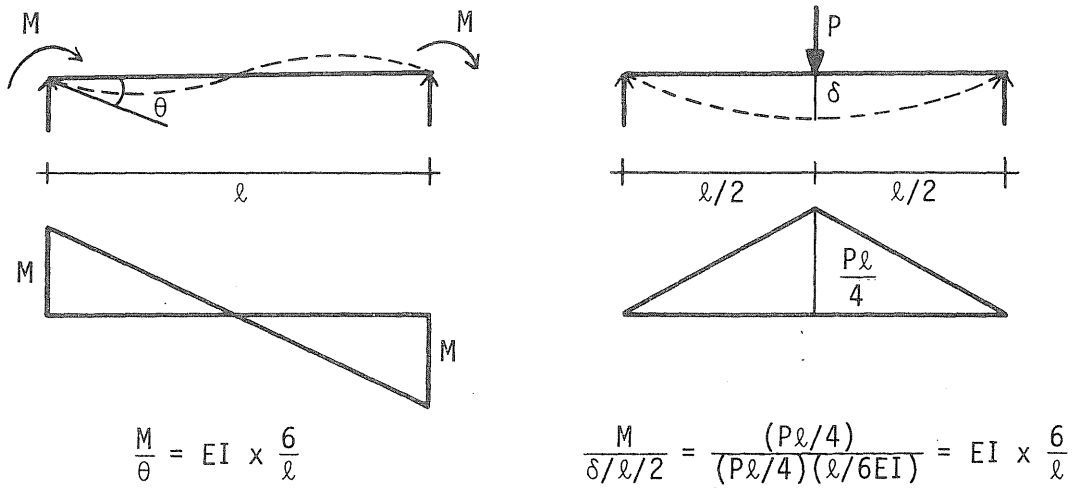
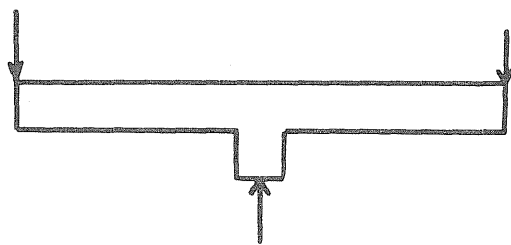
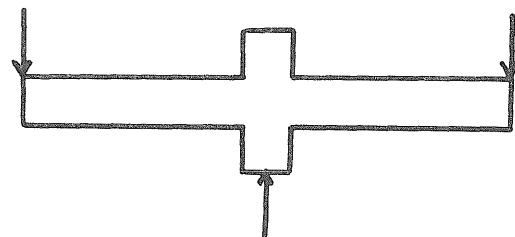


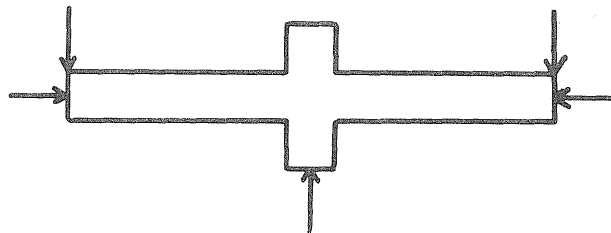
FIG. 3.6 END MOMENT-END ROTATION RELATIONSHIP OF ANTI-SYMMETRIC MEMBERS



McCollister, et al [63]



Burns and Siess [26]



Yamashiro and Siess [103]

FIG. 3.7 TYPES OF ELEMENTS TESTED

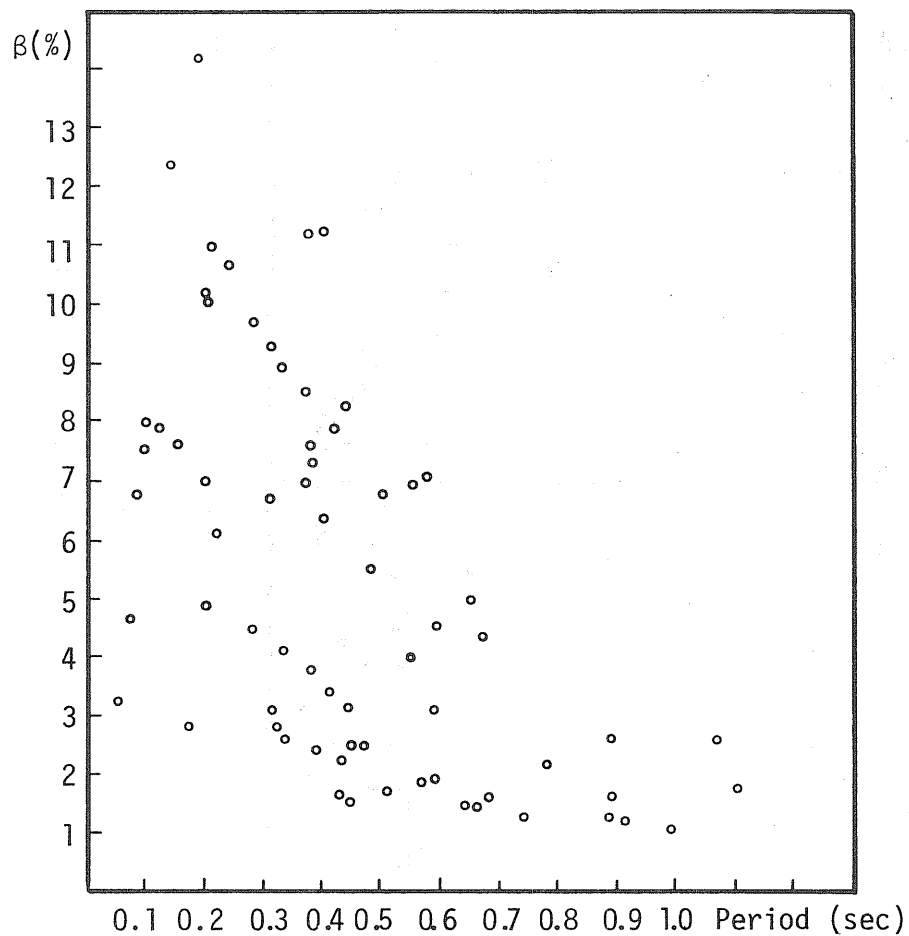


FIG. 3.8 DAMPING VALUES OBTAINED FROM FORCED VIBRATION TESTS OF FULL-SCALE STRUCTURES (ALL DATA)

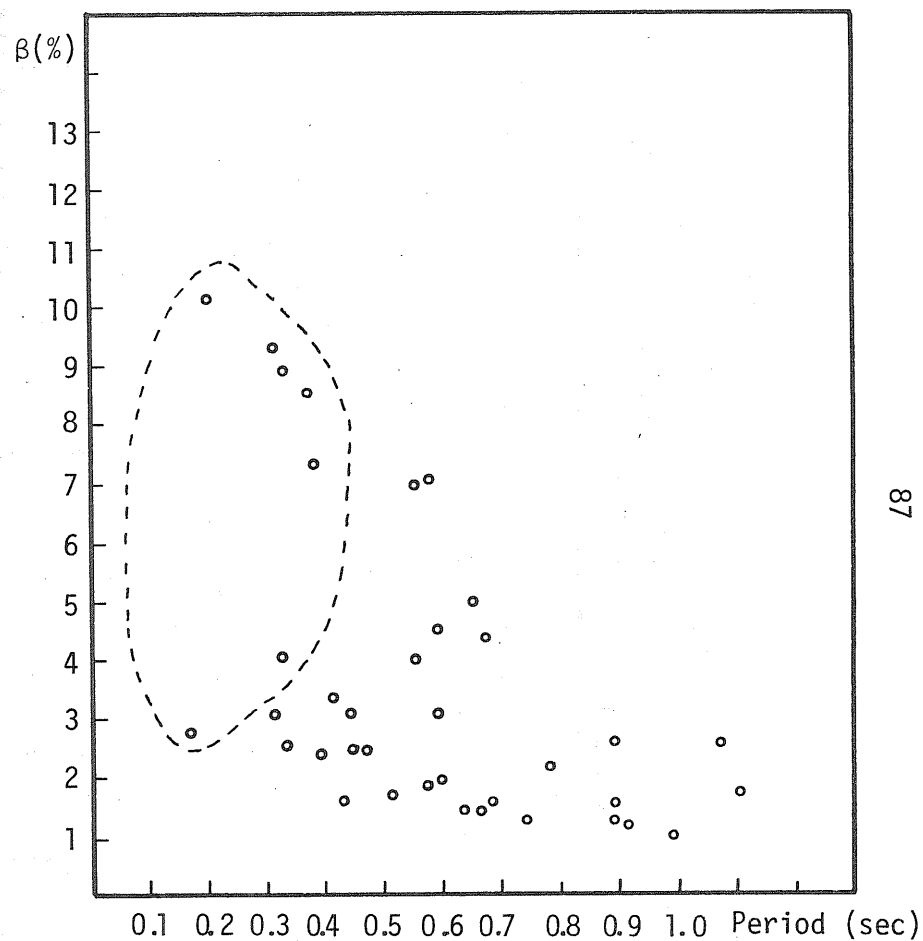


FIG. 3.9 DAMPING VALUES OBTAINED FROM FORCED VIBRATION TESTS OF FULL-SCALE STRUCTURES (DATA OF 1965-1973)

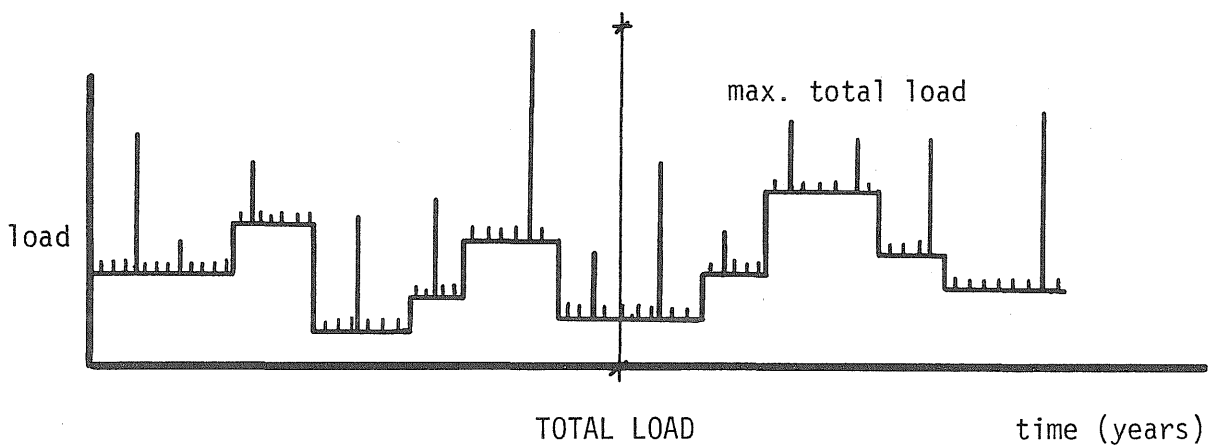
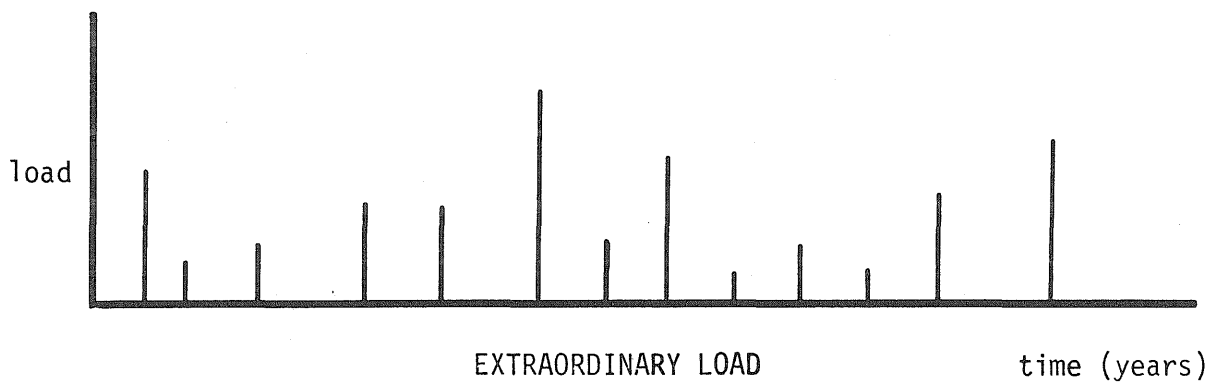
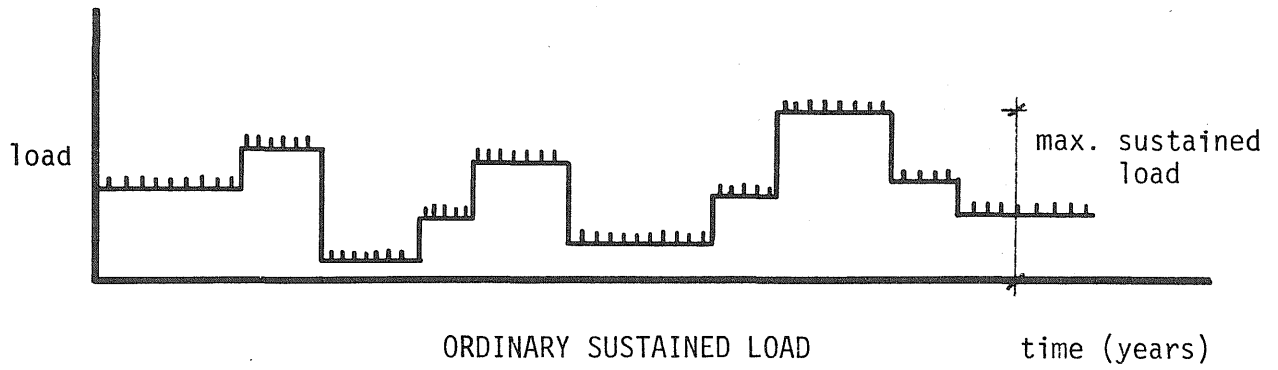


FIG. 4.1 LIVE LOAD MODEL

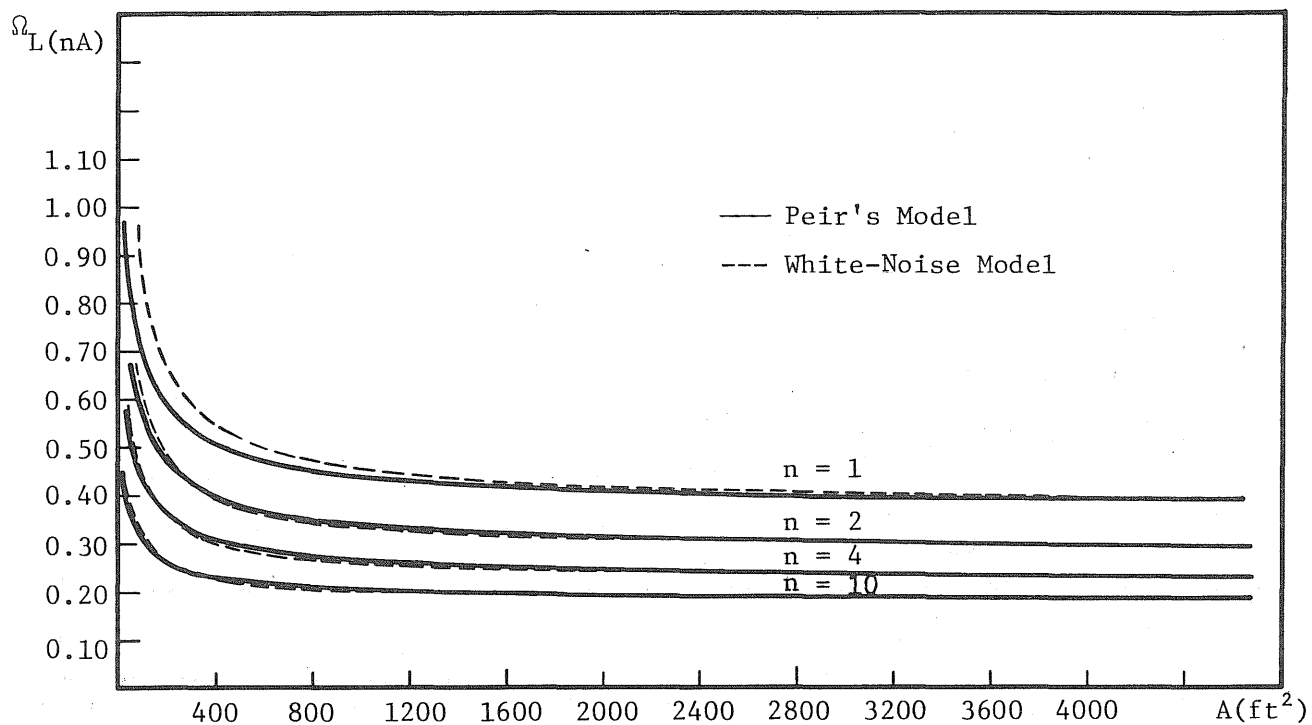


FIG. 4.2 COEFFICIENT OF VARIATION OF UNIT LIVE LOAD INTENSITY

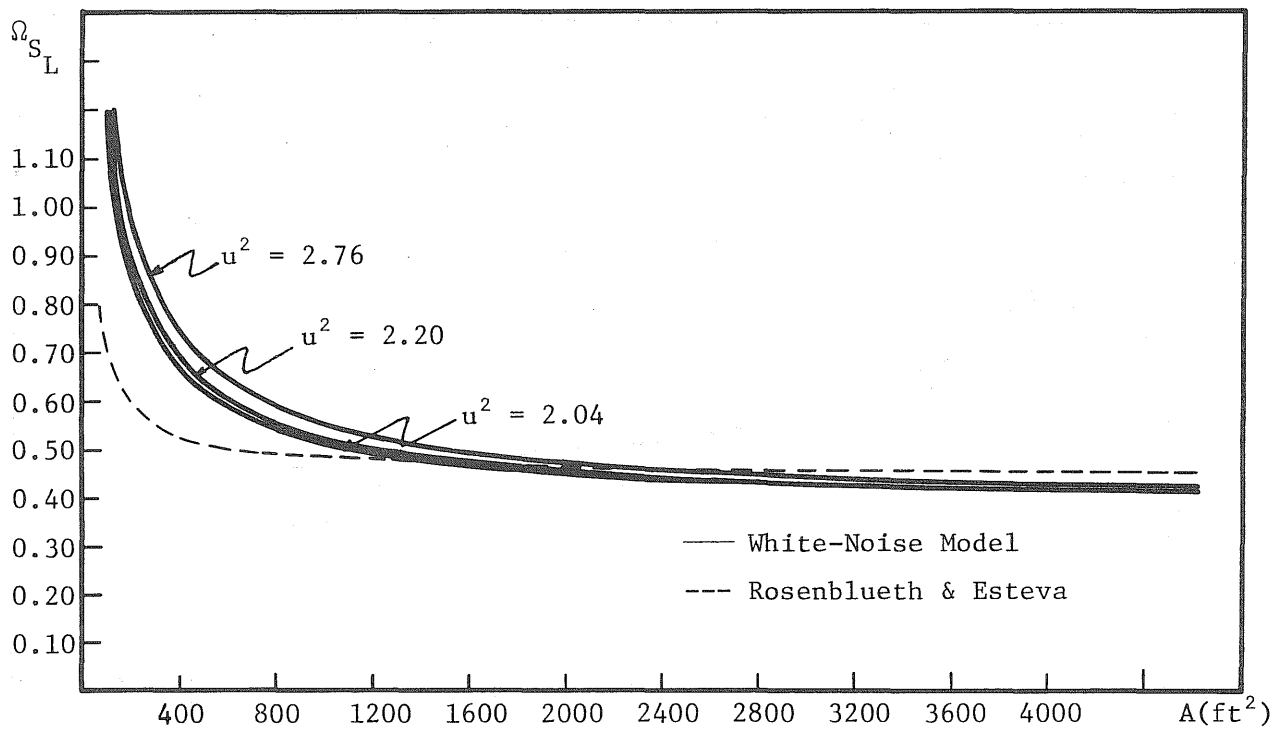


FIG. 4.3 COEFFICIENT OF VARIATION OF LIVE LOAD EFFECT

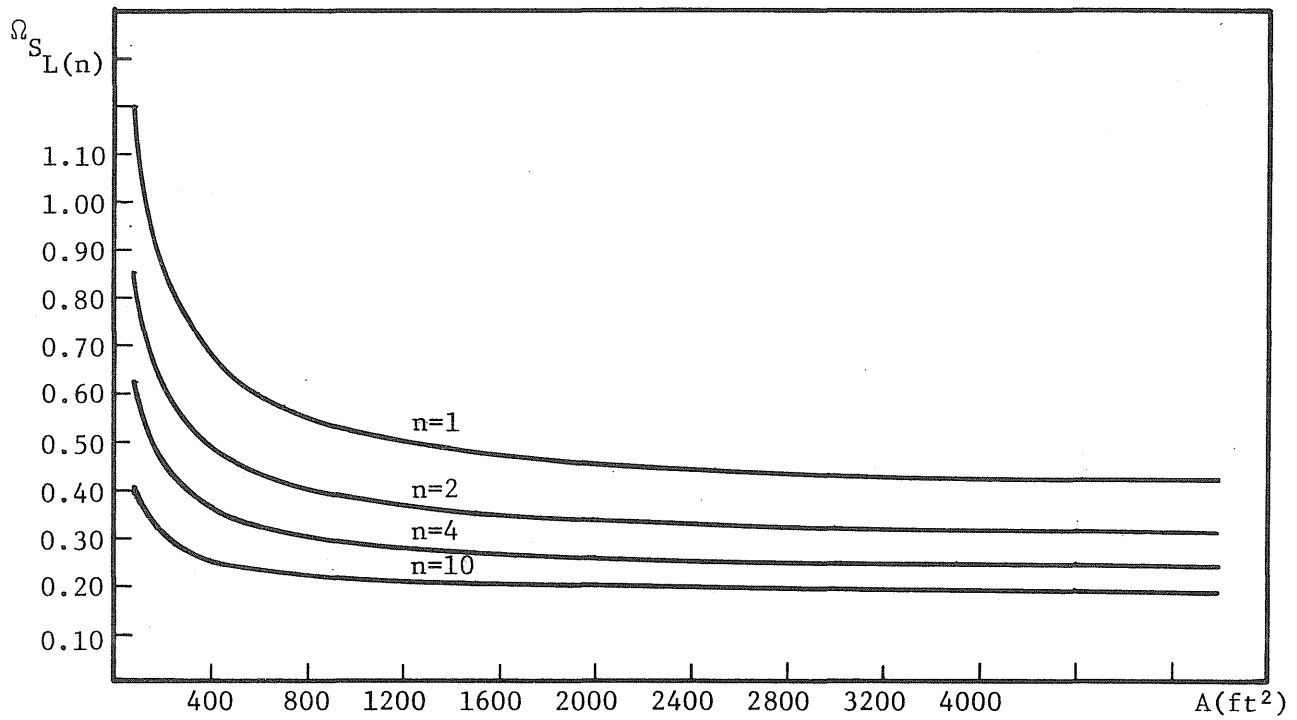


FIG. 4.4 COEFFICIENT OF VARIATION OF AXIAL LOAD IN A COLUMN SUPPORTING n FLOORS

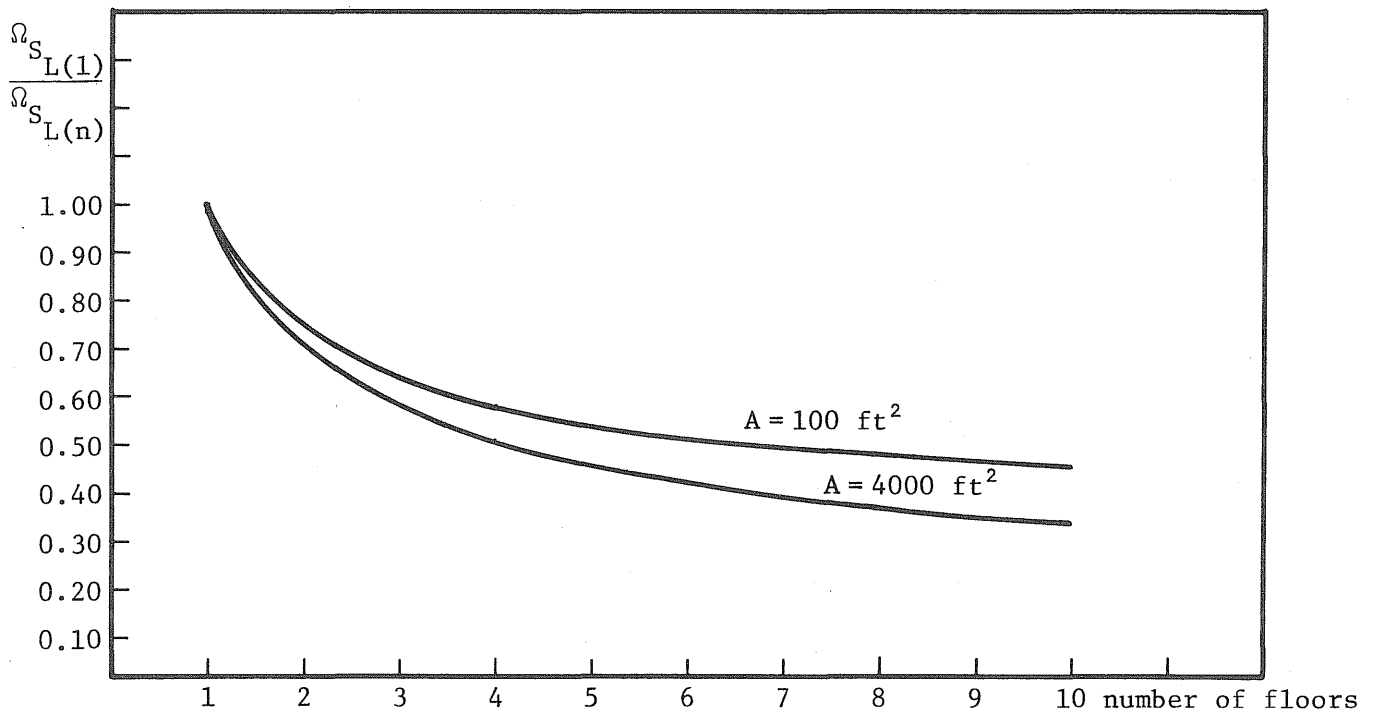


FIG. 4.5 REDUCTION IN COEFFICIENT OF VARIATION OF AXIAL LOAD IN A COLUMN AS A FUNCTION OF NUMBER OF FLOORS SUPPORTED

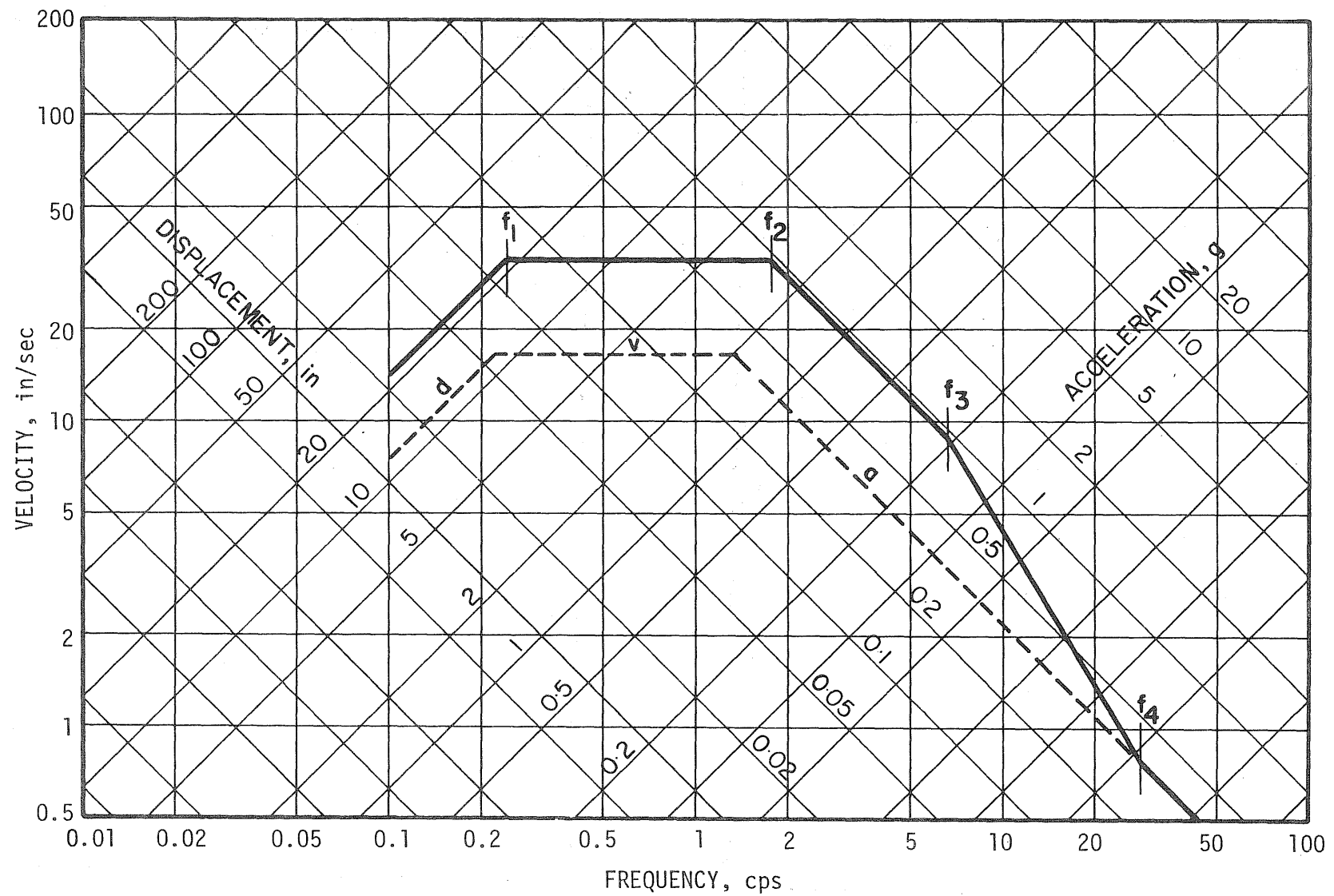


FIG. 4.6 BASIC SHAPE OF THE RESPONSE SPECTRUM [69]

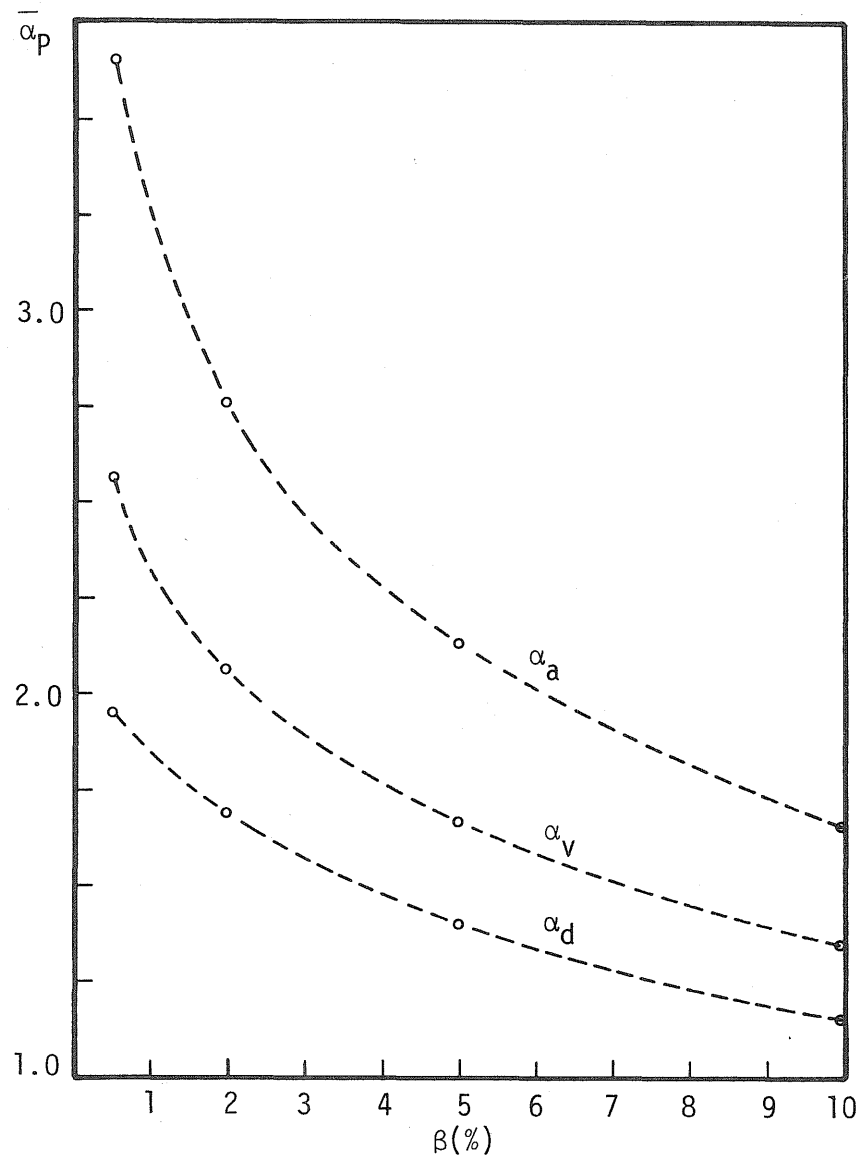


FIG. 4.7 CONDITIONAL MEANS OF AMPLIFICATION FACTORS

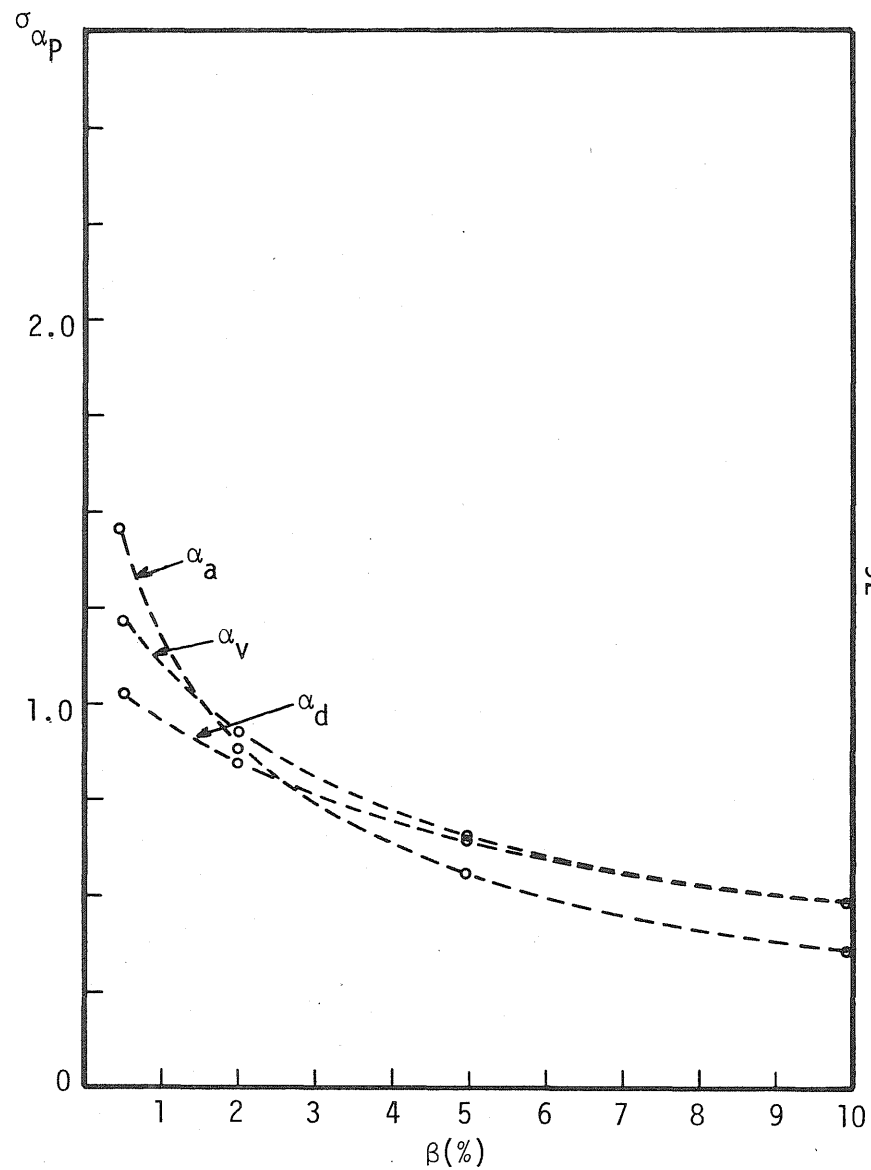


FIG. 4.8 CONDITIONAL STANDARD DEVIATIONS OF AMPLIFICATION FACTORS

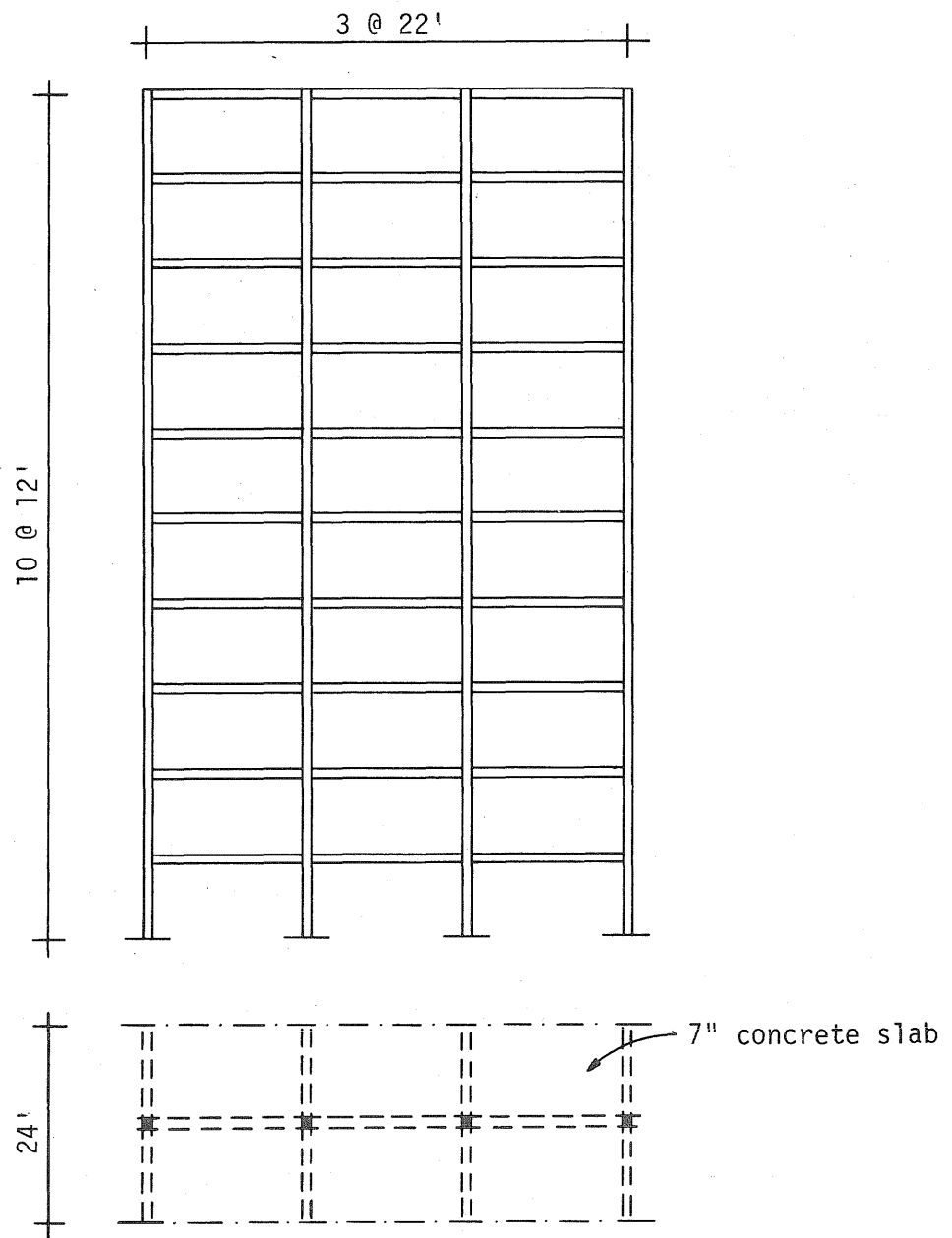


FIG. 5.1 PLAN AND ELEVATION OF STRUCTURES CONSIDERED

STRUCTURE 1				STRUCTURE 2			
16x30	16x30	21 X 21	18 X 18	16x35	16x35	12 X 30	12 X 24
	16x30	21 X 21	18 X 18		16x35	12 X 30	12 X 24
	16x30	21 X 21	18 X 18		16x35	12 X 30	12 X 24
	17x36	23 X 23	20 X 20		17x39	17 X 31	16 X 25
	17x36	23 X 23	20 X 20		17x39	17 X 31	16 X 25
17x36	17x36	23 X 23	20 X 20	17x39	17x39	17 X 31	16 X 25
	17x36	23 X 23	20 X 20		17x39	17 X 31	16 X 25
	17x36	23 X 23	20 X 20		17x39	17 X 31	16 X 25
28 X 28	28 X 28	28 X 28	23 X 23	20 X 37	20 X 37	20 X 37	17 X 31
	28 X 28	28 X 28	23 X 23		20 X 37	20 X 37	17 X 31
28 X 28	28 X 28	28 X 28	23 X 23	20 X 37	20 X 37	20 X 37	17 X 31
	28 X 28	28 X 28	23 X 23		20 X 37	20 X 37	17 X 31

FIG. 5.2 MEMBER DIMENSIONS OF STRUCTURE 1 AND STRUCTURE 2

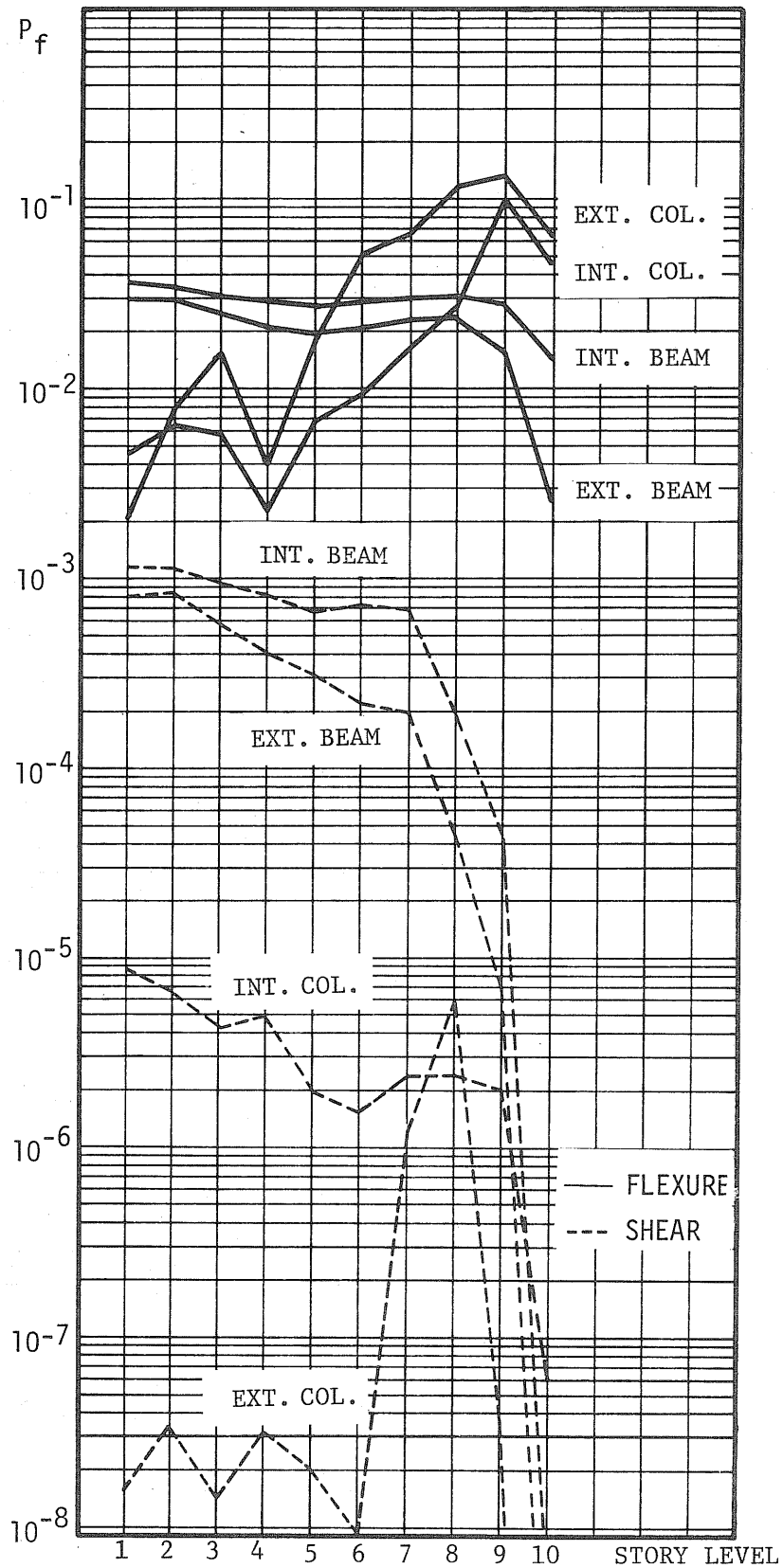


FIG. 5.3 PROBABILITY OF FAILURE OF SEAOC DESIGN, STRUCTURE 1; $a = 0.1 \text{ g}$, $\bar{\beta} = 4\%$

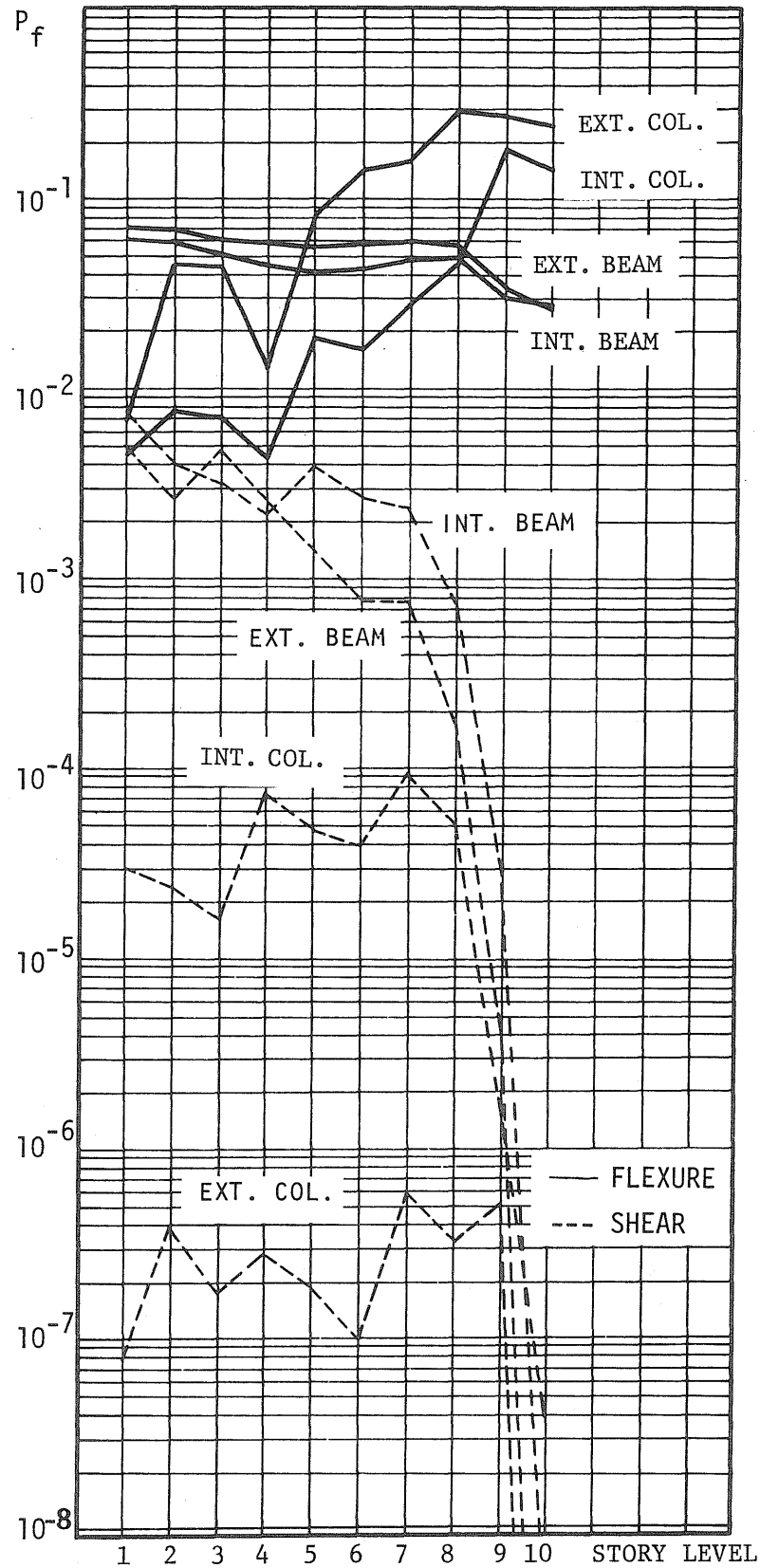


FIG. 5.4 PROBABILITY OF FAILURE OF SEAOC DESIGN, STRUCTURE 2; $a = 0.1 g$, $\beta = 4\%$

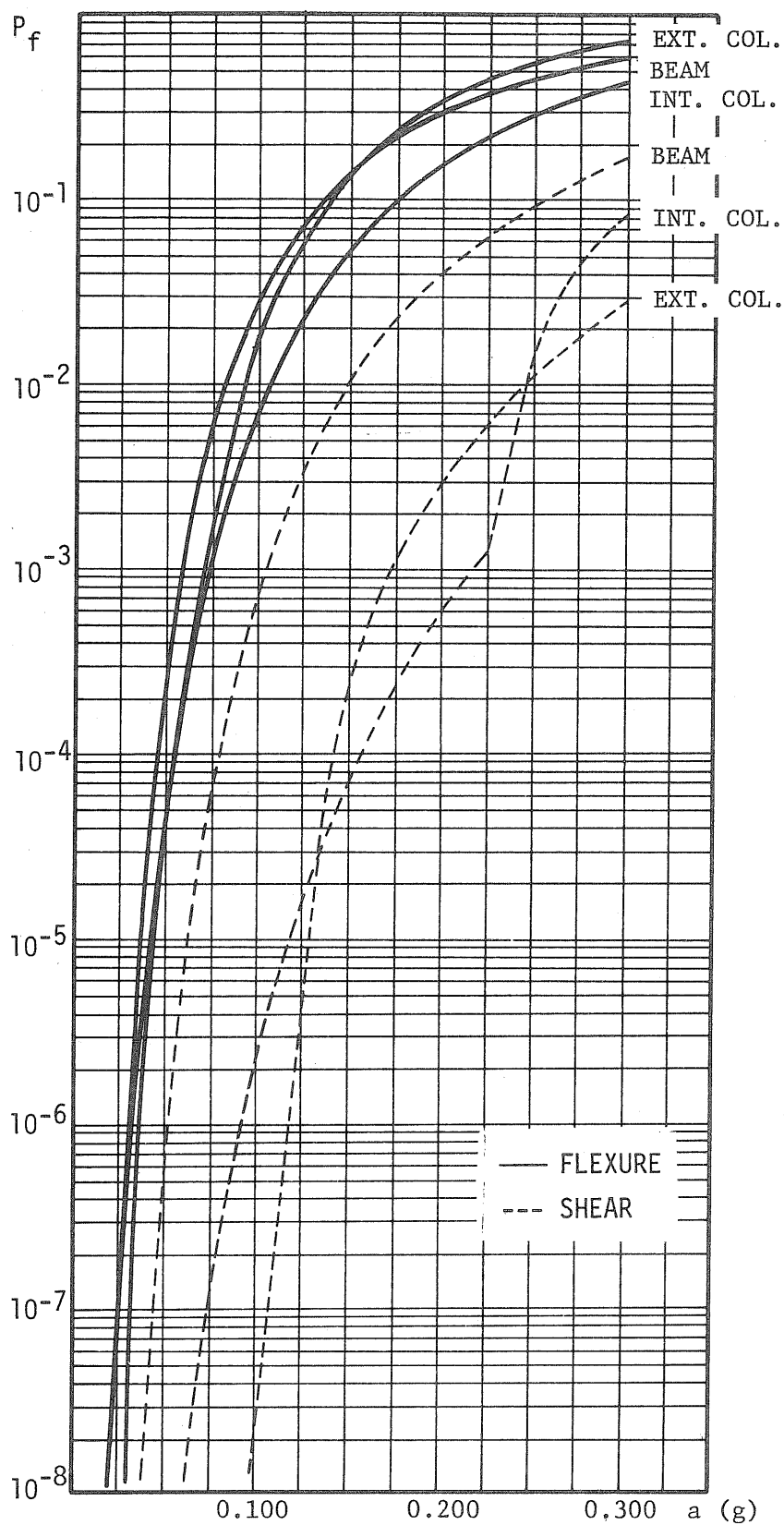


FIG. 5.5 PROBABILITY OF FAILURE OF INTERIOR BEAM AND COLUMNS AT LEVEL 5 OF STRUCTURE 1, $\beta = 4\%$

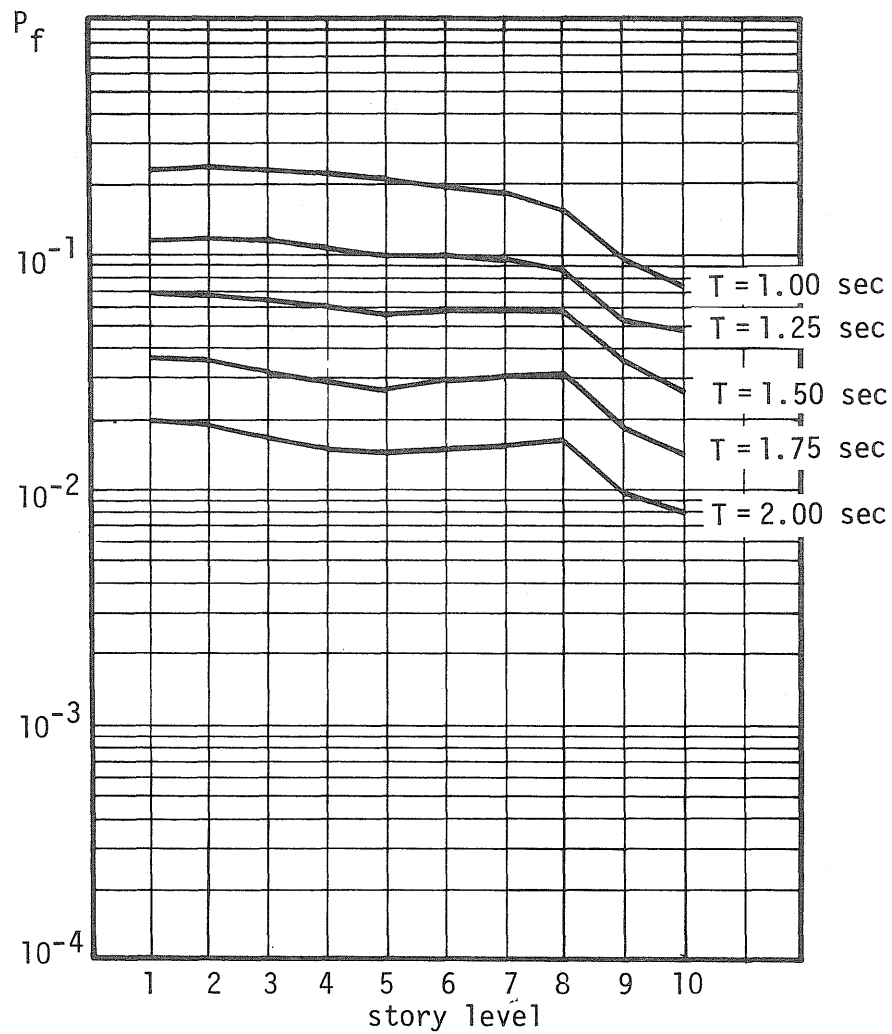


FIG. 5.6 FAILURE PROBABILITY OF INTERIOR BEAMS FOR DIFFERENT NATURAL PERIODS, $\bar{\beta} = 4\%$

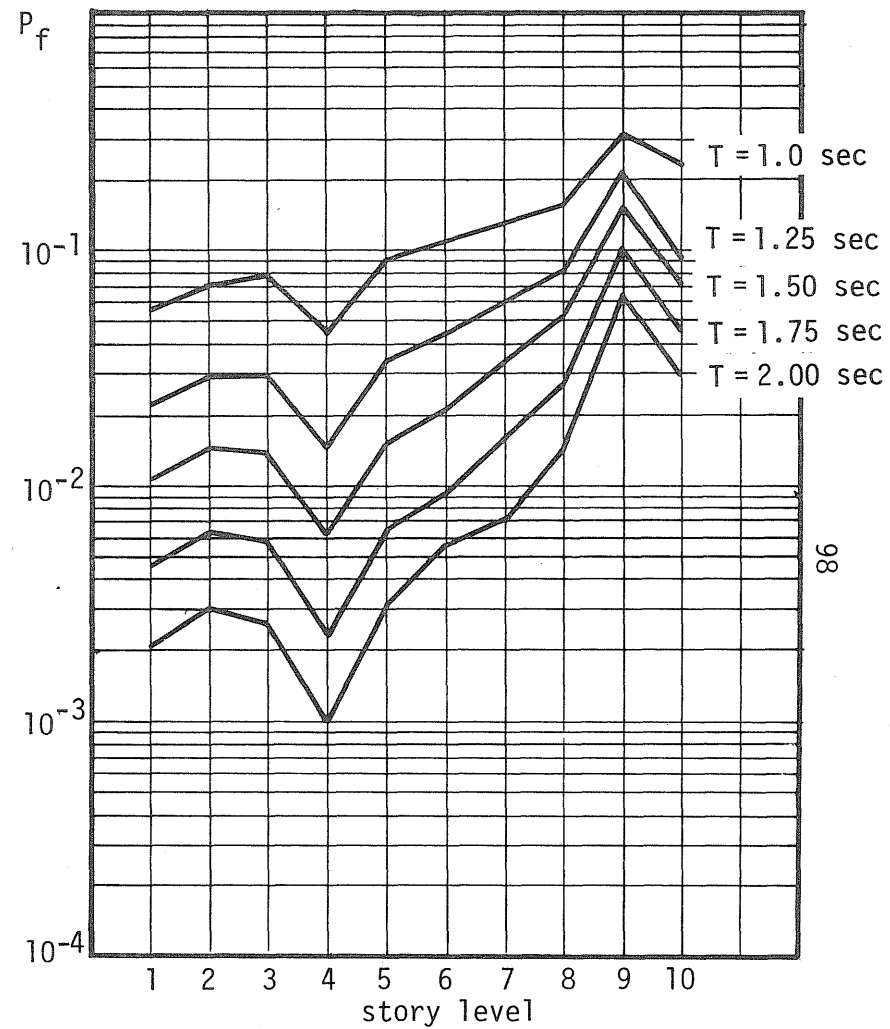


FIG. 5.7 FAILURE PROBABILITY OF INTERIOR COLUMNS FOR DIFFERENT NATURAL PERIODS, $\bar{\beta} = 4\%$

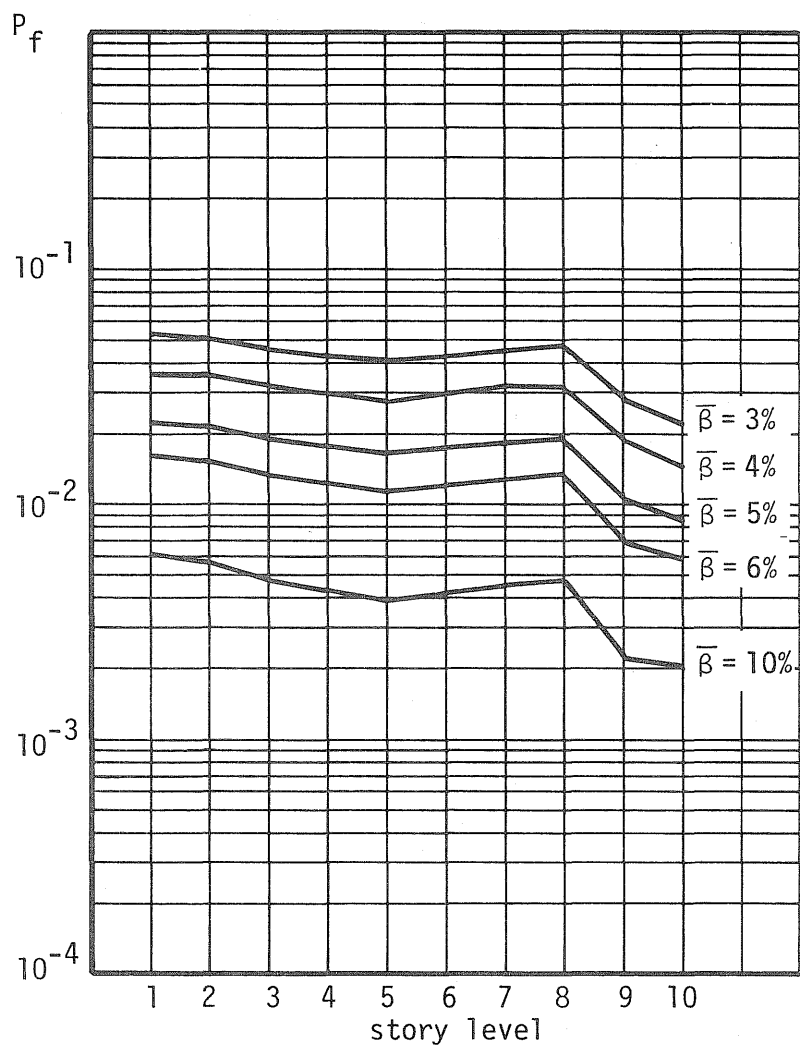


FIG. 5.8 FAILURE PROBABILITY OF INTERIOR BEAMS FOR DIFFERENT DAMPING, $\bar{T} = 1.75$ sec

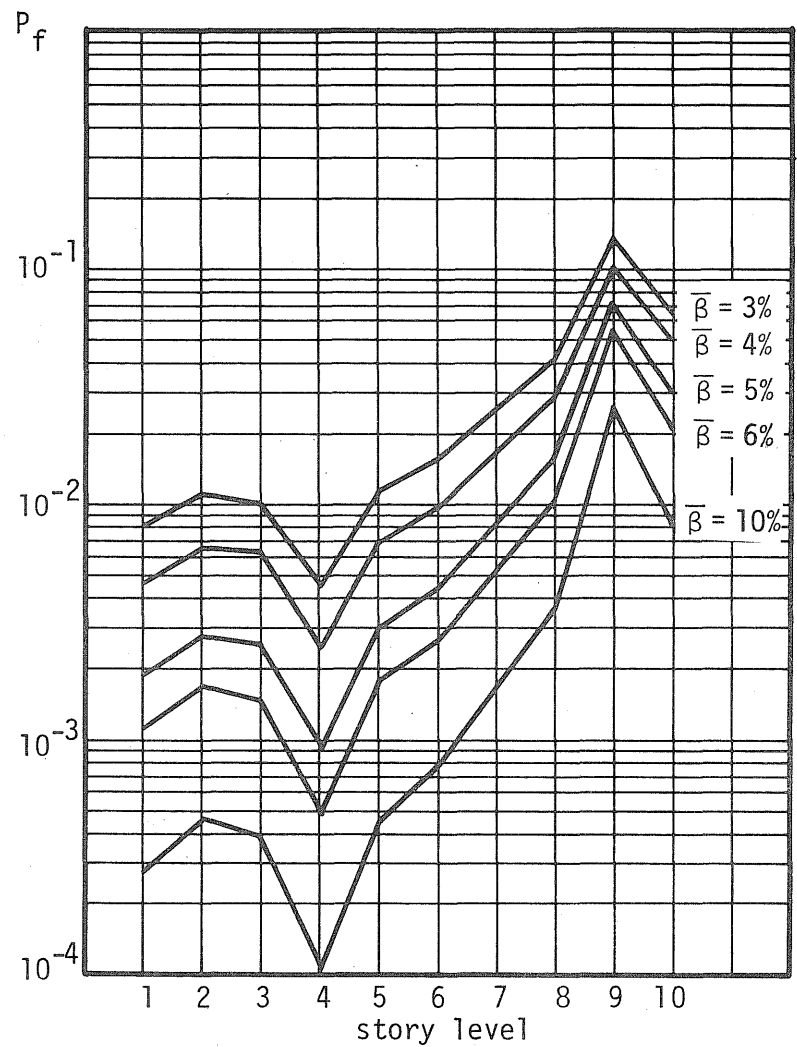


FIG. 5.9 FAILURE PROBABILITY OF INTERIOR COLUMNS FOR DIFFERENT DAMPING, $\bar{T} = 1.75$ sec

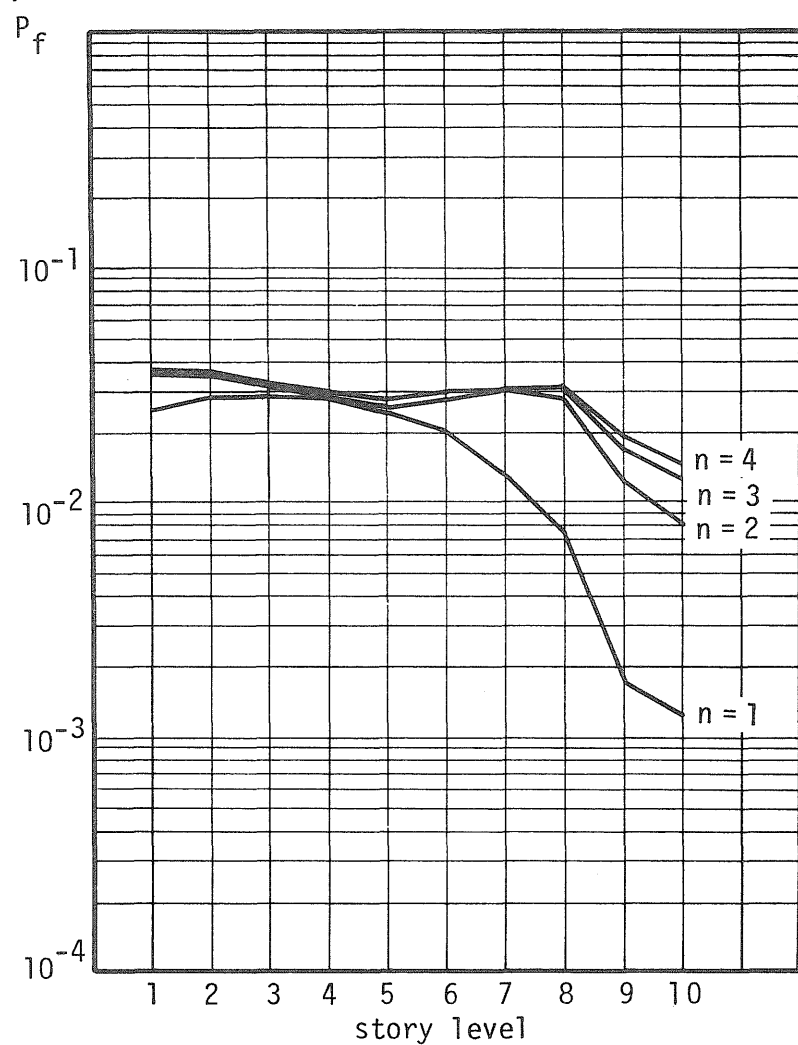


FIG. 5.10 INFLUENCE OF THE NUMBER OF MODES ON PROBABILITY OF FAILURE (INTERIOR BEAMS OF STRUCTURE 1), $\bar{\beta} = 4\%$

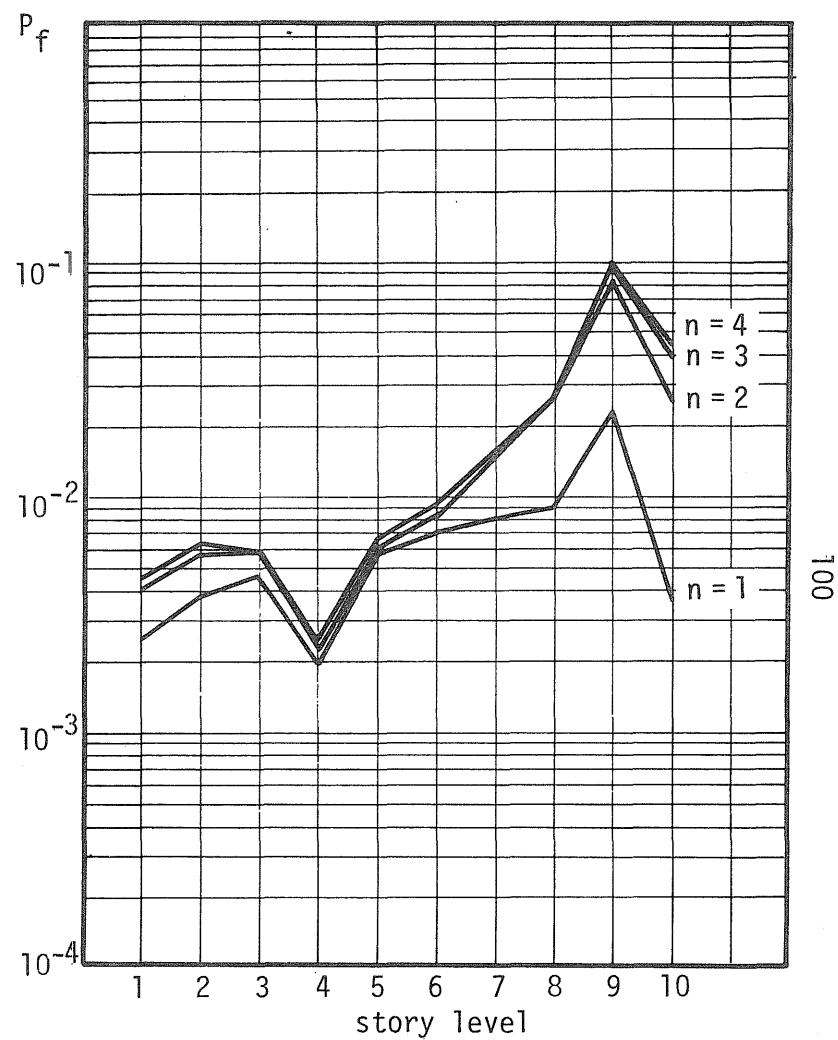


FIG. 5.11 INFLUENCE OF THE NUMBER OF MODES ON PROBABILITY OF FAILURE (INTERIOR COLUMNS OF STRUCTURE 1), $\bar{\beta} = 4\%$

APPENDIX A

COVARIANCE BETWEEN MATHEMATICAL MODELS

In many cases of practical interest, the correlation between two mathematical models, X and Y , depends only on some type of correlation between their component variables. An approximate expression of $\text{COV}[XY]$ for this case, consistent with the first-order approximation is developed here.

Let X and Y be two equations,

$$\begin{aligned} X &= f_1(X_1, X_2, \dots, X_n) = N_{f_1} \hat{f}_1(X_1, X_2, \dots, X_n) \\ \text{and} \\ Y &= f_2(Y_1, Y_2, \dots, Y_m) = N_{f_2} \hat{f}_2(Y_1, Y_2, \dots, Y_m) \end{aligned} \quad (\text{A.1})$$

where N_{f_1} and N_{f_2} are corrective factors for the mathematical functions adopted, and X_1, \dots, X_n and Y_1, \dots, Y_m are the true component variables with true means $\mu_{X_1}, \dots, \mu_{X_n}$ and $\mu_{Y_1}, \dots, \mu_{Y_m}$ and total coefficients of variation $\Omega_{X_1}, \dots, \Omega_{X_n}$ and $\Omega_{Y_1}, \dots, \Omega_{Y_m}$. It is further assumed that X_i and X_j , as well as Y_i and Y_j are, respectively, statistically independent variables for all i and j .

Expanding X and Y in Taylor series about the true mean value of X_i, \dots, X_n and Y_j, \dots, Y_m , respectively,

$$X = N_{f_1} \hat{f}_1(\mu_{X_1}, \dots, \mu_{X_n}) + N_{f_1} \sum_{i=1}^n \left(\frac{\partial f_1}{\partial X_i} \right)_{\mu} (X_i - \mu_{X_i}) + \dots$$

(A.2)

and

$$Y = N_{f_2} \hat{f}_2(\mu_{Y_1}, \dots, \mu_{Y_m}) + N_{f_2} \sum_{i=1}^m \left(\frac{\partial f_2}{\partial Y_i} \right) (Y_i - \mu_{Y_i}) + \dots$$

The product of X and Y is

$$\begin{aligned}
XY = N_{f_1} N_{f_2} & \left[\hat{f}_1(\mu_{X_1}, \dots, \mu_{X_n}) \hat{f}_2(\mu_{Y_1}, \dots, \mu_{Y_m}) \right. \\
& + \hat{f}_2(\mu_{Y_1}, \dots, \mu_{Y_m}) \sum_{i=1}^n \left(\frac{\partial \hat{f}_1}{\partial X_i} \right)_{\mu} (X_i - \mu_{X_i}) \\
& + \hat{f}_1(\mu_{X_1}, \dots, \mu_{X_n}) \sum_{j=1}^m \left(\frac{\partial \hat{f}_2}{\partial Y_j} \right)_{\mu} (Y_j - \mu_{Y_j}) \\
& \left. + \sum_{i=1}^n \sum_{j=1}^m \left(\frac{\partial \hat{f}_1}{\partial X_i} \right)_{\mu} \left(\frac{\partial \hat{f}_2}{\partial Y_j} \right)_{\mu} (X_i - \mu_{X_i}) (Y_j - \mu_{Y_j}) \right] \quad (A.3)
\end{aligned}$$

and its expected value

$$\begin{aligned}
E[XY] = \bar{N}_{f_1} \bar{N}_{f_2} & \left[\hat{f}_1(\mu_{X_1}, \dots, \mu_{X_n}) \hat{f}_2(\mu_{Y_1}, \dots, \mu_{Y_m}) \right. \\
& + \sum_{i=1}^n \sum_{j=1}^m \left(\frac{\partial \hat{f}_1}{\partial X_i} \right)_{\mu} \left(\frac{\partial \hat{f}_2}{\partial Y_j} \right)_{\mu} \{ E[X_i Y_j] - \mu_{X_i} \mu_{Y_j} \} \left. \right] \quad (A.4)
\end{aligned}$$

but (from Chapter 1)

$$\bar{N}_{f_1} \hat{f}_1(\mu_{X_1}, \dots, \mu_{X_n}) = \mu_X \quad (A.5)$$

and

$$\bar{N}_{f_2} \hat{f}_2(\mu_{Y_1}, \dots, \mu_{Y_m}) = \mu_Y$$

then, Eq. (A.4) may be written as

$$E[XY] = \mu_X \mu_Y + \bar{N}_{f_1} \bar{N}_{f_2} \sum_{i=1}^n \sum_{j=1}^m \left(\frac{\partial \hat{f}_1}{\partial X_i} \right)_{\mu} \left(\frac{\partial \hat{f}_2}{\partial Y_j} \right)_{\mu} \{ E[X_i Y_j] - \mu_{X_i} \mu_{Y_j} \} \quad (A.6)$$

Recalling from elementary probability theory that

$$\text{COV}[Z_i, Z_j] = E[Z_i Z_j] - E[Z_i] E[Z_j] = \rho_{Z_i, Z_j} \sigma_{Z_i} \sigma_{Z_j} \quad (A.7)$$

where ρ_{Z_i, Z_j} is the correlation coefficient between Z_i and Z_j , and σ_{Z_i}

is the standard deviation of Z_i , it is easily shown that

$$\text{COV} [XY] = \bar{N}_{f_1} \bar{N}_{f_2} \sum_{i=1}^n \sum_{j=1}^m \left(\frac{\partial f_1}{\partial X_i} \right)_{\mu} \left(\frac{\partial f_2}{\partial Y_j} \right)_{\mu} \rho_{X_i, Y_j} \Omega_{X_i} \Omega_{Y_j} \mu_{X_i} \mu_{Y_j} \quad (\text{A.8})$$

For the case in which some of the component variables of X and Y are the same, otherwise statistically independent, i.e.,

$$\begin{aligned} \rho_{X_i, Y_j} &= 0 & \text{for } X_i \neq Y_j \\ \rho_{X_i, Y_j} &= 1 & \text{for } X_i = Y_j \end{aligned}$$

it can be shown that

$$\text{COV} [XY] = \bar{N}_{f_1} \bar{N}_{f_2} \sum_{i=1}^p \left(\frac{\partial f_1}{\partial X_i} \right)_{\mu} \left(\frac{\partial f_2}{\partial X_i} \right)_{\mu} \bar{N}_{X_i}^2 \bar{X}_i^2 \Omega_{X_i}^2 \quad (\text{A.9})$$

where X_i for $i = 1, \dots, p$ are the variables common to both X and Y , and μ_{X_i} has been substituted by $\bar{N}_{X_i} \bar{X}_i$.

APPENDIX B

ANALYSIS OF M_t

The moment capacity of reinforced concrete elements failing through yielding of the tension reinforcement may be expressed as

$$M_t = C_c \left[1 - C_c \frac{n}{f'_c b d} \right] d + C_s (d - d') - P \left(\frac{d - d'}{2} \right) \quad (B.1)$$

where

$$C_c = P + T_s - C_s \quad (B.2)$$

$$T_s = A_s f_y \quad (B.3)$$

and

$$C_s = A'_s \left(\frac{\bar{f}'_s}{\bar{f}_y} f_y - k_3 f'_c \right) = A'_s (c_5 f_y - k_3 f'_c) \quad (B.4)$$

The c.o.v. of M_t may be expressed as

$$\Omega_{M_t}^2 = \sum C_k^2 \Omega_k^2 \quad (B.5)$$

in which

$$C_k = \frac{1}{\bar{M}_t} \left(\frac{\partial M_t}{\partial X_k} \right)_{\mu} \mu_{X_k} \quad (B.6)$$

The derivatives of M_t with respect to its component variables are

$$\frac{\partial M_t}{\partial b} = C_c^2 \left[\frac{n}{f'_c b^2} \right]$$

$$\frac{\partial M_t}{\partial d} = C_c + C_s - \frac{P}{2}$$

$$\frac{\partial M_t}{\partial d'} = -C_s + \frac{P}{2}$$

$$\frac{\partial M_t}{\partial A_s} = \left[f_y - \frac{A'_s}{A_s} (c_5 f_y - k_3 f'_c) \right] \left[d - 2C_c \frac{\eta}{f'_c b} \right] +$$

$$+ \frac{A'_s}{A_s} (c_5 f_y - k_3 f'_c) (d - d')$$

(in which A'_s and A_s are assumed to be perfectly correlated)

$$\frac{\partial M_t}{\partial f'_c} = A'_s k_3 \left[d' - 2C_c \frac{\eta}{f'_c b} \right] + C_c^2 \frac{\eta}{f'^2_c b}$$

$$\frac{\partial M_t}{\partial P} = \frac{d + d'}{2} - 2C_c \frac{\eta}{f'_c b}$$

$$\frac{\partial M_t}{\partial \eta} = - \frac{C_c^2}{f'_c b}$$

$$\frac{\partial M_t}{\partial f_y} = A_s d - c_5 A'_s d' - 2C_c \frac{\eta(A_s - c_5 A'_s)}{f'_c b} \quad (B.7)$$

APPENDIX C

CORRELATION BETWEEN THE TOTAL LOAD ACTING ON TWO FLOORS

The total load acting on a given floor may be expressed as

$$W_i = [D_i + L(A_i)] A_i \quad (C.1)$$

where D_i and $L(A_i)$ are the average unit dead and live loads, and A is the area of the floor under consideration.

For statistically independent D and L , the covariance between the total loads acting on two different floors, W_i and W_j , is

$$\text{COV}[W_i W_j] = \{ \text{COV}[D_i D_j] + \text{COV}[L(A_i) L(A_j)] \} A_i A_j \quad (C.2)$$

If D_i and D_j are perfectly correlated, then

$$\text{COV}[D_i D_j] = \sigma_{D_i} \sigma_{D_j} = \bar{D}_i \bar{D}_j \Omega_D^2 \quad (C.3)$$

Also, on the basis of the assumptions given in Sect. 4.3.2, it may be shown that

$$\begin{aligned} \text{COV}[L(A_i) L(A_j)] &= \frac{1}{A_i A_j} \iiint \iiint \text{COV}[\omega_L(x_0, y_0) \omega_L(x_2, y_2)] dx_0 dy_0 dx_2 dy_2 \\ &= \sigma_{\gamma_{bld}}^2 + \frac{1}{A_i A_j} \iiint \iiint \text{COV}[\epsilon(x_0, y_0) \epsilon(x_2, y_2)] dx_0 dy_0 dx_2 dy_2 \quad (C.4) \end{aligned}$$

and the corresponding correlation coefficient becomes

$$\begin{aligned}
\rho_{W_i, W_j} &= \frac{\text{COV}[W_i, W_j]}{\sigma_{W_i} \sigma_{W_j}} = \\
&= \frac{\bar{D}_i \bar{D}_j \Omega_D^2 + \sigma_{\gamma_{bld}}^2 + \frac{1}{A_i A_j} \iiint_{A_i A_j} \text{COV}[\varepsilon(x_0, y_0) \varepsilon(x_2, y_2)] dx_0 dy_0 dx_2 dy_2}{[\bar{D}_i^2 \Omega_D^2 + L(A_i)^2 \Omega_L^2(A_i)]^{1/2} [\bar{D}_j^2 \Omega_D^2 + L(A_j)^2 \Omega_L^2(A_j)]^{1/2}} \quad (C.5)
\end{aligned}$$

For the case of equal areas, i.e., $A_i = A_j = A$, and $D_i = D_j = D$, Eq. C.5 becomes

$$\rho_{W_i, W_j} = \frac{\bar{D}^2 \Omega_D^2 + \sigma_{\gamma_{bld}}^2 + \frac{1}{A^2} \iiint_A \text{COV}[\varepsilon(x_0, y_0) \varepsilon(x_2, y_2)] dx_0 dy_0 dx_2 dy_2}{\bar{D}^2 \Omega_D^2 + L(A)^2 \Omega_L^2(A)} \quad (C.6)$$

For the white-noise model (see Eq. 4.7)

$$\iiint_A \text{COV}[\varepsilon(x_0, y_0) \varepsilon(x_2, y_2)] dx_0 dy_0 dx_2 dy_2 = 0 \quad (C.7)$$

thence,

$$\rho_{W_i, W_j} = \frac{\bar{D}^2 \Omega_D^2 + \sigma_{\gamma_{bld}}^2}{\bar{D}^2 \Omega_D^2 + L(A)^2 \Omega_L^2(A)} \quad (C.8)$$

Similarly, for the Peir's model [75, 76] (see Eq. 4.9)

$$\frac{1}{A^2} \iiint_A \text{COV}[\varepsilon(x_0, y_0) \varepsilon(x_2, y_2)] dx_0 dy_0 dx_2 dy_2 = \frac{\rho_m \sigma_{sp}^2 \pi d K(A)}{A} \quad (C.9)$$

$$\text{where} \quad K(A) = \left[\text{erf}\left(\sqrt{\frac{A}{d}}\right) - \sqrt{\frac{d}{A\pi}} (1 - e^{-A/d}) \right]^2 \quad (C.10)$$

and $\text{erf}(-)$ is the error function. Hence,

$$\rho_{W_i, W_j} = \frac{\bar{D}^2 \Omega_D^2 + \sigma_{\gamma_{bld}}^2 + \rho_m \sigma_{sp}^2 \pi d K(A)/A}{\bar{D}^2 \Omega_D^2 + L(\bar{A})^2 \Omega_{L(A)}^2} \quad (C.11)$$

APPENDIX D

ANALYSIS OF EI

The equivalent rigidity of reinforced concrete members may be expressed as

$$EI = \frac{M_y}{\phi_y} \quad (D.1)$$

in which M_y and ϕ_y are, respectively, the yield moment capacity and yield curvature at the critical section.

If a linear stress and strain distribution is assumed, it may be shown that

$$M_y = C_c(d' - \frac{c}{3}) + T_s(d - d') + P\frac{(d - d')}{2} \quad (D.2)$$

and

$$\phi_y = \frac{f_y}{E_s(d - c)} \quad (D.3)$$

in which

$$c = \{ -K_1 + \sqrt{K_1^2 + 2(K_2 + K_3)} \} d = \{-K_1 + R\} d \quad (D.4)$$

and

$$K_1 = \rho'(n-1) + \rho''n \quad (D.5)$$

$$K_2 = \rho'(n-1) d'/d \quad (D.6)$$

$$K_3 = \rho''n \quad (D.7)$$

$$n = E_s/E_c \quad (D.8)$$

$$\rho'' = \frac{A_s + P/f_y}{bd} \quad (D.9)$$

$$C_c = \frac{1}{2} b \frac{c^2}{d - c} \frac{f_y}{n} \quad (D.10)$$

$$T_s = A_s f_y \quad (D.11)$$

If x_k is some parameter, then

$$\begin{aligned} \frac{\partial EI}{\partial x_k} &= \frac{\partial EI}{\partial M_y} \frac{\partial M_y}{\partial x_k} + \frac{\partial EI}{\partial \phi_y} \frac{\partial \phi_y}{\partial x_k} = \\ &= \frac{\phi_y \frac{\partial M_y}{\partial x_k} - M_y \frac{\partial \phi_y}{\partial x_k}}{\phi_y^2} \end{aligned} \quad (D.12)$$

Letting

$$K_4 = -\frac{1}{3} + \left[\frac{2d-c}{c(d-c)} \right] \left[d' - \frac{c}{3} \right] \quad (D.13)$$

The derivatives of M_y are given as

$$\frac{\partial M_y}{\partial b} = \frac{C_c}{b} \left[d' - \frac{c}{3} \right] + C_c K_4 \frac{\partial c}{\partial b}$$

$$\frac{\partial M_y}{\partial d} = -\frac{C_c}{d-c} \left[d' - \frac{c}{3} \right] + C_c K_4 \frac{\partial c}{\partial d} + T_s + \frac{P}{2}$$

$$\frac{\partial M_y}{\partial d'} = C_c + C_c K_4 \frac{\partial c}{\partial d'} - T_s - \frac{P}{2}$$

$$\frac{\partial M_y}{\partial A_s} = C_c K_4 \frac{\partial c}{\partial A_s} + f_y (d - d')$$

$$\frac{\partial M_y}{\partial P} = C_c K_4 \frac{\partial c}{\partial P} + \frac{d - d'}{2}$$

$$\frac{\partial M_y}{\partial f_y} = \frac{C_c}{f_y} \left[d' - \frac{c}{3} \right] + C_c K_4 \frac{\partial c}{\partial f_y} + A_s (d - d')$$

$$\frac{\partial M_y}{\partial E_c} = \frac{C_c}{E_c} \left[d' - \frac{c}{3} \right] + \frac{C_c n}{E_c} K_4 \frac{\partial c}{\partial n} \quad (D.14)$$

and those of ϕ_y as

$$\frac{\partial \phi_y}{\partial b} = \frac{\phi_y}{d-c} \frac{\partial c}{\partial b}$$

$$\frac{\partial \phi_y}{\partial d} = \frac{\phi_y}{d-c} \left[-1 + \frac{\partial c}{\partial d} \right]$$

$$\frac{\partial \phi_y}{\partial d'} = \frac{\phi_y}{d-c} \frac{\partial c}{\partial d'}$$

$$\frac{\partial \phi_y}{\partial A_s} = \frac{\phi_y}{d-c} \frac{\partial c}{\partial A_s}$$

$$\frac{\partial \phi_y}{\partial P} = \frac{\phi_y}{d-c} \frac{\partial c}{\partial P}$$

$$\frac{\partial \phi_y}{\partial f_y} = \frac{\phi_y}{f_y} \left[1 + \frac{f_y}{d-c} \frac{\partial c}{\partial f_y} \right]$$

$$\frac{\partial \phi_y}{\partial E_c} = \frac{\phi_y}{(d-c)} - \frac{n}{E_c} \frac{\partial c}{\partial n} \quad (D.15)$$

The derivatives of c are

$$\frac{\partial c}{\partial b} = \frac{d}{b} \left[K_1 - \frac{K_1^2 + K_2 + K_3}{R} \right]$$

$$\frac{\partial c}{\partial d} = \frac{1}{d} \left[K_1 d - \frac{(K_1^2 + 2K_2 + K_3) d}{R} + c \right]$$

$$\frac{\partial c}{\partial d'} = \frac{d}{d'} \left[\frac{K_2}{R} \right]$$

$$\begin{aligned}
\frac{\partial c}{\partial A_s} &= \frac{d}{A_s} \left[-[\rho'(n-1) + \rho n] + \frac{K_1[\rho'(n-1) + \rho n] + K_2 + \rho n}{R} \right] \\
\frac{\partial c}{\partial n} &= \frac{d}{n} \left[-(\rho'n + K_3) + \frac{K_1(\rho'n + K_3) + \rho'n d'/d + K_3}{R} \right] \\
\frac{\partial c}{\partial P} &= \frac{n}{bf_y} \left[-1 + \frac{K_1 + 1}{R} \right] \\
\frac{\partial c}{\partial f_y} &= \frac{-Pn}{bf_y^2} \left[-1 + \frac{K_1 + 1}{R} \right]
\end{aligned} \tag{D.16}$$

The uncertainty in EI is found from

$$\Omega_{EI}^2 = \sum_k C_k^2 \Omega_k^2 \tag{D.17}$$

where

$$C_k = \frac{1}{EI} \left(\frac{\partial EI}{\partial x_k} \right)_\mu \mu_{x_k} \tag{D.18}$$

APPENDIX E

ANALYSIS OF W_i and $\{\phi_i\}$

The eigenvalue problem of linear structural systems is formulated in terms of the characteristic equation

$$([K] - \lambda[M]) \{\phi\} = 0 \quad (E.1)$$

where $[K]$ and $[M]$ are, respectively, the effective stiffness and mass matrices, λ_i is the i^{th} eigenvalue and $\{\phi_i\}$ the i^{th} eigenvector.

In the case of systems in which the floor masses, as well as the members stiffnesses, are perfectly correlated and with equal coefficients of variations, $[K]$ and $[M]$ may be expressed as (see Sect. 3.2.3)

$$[K] = K^* [\bar{K}] \quad (E.2)$$

and

$$[M] = M^* [\bar{M}] \quad (E.3)$$

in which K^* and M^* are random variables, and $[\bar{K}]$ and $[\bar{M}]$ are deterministic matrices consisting of the mean values of the floor masses and stiffness coefficients, respectively.

Substituting Eqs. E.2 and E.3 into Eq. E.1 and dividing by K^* , it follows that

$$([\bar{K}] - \lambda' [\bar{M}]) \{\phi\} = 0 \quad (E.4)$$

in which

$$\lambda' = \frac{M^*}{K^*} \lambda \quad (E.5)$$

Since $[\bar{K}]$ and $[\bar{M}]$ are deterministic matrices, it follows that the eigenvalues λ'_i for $i = 1, \dots, n$ of Eq. E.4 are also deterministic quantities.

The i^{th} eigenvalue of Eq. E.1 then may be expressed as

$$\lambda_i = \frac{K^*}{M^*} \lambda'_i \quad (E.6)$$

from which the mean and c.o.v. of λ_i may be found. The corresponding eigenvector is found by substituting Eq. E.6 into Eq. E.1, yielding

$$([K] - \frac{K^*}{M^*} \lambda_i^! [M]) \{\phi_i\} = 0 \quad (E.7)$$

Using Eqs. E.2 and E.3, Eq. E.7 becomes

$$([\bar{K}] - \lambda_i^! [\bar{M}]) \{\phi_i\} = 0 \quad (E.8)$$

Since $[\bar{K}]$, $[\bar{M}]$ and $\lambda_i^!$ are deterministic, it follows then that $\{\phi_i\}$ is also deterministic.